INFORMATION TO USERS

This manuscript has been reproduced from the microfilm master. UMI films the text directly from the original or copy submitted. Thus, some thesis and dissertation copies are in typewriter face, while others may be from any type of computer printer.

The quality of this reproduction is dependent upon the quality of the copy submitted. Broken or indistinct print, colored or poor quality illustrations and photographs, print bleedthrough, substandard margins, and improper alignment can adversely affect reproduction.

In the unlikely event that the author did not send UMI a complete manuscript and there are missing pages, these will be noted. Also, if unauthorized copyright material had to be removed, a note will indicate the deletion.

Oversize materials (e.g., maps, drawings, charts) are reproduced by sectioning the original, beginning at the upper left-hand corner and continuing from left to right in equal sections with small overlaps.

Photographs included in the original manuscript have been reproduced xerographically in this copy. Higher quality 6" x 9" black and white photographic prints are available for any photographs or illustrations appearing in this copy for an additional charge. Contact UMI directly to order.

Bell & Howell Information and Learning
300 North Zeeb Road, Ann Arbor, MI 48106-1346 USA
800-521-0600

UMI®

DISCHARGE ESTIMATION TECHNIQUES FOR HYDRAULIC EFFICIENCY TESTING

PAMELA D. HANS

A THESIS
SUBMITTED TO THE FACULTY OF GRADUATE STUDIES
IN PARTIAL FULFILLMENT FOR THE DEGREE OF

MASTER OF SCIENCE

DEPARTMENT OF CIVIL ENGINEERING
UNIVERSITY OF MANITOBA
WINNIPEG, MANITOBA

THE UNIVERSITY OF MANITOBA

FACULTY OF GRADUATE STUDIES

COPYRIGHT PERMISSION

DISCHARGE ESTIMATION TECHNIQUES FOR HYDRAULIC EFFICIENCY TESTING

by

PAMELA D. HANS

A Thesis submitted to the Faculty of Graduate Studies of the University of Manitoba in partial fulfillment of the requirements of the degree of

MASTER OF SCIENCE

ABSTRACT

Field performance testing of hydraulic turbines is used to define the head-power-discharge relationship for a turbine/generator; this relationship is used to identify the peak operating point for a turbine. Of the variables used to determine this relationship, discharge is most difficult to measure accurately in real time and is most susceptible to measurement error. The velocity-area method of discharge measurement is favored by many hydroelectric utilities as it is well suited to application at low-head plants, and is therefore the subject of this research.

Velocity data collected during field performance tests were used to compare discharge estimates obtained using various distributions of metering points. This analysis suggests that an accurate estimate of discharge may be obtained by establishing the arrangement of measurement points based on the true intake velocity profile, rather than on an idealized velocity distribution.

Laboratory testing was undertaken to investigate the results of the numerical analysis. Seven arrangements of velocity points were used to compute discharge through a model of a turbine intake. The reliability of discharge estimate was evaluated by comparison to a reference discharge. The results of the laboratory testing are comparable to the numerical analysis and indicate that a more accurate discharge estimate may be obtained with fewer velocity measurements combined with a numerical integration strategy than code based methods.

An observed relationship between the horizontal velocity profile and unit discharge prompted analysis of a Reduced Data Set (RDS) method of estimating discharge. Field data was used to investigate the statistical relationship between discharge and horizontal velocity profile at three locations within the vertical traverse. The analysis was used to evaluate the reliability of a discharge estimate made based on the relationship between the two variables. The results of this analysis suggest that the relationship between horizontal velocity profile and discharge is strongest in proximity to 0.11 D (from top and bottom of the intake).

ACKNOWLEDGEMENTS

Many individuals have assisted me in completion of this research work. In particular, I would like to thank Manitoba Hydro and NSERC for providing financial support for this project.

Although it is not possible to name each person who has assisted me during this research, I would like to take this opportunity to sincerely thank the following individuals.

H. Zbigniewicz and M. Drouin, Hydraulic Engineering and Operations Department, Manitoba Hydro for providing motivation for this research as well as technical expertise necessary to complete this project.

Thanks also to my advisor, J. Doering for giving me the opportunity to pursue graduate studies; whose unbounded enthusiasm for research is infectious, and pursuit of knowledge, inspiring.

Halina, my mentor and friend for her constant encouragement and guidance.

My friends in the HRTF whose friendship has made my graduate studies a most memorable experience.

Finally, to my Mom and Dad. Thank you for your infinite wisdom, patience, and understanding. Your have shown me that there are no bounds to achievement and given me the confidence to strive for excellence.

This thesis is dedicated to Tom and Dan.

All hard work is rewarded.

TABLE OF CONTENTS

Abstract		ii
Acknowledgements		iii
Dedication		iv
Table of Contents		v
List of Figures		viii
List of Tables		x
CHAPTER 1		1
Introduction		1
1.1	Background	1
1.2	Objectives of this Research	2
1.3	Outline	2
CHAPTER 2		4
Performance Testing		4
2.1	Equations and Theory	4
2.2	Homologous Equations	6
2.3	Performance Tests Methods	7
	2.3.1 Gibson Pressure-Time	8
	2.3.2 Tracer Dilution	9
	2.3.3 Transit Time (Allen Salt Velocity) Method	9
	2.3.4 Acoustic Methods	10
	2.3.5 Velocity-Area Method	11
2.4	Performance Testing Codes	11
	2.4.1 American Society of Mechanical Engineers (ASME PTC-18)	12
	2.4.2 International Standards Organization (ISO 3354)	13
	2.4.3 International Electrotechnical Commission (IEC 41)	14
	2.4.4 German Testing Code	14
2.5	Performance Curves	16
CHAPTER 3		23
3	A Comparison of Discharge Estimates	23
3.1	Intoduction	23
3.2	Code Specifications	24
3.3	Gauss-Legendre Quadrature Method	24
3.4	Data	26
	3.4.1 Data Interpolation	27
	3.4.2 Discharge Estimates	28

CHAPTER 4 39
Laboratory Testing 39
4.1 Introduction 39
4.2 Hydraulic Models 40
4.3 Physical Model 41
4.4 Physical Characteristics 42
4.4.1 Velocity Measurement 43
4.4.2 Positioning System 44
4.4.3 Flow Measurement 44
4.5 Testing Schedule 45

CHAPTER 5 53
5 Data Post-Processing 53
5.1 Velocity Data 53
5.2 Discharge Data 54
5.2.1 MAG Reference Discharge Error 54
5.2.2 Velocity Measurement Error 55
5.2.3 Positioning Error 55
5.2.4 Geometric Error 56
5.3 Error Calculations 56

CHAPTER 6 58
Laboratory Results 58
6.1 Favorable Flow Conditions 58
6.1.1 Gauss Legendre Quadrature 59
6.1.2 German 60
6.1.3 ASME 60
6.2 Disturbed Flow Condition 61
6.2.1 Gauss-Legendre Quadrature 62
6.2.2 German 62
6.2.3 ASME 63

CHAPTER 7 69
Reduced Data Set Testing 69
7.1 Data 69
7.2 Data Interpolation and Integration 70
7.3 Evaluation of the RDS Methodology 71
7.3.1 Statistical Analysis 72
7.3.1.1 RDS at 0.15H 75
7.3.1.2 RDS at 0.67H 75
7.3.1.3 RDS at 0.91H 76
7.4 Summary 76

CHAPTER 8 84
Conclusions and Recommendations 84
8.1 Summary 84
8.2 Conclusions 86
8.3 Recommendations 87

REFERENCES 88

APPENDIX A 90
Position of Velocity Measurements
Motion Control Programs

APPENDIX B 120
Laboratory Testing Results
MATLAB™ Script Files for Data Post-Processing

APPENDIX C
MATLAB™ Script Files for RDS Analysis 138

APPENDIX D
RDS Results 143

LIST OF FIGURES

Figure 2.1. Cross section of low-head turbine unit 18

Figure 2.2. Aluminum space-frame truss. 19

Figure 2.3. Ott type-A propeller 19

Figure 2.4 . Theoretical (a) and measured (b) velocity profiles 20

Figure 2.5. Distribution of velocity measurements used in ASME integration 21

Figure 2.6. Operating Curves for a low-head plant 22

Figure 3.1. Distribution of metering points used to sample the intake at Pine Falls G.S. 33

Figure 3.2 Measured (a) and interpolated (b) velocity profiles 34

Figure 3.3 (a-c). Interpolated velocity profile for unit 3, intakes A. B, and C at 60% gate. 35

Figure 3.4 (a-c). Interpolated velocity profile for unit 6, intakes A, B, and C. 36

Figure 3.5. The location of the metering points required by ASME code relative to the German code. 37

Figure 3.6 (a-c). Locations of metering points required for a 4x5, 5x5, and 5x6 GLQ. 38

Figure 4.1. Relationship between drag and Reynolds number 47

Figure 4.2. Schematic of laboratory model 48

Figure 4.3. Timber flume and intake 49

Figure 4.4. Trash rack 49

Figure 4.5. Aluminum positioning apparatus 50

Figure 4.6 (a-g) Distributions of metering points used to traverse the intake 51

Figure 5.1: Unfiltered ADV record. 57

Figure 5.2 Typical plot of magmeter discharge data. 57

Figure 6.1. Intake velocity profile 64

Figure 6.2. Centerline velocity profile 64

figure 6.3 (a-b). Intake velocity profile from 5x5 GLQ and 6x6 GLQ 65

Figure 6.4. Relative position of ASME and GLQ metering points 66

Figure 6.5. Intake velocity profile for disturbed flow condition 67

Figure 6.6. Error of discharge estimate. 68

Figure 7.1. Velocity-horizontal position curve for Unit 1 at RDS 0.91 H 76

Figure 7.2. Distribution of metering points used at Kettle G.S. 77
Figure 7.3 (a-b). Measured and interpolated intake velocity profiles 78
Figure 7.4 (a-b) Measured and splined velocity profiles at RDS of 0.91 H 79
Figure 7.5. Statistical relationship between Gate and RDS index number 80
Figure 7.6(a-c) Velocity-horizontal position curve for Unit 1, intake a 81
Figure 7.7 (a-c) Standard error of discharge estimate 82
Figure 7.8. Summary of statistical analysis 83

LIST OF TABLES

Table 2.1. German distribution of velocity measurements. 16

Table 3.1 Gauss-Legendre quadrature weights and function arguments 26

Table 3.2 Summary of discharge estimates 32

Table 3.3. Summary of average relative errors for discharge estimates. 31

Table 4.1 Model scale factors 42

Table 4.2 Laboratory testing schedule 46

Table 6.1 Summary of discharge estimates (favorable conditions) 59

Table 6.2 Summary of discharge estimates (unfavorable conditions) 61

Table 7.1 Summary of RDS statistical analysis 74

CHAPTER 1

INTRODUCTION

1.1 Background

Field performance tests of turbine/generator units are necessary for the efficient operation of a hydroelectric generating station. Performance test data are used to determine the head-power-discharge relationship for a turbine/generator unit; this relationship is used to identify the peak operating point for a turbine. The accurate measurement of the variables which influence the efficiency of a turbine is critical to the economic and efficient generation of hydroelectric power as a small deviation from a turbine/generator unit's peak operating point can result in significant economic losses.

Objectives for determining operating curves for turbine/generator units include efficient and economical generation of electricity, evaluating turbine manufacturer guarantees, measuring the need for turbine maintenance, and quantifying the benefits realized from turbine upgrades. Ancillary objectives include responsible use of water resources, as well as decreased fish mortality. An additional benefit of operating at maximum efficiency is reduced cavitation damage to the turbine blades as the point of best efficiency typically coincides with minimum vibrations.

The variables required to establish the operating curves for a turbine/generator unit are discharge, head, and power. Of these variables, discharge is most difficult to measure accurately. Head and power generation are recorded on an hourly basis; this is routine for plant operation. Discharge, however, is not normally measured as it is difficult to estimate accurately in real time. Various techniques are available to measure discharge. The suitability of a given method depends on the flow rate, head, and turbine intake characteristics.

The velocity-area method for discharge measurement is favored by many hydroelectric utilities, because it is well-suited to low-head plants with short, converging intakes. This method involves traversing an array of propeller-type flow meters (*i.e.*, Ott Type A) mounted on a rigid horizontal frame across the flow at the intake stoplog guides. The appropriate summation of the grid of point measurements of velocity, times the corresponding area within the metering plane, yields an estimate of the discharge.

1.2 Objectives of this Research

The complex nature of the velocity profile at the intake of a low-head plant makes it difficult to determine the appropriate sampling strategy to accurately represent the velocity profile. Although the codes which govern the testing of hydraulic turbines specify a distribution and summation of velocity measurements to estimate discharge, the codes do not agree on the number, or the distribution of velocity measurements required to adequately sample the velocity profile.

The objective of this research is to improve the velocity-area method of discharge measurement. Given the complex nature of the intake velocity profile typical of low-head plants, it may be advantageous to develop a sampling strategy that reflects the variability in both the horizontal and vertical dimensions. It is anticipated that the results of this research may be used to improve the accuracy and efficiency of discharge measurement.

1.3 Outline

An overview of performance testing, outlining the need for testing, and the methods of establishing operating curves, with a focus on low-head plants, follows in Chapter 2. Also included in Chapter 2 is a review of the literature pertaining to hydraulic efficiency testing, with a focus on discharge measurement at low-head plants and the associated difficulties. Since the codes which govern hydraulic efficiency testing do not agree on

either the number or the distribution of velocity measurements necessary to estimate discharge, Chapter 3 provides a comparison of discharge estimates (based on field data) resulting from the different distributions of metering locations. as outlined in the testing codes. Included in the analysis is an evaluation of the Gauss-Legendre quadrature numerical integration method, which is proposed as a noncode-based method to estimate discharge. Chapter 4 presents the laboratory model used to test the numerical analyses outlined in Chapter 3. The post processing of data is described in Chapter 5. Chapter 6 presents the data collected using the laboratory model, as well as an analysis of the data. Chapter 7 explores the statistical relationship between discharge and the horizontal velocity profile at a given location in the vertical traverse. Chapter 8 summarizes the research and provides conclusions that may be drawn from the analysis. Included in this chapter are recommendations for further research in both laboratory and field environments.

CHAPTER 2

PERFORMANCE TESTING

In general, performance tests are used to determine either relative or absolute efficiency. Tests used to determine relative efficiency are index tests, and are used primarily to assess the manufacturer's guaranty (Voaden, 1951; Voigt, 1989) . Absolute efficiency tests are used to define operating curves for turbine/generator units and use unit discharge in their calculation of efficiency. The principle difference between relative and absolute efficiency tests is, in the case of absolute tests, it is necessary to determine the flow rate (Almquist *et. al.*, 1995); index tests determine efficiency relative to a reference discharge.

There are three primary objectives for conducting performance tests of hydroelectric turbine/generator units. The first objective is to measure the variables which define generating efficiency, *i.e.*, head, power, and discharge. From the relationship between these variables it is possible to establish performance curves for a hydraulic turbine/generator unit. Performance curves are used to operate turbines at their most efficient operating point, *i.e.*, best gate. A second objective is to provide the hydraulic relationships required for accurate calculations of discharge through the unit; this information is useful for the management of water resources, as well as determining efficiency of power generation. A third objective is to quantify the benefits realized from turbine maintenance measures (Hans & Louka, 1996).

2.1 Equations and Theory

Evaluation of hydroelectric performance requires measurement of flow, effective head, and electrical output. Of these variables, absolute discharge is typically the most difficult to measure and is most susceptible to measurement error. Hydraulic head is readily obtained from the difference between the forebay and tailrace water surface elevations.

Power output for each turbine is accurately measured and monitored as part of routine plant operation.

The efficiency of power generation, when related to discharge, can be used to establish operating curves for turbine/generator units. These operating curves are essential to optimize the efficiency of power generation. Among the advantages of operating a turbine at its most efficient operating point are: responsible use of water resources, and minimizing cavitation damage, as typically the point of peak efficiency also coincides with minimum vibrations (Howe, 1995).

By definition, efficiency is the ratio of the power output, to the power input given by

$$\eta = \frac{P}{\rho g Q H}, \tag{2.1}$$

where P is the power output, ρ is the density of water, g is the acceleration due to gravity, Q is the volumetric water flow rate, H is the difference between the headwater and tailwater elevations, and η is efficiency (Almquist *et. al.*, 1995).

Power output is measured either as the shaft power delivered by the turbine to the generator, or as the electrical power delivered by the generator, and is typically measured by a watt-hour meter. Using shaft power as P in equation (2.1) determines *turbine efficiency*; electrical power measures the combined efficiency of the turbine and generator unit, and is referred to as *unit efficiency*. The denominator of equation (2.1) is the power input, or the power of the water passing through the unit that is available for conversion to electricity. Power input varies according to unit discharge and head.

From Bernoulli, the total hydraulic head is given as the sum of the potential, pressure, and velocity heads, expressed as

$$H = z + \frac{p}{\gamma} + \alpha \frac{v^2}{2g} \tag{2.2}$$

where z is the potential head available (measured as height above datum); $\frac{p}{\gamma}$ is the pressure head (measured as the ratio of pressure at z to the specific weight of water, γ); and. $\frac{v^2}{2g}$ is the velocity head (v is velocity and g is acceleration due to gravity), and α is the kinetic energy correction factor for non-uniform flow (Craeger and Justin, 1927).

The difference between the forebay and tailrace water surface elevations is defined as gross head, as illustrated in figure 2.1; gross head is the sum of the potential and pressure heads. As gross head does not take into account the losses that occur as the water passes through the unit (*i.e.*, kinetic energy losses), net head is used as the effective hydraulic head available for power generation.

Net head is the hydraulic head, or energy available to the turbine for conversion to rotational energy. It is equivalent to the gross head, less the losses due to the trash rack, intake, scroll case, and exit losses, as well as the losses that occur at the draft tube outlet.

2.2 Homologous Equations

Stationarity of testing conditions such as head and power output, during performance testing is important to ensure that the velocity data collected during a single test are commensurate. Forebay and tailwater levels are recorded continuously throughout performance testing , and as part of routine plant operation. As shown in figure 2.1, the difference between these water surface elevations is the head available for power generation. Gross head is affected by plant discharge as well as backwater effects. Since (both gross and net) head influences both efficiency and discharge, it is necessary to correct for the fluctuations in head that take place during the course of a single performance test. As plant discharge varies with power generation, it is unlikely that constant plant discharge will be maintained for the duration of an intake traverse, and less likely that constant conditions will be maintained for the complete performance test

schedule of a unit. A complete test schedule involves measuring unit performance at numerous gate settings. This process is lengthy and increases with the size of the turbine intake, number of gate setting, and in the case of variable pitch turbines, number of blade angles tested.

Homologous equations are used to correct performance test data for changing conditions. These equations relate power, head, and discharge values. Using the homologous equations allows a comparison of performance test data collected at different conditions of head, and power output (Winstone, 1989). In addition, as in the case of conducting acceptance tests to verify turbine manufacturer guarantees, homologous equations are used to compare the results of performance tests conducted at rated head, to the tested head. The homologous equations used to relate discharge, power, and head are given by Winstone (1989)

$$\frac{Q_1}{Q_2} = \left[\frac{H_1}{H_2}\right]^{1/2} \tag{2.3a}$$

$$\frac{Q_1}{Q_2} = \left[\frac{P_1}{P_2}\right]^{1/3} \tag{2.3b}$$

$$\frac{P_1}{P_2} = \left[\frac{H_1}{H_2}\right]^{3/2} \tag{2.3c}$$

where Q_1 is the flow at rated head conditions and Q_2 is the flow at testing conditions. H_1 is the rated head and H_2 is the head at testing conditions. P_1 is the rated power and P_2 is the power at testing conditions.

2.3 Performance Tests Methods

An accurate measurement of discharge, is difficult to obtain but is central to the efficient management of water resources. In addition, measuring absolute discharge is essential to

determining absolute power generation efficiency. Five techniques have been used to measure the discharge through a turbine (Winstone, 1989); they include: Gibson pressure-time, tracer dilution, Allen salt velocity, acoustic, and velocity-area methods. The suitability of a given method depends on the characteristics of the turbine, intake conduit, as well as the hydraulic characteristics of the plant (*i.e.*, head and discharge) (Hecker and Nystrom, 1987).

The following presents a discussion of these discharge measurement methods with the objective of providing a general background into the discharge measurement component of hydraulic performance testing. Particular attention is given to the suitability of each method to low-head plants, with short, converging intake conduits. In addition, the codes which govern the performance testing of hydraulic turbine/generator units will be reviewed.

2.3.1 Gibson Pressure-Time

The Gibson pressure-time method of discharge measurement is used to determine absolute discharge. This technique uses the differential pressure required to decelerate a mass of water between two piezometer stations in a straight section of penstock. From the time integral of the pressure-time relationship, it is possible to derive the momentum exerted by the mass of water, and hence the rate of flow (Nystrom, 1991).

The procedure for conducting pressure-time measurements is as follows. Primary hydraulic testing parameters such as gate opening, forebay and tailrace water levels, hydraulic pressures, and generator output are collected, as part of the test data set. The turbine/generator unit is set at the desired gate opening, for a short stabilization period. The wicket gates are abruptly closed, and simultaneous pressure measurements are made at two piezometer stations. When conducting the pressure-time test, it is important to have steady conditions of head and discharge during the time of wicket gate closure.

This method of discharge measurement is best suited to plants with long conduits that have two well-spaced metering sections for pressure measurement. The primary disadvantage of this method is the disruption to normal plant operation, as a load rejection is required for full closure of the wicket gates (Levesque, 1994).

2.3.2 *Tracer Dilution*

The tracer dilution method uses a continuous injection of a conservative tracer, at a known concentration and flow rate, to measure unit discharge. The dye is injected at the intake and the concentration is measured at the draft tube outlet. Using a mass balance, the ratio of the initial concentration, to the concentration in the draft tube, multiplied by the rate of dye injection, yields the total discharge.

As the accuracy of this method relies on the rate of mixing as well as complete mixing of the tracer it is not well-suited to low-head plants with short penstocks, as it is not possible to guarantee complete mixing (Nystrom, 1991; Winstone, 1989).

2.3.3 *Transit Time (Allen Salt Velocity) Method*

The transit time method uses the travel time of a cloud of salt water injected into a control volume to measure discharge. The conductivity of the salt brine solution is used to measure the travel time. Electrodes are used to establish a conductance trace for the salt water cloud, with the transit time calculated as the difference between the centroid of the two conductivity traces. Among the disadvantages of this method, is the disruption to plant operations which arises due to the time required to install and remove the testing equipment. Since the accuracy of the transit time method increases with transit time, this method is best suited to plants with long penstocks (Spencer, 1986; Levesque 1987).

2.3.4 Acoustic Methods

Acoustic discharge measurement techniques are relatively new technology for hydroelectric performance testing. They were originally developed for oceanographic flow measurement and have recently been developed for application in hydroelectric turbine discharge measurement (Birch & Lemon, 1995). Acoustic methods can be divided into three categories: Doppler, scintillation, and transit-time. Doppler measures the phase shift of an acoustic pulse to determine the component of the flow along the acoustic path. This principle assumes flow homogeneity along the acoustic path. Scintillation uses the time delay in the "signature" of an acoustic pulse to determine velocity. Both methods use an array of separate transmitters and receivers. Transit time acoustic velocimetry is based on the principle that the velocity of an acoustic signal is influenced by the velocity component of the medium parallel to the direction of acoustic propagation (Gawne, 1997). The average water velocity along a path between a pair of acoustic cells is determined by the difference in the travel time of the upstream and downstream acoustic signals. Problems associated with the acoustic method are accurate positioning of the transducers when applying integration methods that use a fixed weighting scheme, such as Gauss Jacobi. Voser *et al.* (1996) have developed a method of improving acoustic flow measurement by incorporating positioning error into the weighting scheme used in Gauss-Jacobi quadrature integration. Accurate alignment of the acoustic pairs is also critical to meaningful results. It has been shown that misalignment of acoustic paths can lead to significant errors (Grego, 1996; Sugishita 1996).

Among the advantages of acoustic methods are the ability to perform continuous sampling of the velocity profile, minimum disruption to normal plant operation, and a real time flow measurement. Due to the relatively recent application of acoustic methods to hydraulic performance testing, the codes do not include acoustic methods in current testing codes (Hecker and Nystrom, 1987).

2.3.5 *Velocity-Area Method*

Of the methods available for measuring unit discharge, the velocity-area method is favored by many hydroelectric utilities because of its relatively low start-up costs and ease of application (Levesque, 1987). In addition, when the metering plane is located at the intake stop-log guides minimal disruption to normal plant operation is required.

The velocity-area method involves traversing an array of propellers (Ott type A), mounted as shown in figure 2.2, across the intake velocity profile. This process is repeated for numerous power settings, and in the case of variable pitch turbines, blade angles, to determine the operating curves for a turbine/generator unit.

The Ott meters (figure 2.3) provide a point measurement of velocity based on the number of propeller revolutions within a given time interval. The number of revolutions is converted into a time averaged velocity measurement using tow tank calibration equations. The location of velocity measurement, or metering plane, depends on site specific characteristics. In the case of high-head plants, with long penstocks, the metering plane is located within the penstock, where the flow profile is fully-developed (Nguyen *et. al.*, 1991) . In these circumstances, the meters are located in fixed positions, appropriately distributed across the metering plane. At low-head plants, with short intake conduits, the metering plane is typically located at the intake stoplog guides. The advantage of locating the metering plane at the intake is it is possible to traverse the flow at the intake, rather than de-watering the unit and locating the current meters at fixed positions. The number of point velocity measurements required to ensure accurate integration of the velocity profile is dependent on the size of the conduit (Halas *et. al.*, 1991), provided that the velocity profile is fully-developed.

2.4 Performance Testing Codes

Four codes govern the performance testing of hydraulic turbines: the American Society of Mechanical Engineers (ASME PTC-18, 1992), the International Standards Organization

(ISO 3354, 1975), the International Electrotechnical Commission (IEC 41, 1991), and the German code (DIN, 1948) for hydraulic efficiency testing. These codes outline the procedures, limitations, and specifications to be met when conducting performance tests. The codes differ primarily with respect to the number, and distribution of velocity measurements, or metering points, used to sample the velocity profile.

All performance testing codes recommend that the intake velocity profile be measured at a location where the flow profile is fully-developed. If the velocity profile is measured in a penstock, the location of velocity measurement (*i.e.*, the metering plane), must be located a sufficient distance, both upstream and downstream, from any bends or changes in cross-section. These conditions are meant to ensure fully-developed flow exists; the velocity profile for fully-developed flow is represented by Von Karman's 1/n power law, shown in figure 2.4a. For low-head plants the metering plane is typically located at the emergency stop-log guides, where the flow profile is typically converging, and not fully-developed. A typical velocity profile for these non-ideal conditions is given in figure 2.4b. In this case flow modifications, such as bell-mouth nozzle, are necessary to obtain the required velocity profile. However such flow modifications are quite costly, and consequently, not implemented. As a result, the metering plane is often located where the velocity profile is much different from the idealized flow profile required by performance testing code. A brief outline of each of the performance testing codes as they apply to the velocity-area method of discharge measurement at a low-head plant follows.

2.4.1 *American Society of Mechanical Engineers (ASME PTC-18)*

For measurements in closed conduits, the ASME PTC-18 (1992) recommends an arrangement of at least 26 velocity measurements, and associated weights to represent the velocity profile. Figure 2.5 shows the arrangement of velocity measurements, as well as the weights associated with each measurement. The location of metering points, as well

as the weights assigned to each measurement is based on a log-linear method of integration and is contingent upon fully-developed turbulent flow.

Discharge using the log-linear integration method is calculated based on a weighted average of velocity measurements, *i.e.*,

$$\overline{V} = \frac{\sum k_i v_i}{\sum k_i} = \frac{\sum k_i v_i}{96}, \tag{2.3}$$

where k_i is the weight given in figure 2.6, v_i is the corresponding velocity, and $\overline{V}$ is the average weighted velocity.

Discharge is calculated by

$$Q = \overline{V} \cdot A, \tag{2.4}$$

where A is the area of the metering plane. The primary advantage of the ASME log-linear integration method is the relatively small number of velocity measurements required to estimate discharge.

2.4.2 *International Standards Organization (ISO 3354)*

The arrangement of point velocity estimates recommended by the ISO 3354 (1975) is based on the assumption of a velocity profile that can be represented by a mathematical relationship, *i.e.*, a 1/n power law for the velocity distribution in fully-developed, turbulent flow conditions. Based on this assumption, a minimum of 25 metering points, arranged in a 5x5 grid, is used to sample the velocity profile. ISO specifies arranging the velocity measurements in such a way that equal flow passes through each element, thereby placing the same importance on each measurement point. Discharge is calculated based on the product of velocity, times flow area.

2.4.3 International Electrotechnical Commission (IEC 41)

The IEC 41 (1991) states that if the metering plane is located so as to satisfy the assumption of fully-developed, turbulent flow, then the number and distribution of metering points need only be sufficient to adequately represent the flow profile. Given the flow conditions which prevail at low-head plants, the IEC does not advocate using the velocity-area technique to measure discharge. Provided that the requirement of uniform flow profile is upheld, the IEC recommends a minimum of 25 velocity measurements be used to estimate discharge. Should a non-uniform velocity profile exist, the number of metering points should be between $24\sqrt[3]{A}$ and $36\sqrt[3]{A}$, where A is the area of the metering plane in [m^2].

2.4.4 German Testing Code

The German code for hydraulic efficiency testing defines three representative elements (*i.e.*, interior, edge, and corner) within the metering plane. Discharge through an interior element is calculated by using the average of the four corner velocities, multiplied by the element area. Flow in proximity to a boundary (*i.e.*, an edge element) is calculated as

$$Q = \int_{y=0}^{H} \int_{x=0}^{W} \left[\frac{w}{x}\right]^{1/7} \cdot V_e \, dx \, dy, \tag{2.5}$$

which yields

$$Q = \frac{7}{8} W \cdot V_e \cdot H, \tag{2.6}$$

where W is the width of an element, H is the height of an element, and $V_e = (v_1 + v_2)/2$ is the average edge velocity; v_1 and v_2 are measured point velocities.

Discharge through a corner element is based on the formula for edge flow, expanded to account for the additional edge influence. The resulting form is given by

$$\frac{1}{2}Q = \int_{y=0}^{W} \int_{x=0}^{y \cdot W/H} \left[\frac{w}{x}\right]^{1/4} \cdot V_c \, dx \, dy, \tag{2.7}$$

which yields

$$Q = \frac{49}{60} H \cdot W \cdot V_c, \tag{2.8}$$

where V_c is the measured point velocity near the corner. The total discharge is computed from the summation of the discharge through all elements.

The German code recommends using between $20\sqrt[3]{A}$ and $40\sqrt[3]{A}$ metering points for a rectangular cross-section, where A is the area [m^2] of the intake. Table 2.1 shows the relative location of the metering points as a function of intake width. The vertical distribution of metering points is determined in the same manner as the horizontal distribution; *i.e.*, the vertical distribution of metering points is determined by simply setting M in table 2.1 equal to the height of the intake. The horizontal and vertical distribution of metering points defined by the German testing code is based on an ideal velocity profile described by a $1/n$ power law, where n varies from 7 to 10.

In addition to specifying the distribution of metering points to be used to represent the velocity profile, the German code stipulates a minimum horizontal spacing of at least one propeller diameter between any metering point and the flow boundaries, as well as between adjacent metering points. The space-frame truss used to traverse the intake velocity profile must also meet code specifications. In particular, the projected area of the apparatus used to traverse the intake may not exceed 2% of the gross metering area. The propeller must be mounted on support arms projected at least one meter (five propeller diameters from the main support of the truss. A minimum sample length of two minutes is required for each metering section.

Given the relatively high density of metering point required, the German code yields a relatively accurate estimate of discharge, even when the velocity profile is less than ideal. Mikhail (1992) has estimated the German method of computing discharge to be accurate to approximately 2%. It is, however, relatively labor intensive due to the high density of metering points required.

Table 2.1 German distribution of velocity measurements. M is the width of the intake in meters. x is the number of metering points.

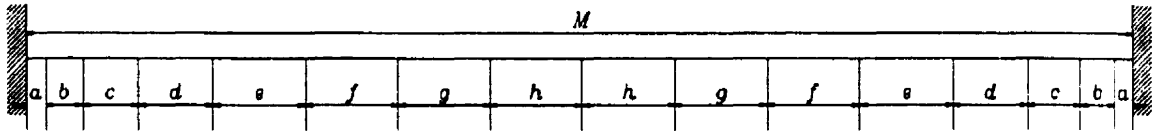

M	*0.6-3.5 m*	*3.0-5.5 m*	*5.0-8.0 m*	*7.5-10.5 m*	*10.0-12.0 m*	*11.5-15.0 m*
x	*5 by 8*	*7 by 8*	*9 by 10*	*11 by 12*	*13 by 14*	*14 by 15*
Size with respect to M						
a	1/10 to 1/20	1/30	1/35	1/45	1/50	1/60
b	3a	3a	2a	2a	2a	2a
c	6a	4a	4a	3a	3a	3a
d	-	6a	5a	4a	4a	4a
e	-	-	6a	6a	5a	5a
f	-	-	-	6a	5a	5a
g	-	-	-	-	5a	5a
h	-	-	-	-	-	5a

2.5 Performance Curves

In addition to discharge, head and power are recorded as part of performance test data. From the information collected through field performance tests, it is possible to determine the operating curves for turbine/generator units. Operating curves are based on

the relationship between efficiency, discharge, and head, or head, gate and power. Typically, a series of efficiency curves are generated for varying head conditions. The set of operating curves for a typical low-head turbine/generator unit are given in figure 2.6.

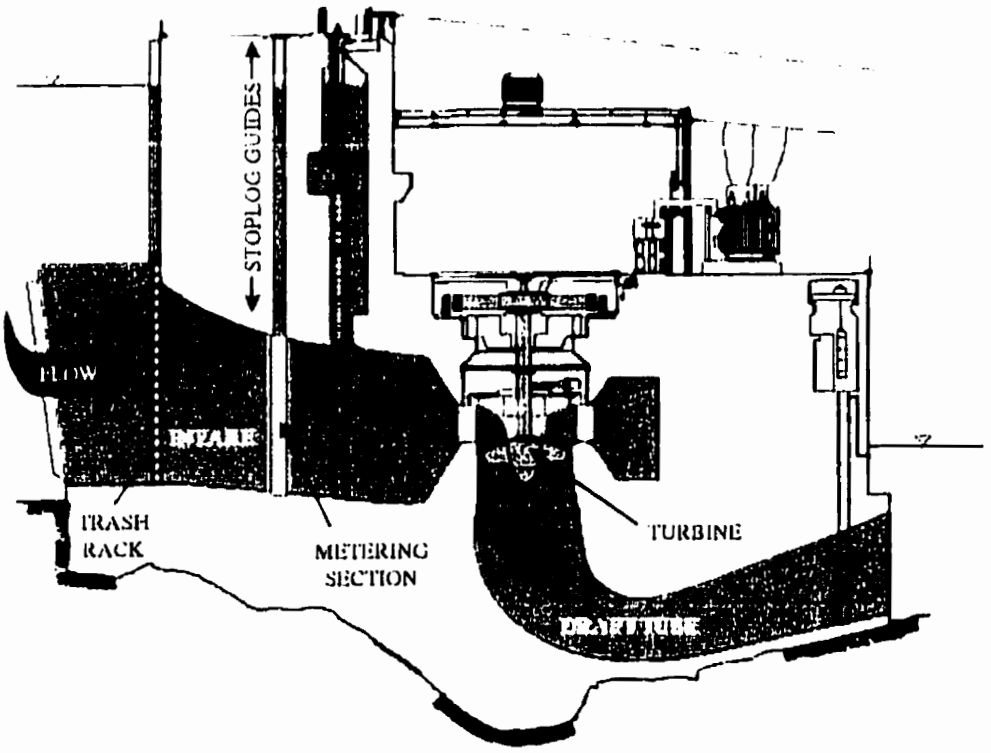

Figure 2.1. Cross-section of a low-head turbine unit. The difference between forebay and tailrace water surface elevations is gross head. The metering plane is located at the intake stop-log guides.

Figure 2.2. An aluminum space-frame truss is used for traversing the Ott meters across the intake. The meters are mounted on 1 m long support arms that are extended into the flow during data collection.

Figure 2.3. Ott type-A propellers used to collect velocity data. The meters provide a point estimate of velocity by recording the number of propeller revolutions. The number of revolutions is converted to a velocity based on calibration equations specific to each meter.

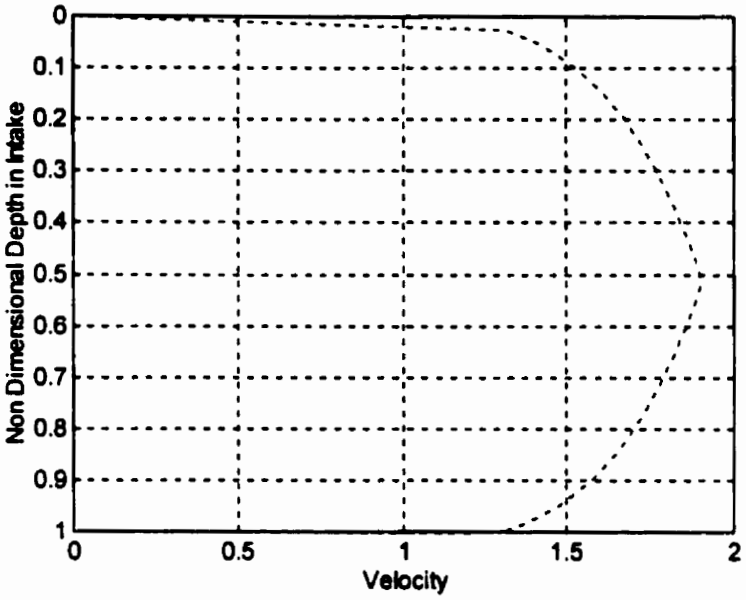

Figure 2.4 (a) Theoretical (idealized) velocity profile represented by Von Karman's power law for turbulent fully-developed pipe flow. The velocity profile is given by a 1/n power-law; in this figure n=7.

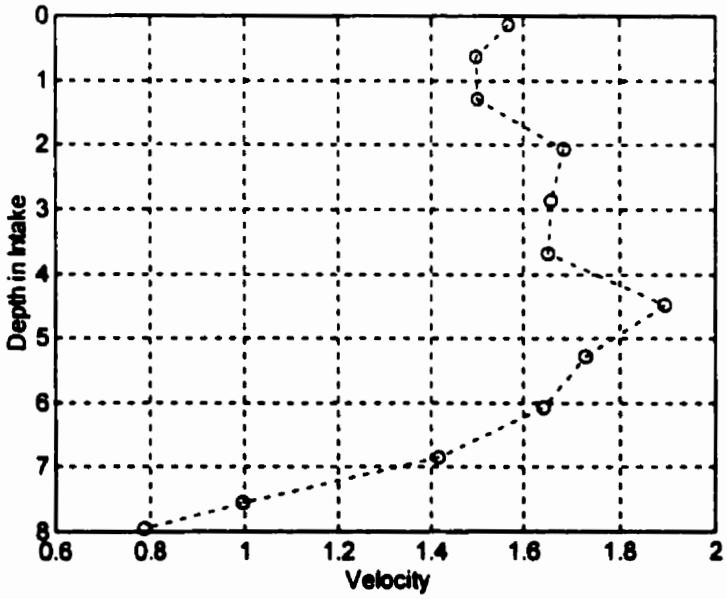

Figure 2.4 (b). The measured velocity profile shown above was obtained from the center-line of a vertical traverse at Pine Falls; unit 5, intake A. The test was conducted October 1989. Measured velocities are shown by 'o'.

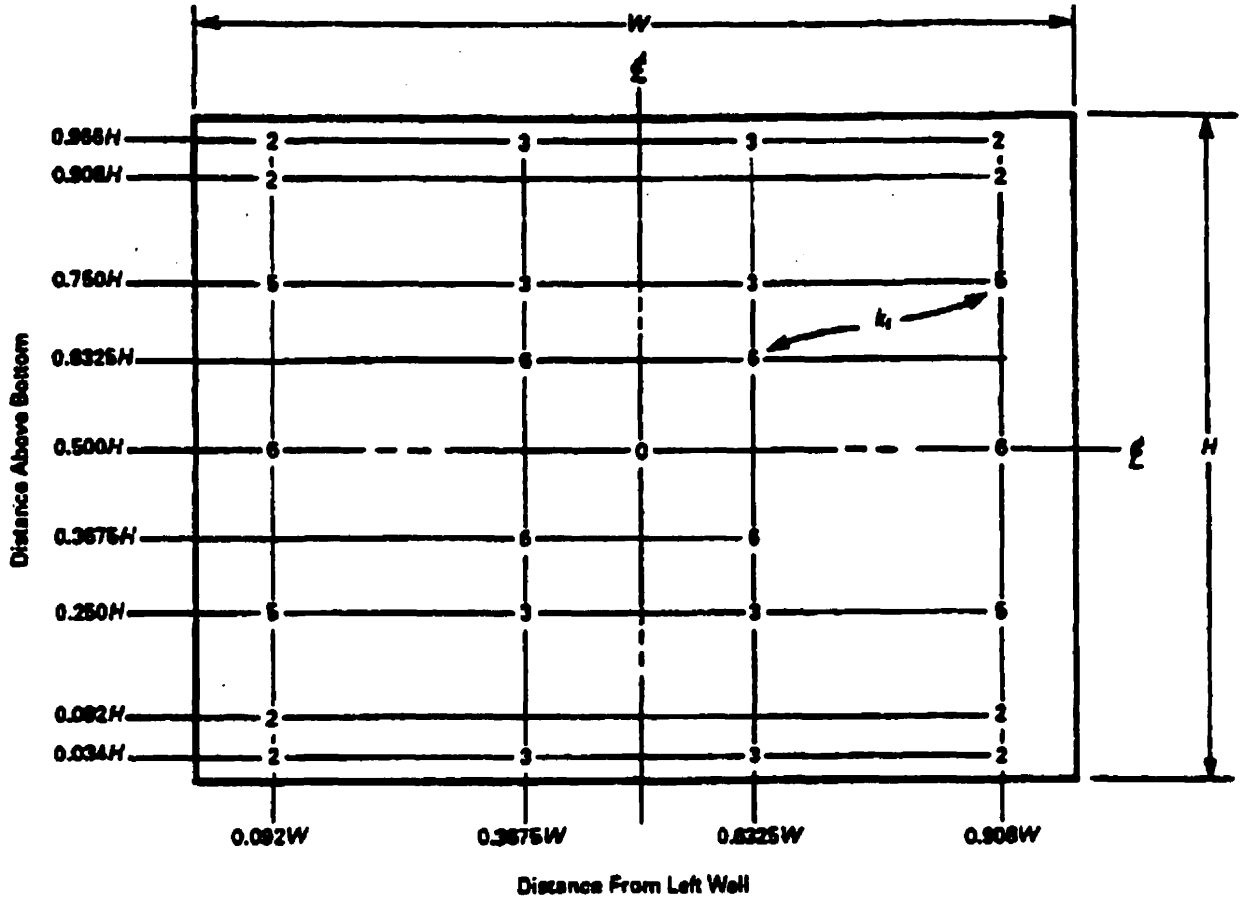

Figure 2.5. Distribution of velocity measurements and weights used in ASME log-linear method of discharge estiamtion. The weighting scheme tends to place more emphasis on velocity measurements through the (horizontal and vertical) center of the intake and less empahsis on those measurements in proximity to the flow boundaries.

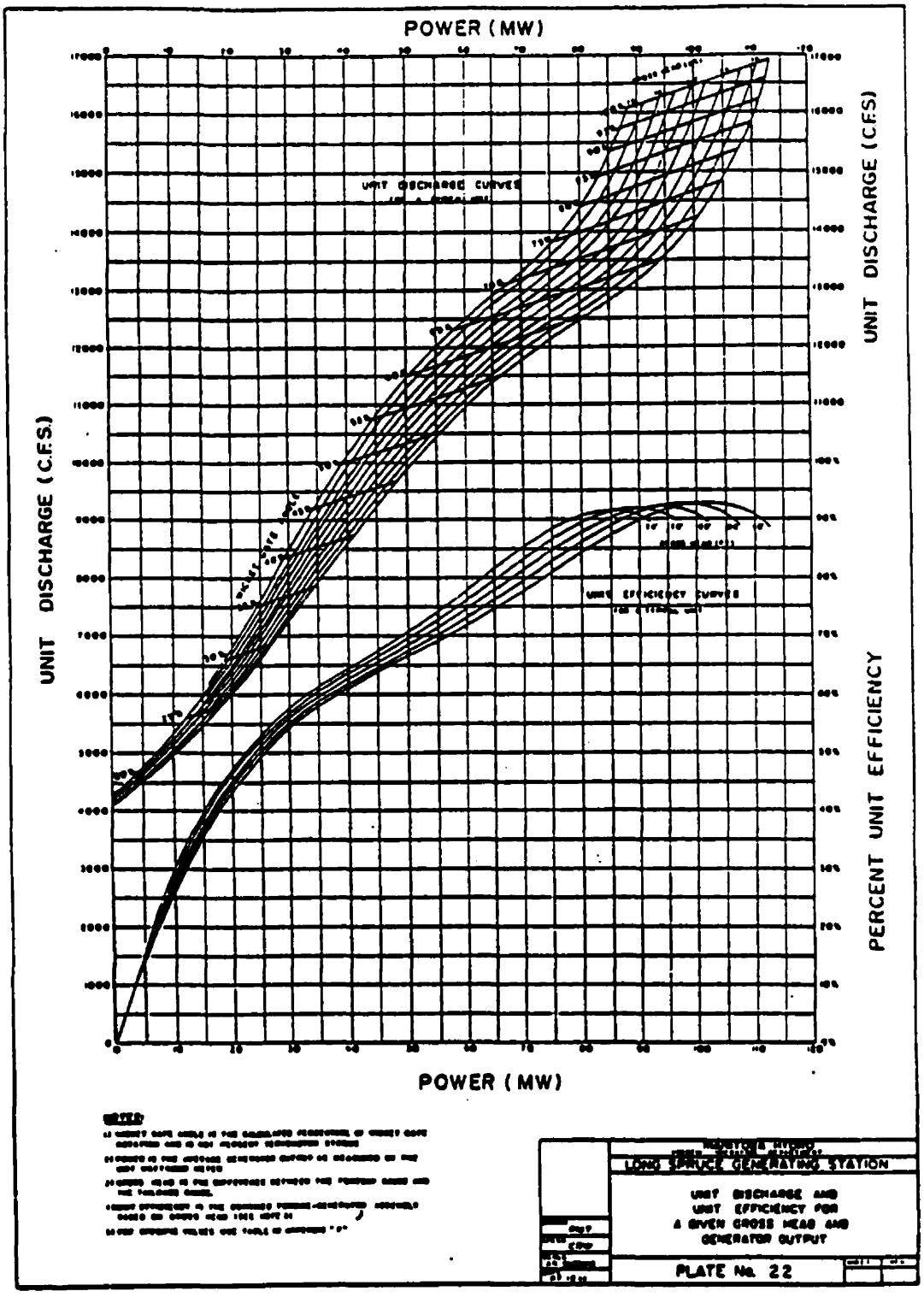

Figure 2.6. Operating curves for a typical low-head unit.

CHAPTER 3

A COMPARISON OF DISCHARGE ESTIMATES

3.1 Introduction

The codes for the performance testing of hydraulic turbines rely on a (theoretical) fully-developed flow profile to establish the distribution of metering points used in the velocity-area method of discharge estimation. Comparison of the theoretical and idealized profiles (Figures 2.4a and 2.4b) suggests that the two profiles are not commensurate. As the theoretical profile is used to determine the location of the velocity measurements, the discrepancy between these two profiles raises questions about the reliability and efficacy of positioning the metering points for low-head plants according to an unsatisfied idealized flow profile requriement.

If the assumed fully-developed flow condition is not satisfied, it may be advantageous to position the metering points to judiciously resolve the existent or anticipated velocity profile. A numerical technique well-suited to this task is the Gauss-Legendre quadrature integration method. This integration method requires functional values (*i.e.*, velocity) at non-uniformly spaced points in the plane of integration. The primary advantage of this method is a complex velocity profile can be very closely approximated with relatively few velocity measurements.

The primary objective of this chapter is to use a densely spaced array of metering points to compare estimates of discharge according to the ASME and German code based estimates of discharge. An alternative non-code based method of resolving and integrating the velocity profile using Gauss-Legendre quadrature integration is also considered. The discharge estimates computed using these methods are compared using data collected during turbine performance tests.

3.2 Code Specifications

Four codes govern the performance testing of hydraulic turbines, German, ASME, IEC, and ISO. The hydraulic testing codes that will be used in this analysis are the German and ASME codes as both specify the number and distribution of metering points to be used to sample the intake velocity profile. The IEC and ISO standards will not be considered in this analysis as they do not provide a specific distribution of metering points.

3.3 Gauss-Legendre Quadrature Method

Given the discrepancy between measured and theoretical velocity profiles, such as that shown in figures 2.4a and 2.4b, an alternative method of sampling the velocity profile which optimizes a fit to the actual velocity profile could improve the accuracy of computing discharge. As the velocity profile is not known *a priori*, the number of metering points should be commensurate with the anticipated, (or previously measured) profile. A numerical technique well-suited to this task is the Gauss-Legendre quadrature method of integration. This integration method requires functional values (in this case velocity) at non-uniformly spaced points in the plane of integration. The primary advantage of this method is the discharge of a complex velocity profile can be very closely approximated with relatively few measurements.

The acoustic method of discharge measurement applies a variant of the Gauss Legendre quadrature method of integration, known as Gauss-Jacobi for discharge measurement in a penstock, because of its accuracy and efficiency (Voser *et al.*, 1996; ASME, 1992). Voser *et al.* (1996) have shown that 8 acoustic paths (in 2 crossed planes) in fully-developed turbulent pipe flow can be used to measure discharge accurately (<1% error).

The Gauss-Legendre quadrature (hereinafter denoted GLQ) method exactly integrates a polynomial of order 2n-1 using n points. For an arbitrary velocity profile, $v(x)$, between spatial locations x_1 and x_2, the integral of the profile is given by

$$I = \int_{x_1}^{x_2} v(x)\,dx \tag{3.1}$$

For GLQ integration the integration limits are transformed from $x_1 \rightarrow x_2$ to $-1 \rightarrow +1$. The resulting integral is

$$I = \int_{-1}^{+1} f(x)\,dx \tag{3.2}$$

which may discretely expressed as

$$I = \sum_{0}^{n-1} w_i f(x_i) \tag{3.3}$$

where $f(x)$ denotes the transformed velocity profile. w_i is a Gauss-Legendre weight and n is the number of points to be used. The position of the (transformed) velocity measurements, $f(x_i)$, required for an n point GLQ integration, and the corresponding weights, w_i, are given in Table 3.1.

To determine the integral of a surface, for example, the discharge associated with a velocity profile through an intake, the function is simply integrated in one-dimension to reduce the problem to a line-integral, then integrated again to obtain the required value. Unlike the German and ASME codes, GLQ integration does not position the metering points according to an expected theoretical profile; rather, the metering points are located at the zeros of a Legendre polynomial.

Table 3.1 Gauss Quadrature Weights and Function Arguments for n Point Quadrature (from Chapra & Canale, 1988)

n	$f(x_i)$	w_i
4	± 0.861 136 312	0.347 854 845
	± 0.339 981 044	0.652 145 155
5	+ 0.000 000 000	0.568 888 889
	± 0.538 469 310	0.478 628 671
	± 0.906 179 846	0.236 926 885
6	± 0.238 619 186	0.467 913 935
	± 0.661 209 387	0.360 761 573
	± 0.932 469 514	0.171 324 492

3.4 Data

The data used in this analysis were collected during performance tests conducted at the Pine Falls Generating Station during October 12th to 24th, 1989. Pine Falls is part of the Manitoba Hydro system and is located on the Winnipeg River. It is a low-head plant (4 m) with six fixed blade turbines yielding a maximum production of 82 MW. Each unit has 3 intake openings measuring 4.4 m (wide) × 8.1 m (high).

Each intake trash rack was cleaned prior to testing. The turbines were tested one at a time. The performance tests were conducted in accordance with the German code for hydraulic efficiency testing. Propeller-type flow meters (figure 2.3) were mounted on a rigid support frame and traversed across the intake at the emergency stop log gains for various gate settings. Frames were traverse simultaneously across all three intakes when testing a given unit. The distribution of metering points is shown in figure 3.1. A 7 (horizontal) × 12 (vertical) grid of metering points was obtained for each intake with close spacing in the vicinity of the flow boundaries and fewer points through the center of

the intake where the velocity profile is assumed to be more uniform. The horizontal and vertical dimensions have been non-dimensionalized to show the relative location of the metering points in the intake and to indicate the horizontal and vertical symmetry of the metering point distribution. Estimates of velocity are based on two minute averages as delineated by German performance testing code. The testing of each unit (at a given gate setting) takes approximately one hour (12 metering levels at 2 minutes each, carriage traversing time, data acquisition start-up logging, *etc.*). During this time the conditions are monitored to ensure stationarity, *i.e.*, forebay and tailrace elevations are monitored during the course of a test.

Hydraulic performance testing was conducted for all six units. Testing was undertaken for turbine wicket gate settings of 40, 60, 70, 80, 85, 90 , 95, and 100 %. The data from all of the units were examined, however the analysis here focuses on unit 3 (a center unit) with relatively little velocity structure and unit 6 (an end unit) with considerable velocity structure.

3.4.1 Data Interpolation

The ASME log-linear and the Gauss quadrature integration techniques require velocity measurements at points close to, but not coincident with the measurements obtained at Pine Falls. In order to obtain the appropriate velocity measurements it was necessary to interpolate between the measured points. MATLAB™ algorithms were used to perform 2-D cubic spline interpolation on the measured velocity data. Cubic splines were used for the interpolation for several reasons. First, a cubic spline provides an exact fit to the data. Second, the use of cubic splines avoids the pitfalls of over-fitting the data with high-order polynomials. A cubic spline ensures that the slope (first derivative) and curvature (second derivative) are continuous at each of the measured points, thus providing a fit similar to that of a flexible curve. The 2D cubic spline interpolation was performed as follows. Cubic splines were fit to each of horizontal and vertical array of points. The resulting (unique) cubic splined surface provided a parametric description of

the intake velocity profile that could then be interpolated to the desired resolution to obtain velocity estimates at the required locations.

Figure 3.2a shows the velocity profile obtained from the 84 metering points while figure 3.2b shows the velocity profile resulting from the 2-D cubic spline interpolation. One of the primary visual differences between these figures is the points in figure 3.2a are connected by straight line segments while those in figure 3.2b are connected by cubic splines.

The interpolated velocity profiles through units 3 and 6 are shown in figures 3.3 and 3.4, respectively. These figures indicate the range in velocity structure that can occur. The flow through unit 3, intakes A, B, and C, is relatively uniform. The vertical structure in the flow is due, in part, to the large horizontal I-beams that support the trash rack. Unit 6, an end unit, has considerably more variation than center unit 3. As for unit 3, the vertical variation in the flow through unit 6 intake is due, in part, to the large horizontal I-beams supporting the trash rack. However, the intakes of unit 6 exhibit considerably more horizontal and vertical velocity structure than the unit 3 intakes. Since the trash racks were cleaned prior to testing the observed variation in velocity is not believed to be due to debris on the trash racks. The flow through the intakes of unit 6 are not atypical of the velocity structure observed at the intake of low-head hydroelectric plants. However, these time averaged velocity profiles are clearly a marked departure from fully-developed flow.

3.4.2 *Discharge Estimates*

The discharge was computed for each unit and for all 8 wicket gate settings using the German code, ASME code, and $n \times m$ point GLQ integration. Figure 3.5 shows the location of the 26 metering points required by ASME code relative to the 7×12 grid of metering points (based on the German code) measured during the performance testing at Pine Falls generating station. To fit the vertical structure observed for the three unit 3

intakes (figure 3.3) would require a minimum of an 8th order polynomial. Since an n point GLQ exactly integrates a polynomial of order $2n$-1, a minimum of 5 points are required in the horizontal direction. Allowing for comparable variation in the horizontal velocity structure, 4×5, 5×5, and 5×6 GLQ integrations were examined. Figures 3.6 a-c, show the location of the metering points required for a 4×5, 5×5, and 5×6 GLQ integration.

The locations of velocity measurements required to compute the discharge according to ASME code and an $n \times m$ point GLQ are all located within the array of metered points. Although it would have been interesting to investigate a denser array of GLQ points (*i.e.*, 6×6, 6×7, *etc.*) the measured data prohibited using more than a 5×5 GLQ integration, as the points required for a denser array lie outside of the measured array.

Table 3.3 provides a summary of the discharge estimates computed using the German, ASME, and $n \times m$ GLQ integration method. In addition, the volume under each splined surface was computed numerically to provide a reference time-averaged discharge, denoted Q_I; this should provide the most accurate estimate of the discharge through each intake and was therefore chosen as the reference. The relative error (expressed as a %age) associated with the various estimates of discharge is defined here as

$$relative\ error = \frac{Q_i - Q_R}{Q_R} \times 100\% \tag{3.4}$$

where Q_i denotes either the German, ASME, or $n \times m$ GLQ estimate of discharge, and Q_R is the reference discharge. Since the relative error can be positive (over-prediction) or negative (under-prediction), the standard deviation of the relative error was also computed to indicate the variation of the average relative error; this quantity is given in brackets following the average relative error.

An examination of table 3.2 indicates that German code consistently over-estimates the discharge for unit 3 by approximately 3.30(0.30)%, while the ASME code under-

estimates the discharge by approximately 1.38(0.72)%. The 4×5, 5×5, and 5×6 point GLQ integrations consistently over-estimate the discharge on average by 0.74(0.66)%, 0.52(0.61)% and 0.00(0.64)%, respectively. On average, the GLQ methods more closely approximate the reference discharge for unit 3 than ASME, and ASME more closely approximates the reference discharge than the German method.

The application of the German code to unit 6, which exhibits considerably more velocity structure than unit 3, yields an over-estimation of 1.55(1.23)% across all intakes and gate settings. The German code tends to over-estimate intakes A and B for all gate settings and yield a near zero relative error for intake C. The ASME estimates tend to under-predict the reference discharge. The 4×5 point GLQ integration under-predicts intakes A and C and over-predicts intake B; the reference discharge is under-predicted on average by 0.69(3.32)%. The 5×5 point GLQ integration under-predicts intake A and over predicts intakes B and C; it under-predicts the reference discharge by 0.17(2.17)% on average. Finally, the 5×6 point GLQ integration over-predicts intake A and under predicts intakes B and C; it over-predicts the reference discharge by 1.13(1.96)% on average.

A summary of the average relative errors for all units, across all intakes and gate setting, is given in Table 3.3. The general tendencies are well-defined. The German code over-predicts discharge (by about 3.09(0.96)% on average) while the ASME code under predicts discharge (by about 1.25(1.07)% on average) relative to the reference value; the ASME code yields estimates closer to the reference value. All three of the GLQ integration methods more closely approximate the reference discharge than the German code approach. This is an intriguing outcome as the German code uses 84 metering points while the GLQ methods use only 20 (4×5) to 30 (5×6) metering points. Comparing the ASME estimates with the 4×5 and 5×5 point GLQ integration indicates that the GLQ estimates tend to more closely approximate the reference discharge. That the GLQ integration approach tends to yield smaller relative errors is perhaps not

surprising. The German and ASME codes position the metering points to resolve a fully-developed flow profile that does not exist, while the GLQ method on the other hand positions the points of evaluation so as to resolve a complex velocity profile.

Table 3.3. Summary of average relative errors [%] for all units, across all intakes and gate settings at Pine Falls. The standard deviation [%] is given in brackets.

Unit	$\frac{(Q_{Germ}-Q_R)}{Q_R}$	$\frac{(Q_{ASME}-Q_R)}{Q_R}$	$\frac{(Q_{4x5}-Q_R)}{Q_R}$	$\frac{(Q_{5x5}-Q_R)}{Q_R}$	$\frac{(Q_{5x6}-Q_R)}{Q_R}$
1	3.71 (0.58)	-0.69 (1.17)	1.85 (1.04)	1.67 (1.08)	-0.19 (1.11)
2	3.39 (0.24)	-1.24 (0.92)	1.21 (0.42)	0.89 (0.40)	-0.11 (0.42)
3	3.30 (0.30)	-1.38 (0.72)	0.74 (0.66)	0.53 (0.61)	0.00 (0.64)
4	3.57 (0.59)	-0.62 (0.55)	1.23 (0.61)	0.94 (0.36)	0.19 (0.46)
5	3.03 (0.27)	-1.72 (0.79)	0.17 (0.69)	0.45 (0.73)	-0.28 (0.40)
6	1.55 (1.23)	-1.84 (1.43)	-0.69 (3.32)	0.17 (2.17)	-1.13 (1.96)
1 to 6	3.09 (0.96)	-1.25 (1.07)	0.75 (1.69)	0.78 (1.17)	-0.25 (1.07)

Table 3.2. Summary of discharge calculation estimates and relative errors.

Setting			Discharge Estimates (cms)						Relative Errors (%)				
Unit	Intake	Gate	Q_{ORS}	Q_{ASME}	Q_{Sc5}	Q_{Sc6}	Q_{Sc8}	Q_R	$(Q_{ORS}-Q_R)/Q_R$	$(Q_{ASME}-Q_R)/Q_R$	$(Q_{Sc5}-Q_R)/Q_R$	$(Q_{Sc6}-Q_R)/Q_R$	$(Q_{Sc8}-Q_R)/Q_R$
3	A	100	41.97	40.07	40.90	40.78	40.69	40.64	3.27	-1.39	0.65	0.35	0.13
3	B	100	49.41	46.81	48.10	48.09	48	48.18	2.57	-2.83	-0.16	-0.18	-0.36
3	C	100	54.76	52.31	53.84	53.55	52.84	53.11	3.11	-1.51	1.37	0.83	-0.51
3	A	95	40.89	39.07	40.03	39.89	39.56	39.58	3.30	-1.30	1.13	0.77	-0.06
3	B	95	48.76	46.24	47.36	47.36	47.53	47.30	3.10	-2.22	0.13	0.18	0.49
3	C	95	53.07	50.72	51.74	51.37	51.37	51.28	3.47	-1.10	0.89	0.17	0.17
3	A	90	40.29	38.36	39.31	39.17	39.02	39.06	3.15	-1.83	0.63	0.27	-0.11
3	B	90	47.29	44.93	45.79	45.9	46.09	45.86	3.12	-2.02	-0.15	0.09	0.51
3	C	90	53.46	50.96	52.55	52.16	51.65	51.76	3.25	-1.60	1.49	0.74	-0.25
3	A	85	38.94	37.23	37.94	37.85	37.76	37.74	3.18	-1.36	0.52	0.29	0.05
3	B	85	46.07	43.82	44.75	44.84	44.79	44.65	3.19	-1.86	0.23	0.43	0.32
3	C	85	50.32	47.99	48.70	48.34	48.86	48.50	3.74	-1.06	0.41	-0.34	0.74
3	A	80	37.60	35.89	36.72	36.57	36.42	36.43	3.24	-1.47	0.81	0.40	-0.01
3	B	80	44.20	41.94	42.98	42.97	43.01	42.87	3.12	-2.15	0.27	0.24	0.34
3	C	80	47.91	45.73	46.81	46.64	46.48	46.41	3.24	-1.45	0.87	0.50	0.16
3	A	70	34.29	32.74	33.40	33.31	33.26	33.22	3.23	-1.44	0.55	0.28	0.13
3	B	70	40.24	38.29	39.06	39.14	39.1	38.99	3.20	-1.79	0.18	0.38	0.28
3	C	70	44.37	42.48	43.35	43.2	43.01	42.87	3.49	-0.93	1.11	0.76	0.31
3	A	60	29.73	28.46	28.91	28.91	28.71	28.80	3.23	-1.20	0.37	0.37	-0.32
3	B	60	34.97	33.28	33.90	33.93	33.96	33.83	3.38	-1.61	0.22	0.30	0.39
3	C	60	40.32	38.50	39.45	39.32	39.07	38.96	3.51	-1.18	1.27	0.93	0.29
3	A	40	20.08	19.48	19.95	19.99	18.96	19.47	3.11	0.07	2.46	2.67	-2.62
3	B	40	24.15	23.17	23.36	23.41	23.34	23.29	3.69	-0.54	0.28	0.50	0.20
3	C	40	27.55	26.60	27.01	26.91	26.39	26.44	4.21	0.61	2.16	1.78	-0.19
								avg	3.30	-1.38	0.74	0.53	0.00
								std	0.30	0.72	0.66	0.61	0.64
6	A	100	43.52	40.88	40.89	41.72	43.25	42.64	2.07	-4.12	-4.11	-2.16	1.43
6	B	100	51.34	49.44	51.83	51.23	48.84	50.00	2.68	-1.12	3.66	2.46	-2.32
6	C	100	53.18	52.55	52.72	53.58	51.86	53.35	-0.31	-1.49	-1.17	0.44	-2.78
6	A	95	42.42	39.80	39.74	40.5	42.27	41.57	2.04	-4.27	-4.41	-2.58	1.68
6	B	95	49.92	48.05	50.33	49.8	47.49	48.58	2.76	-1.10	3.60	2.51	-2.24
6	C	95	51.71	51.39	51.23	52.22	50.38	51.79	-0.17	-0.78	-1.09	0.82	-2.73
6	A	90	41.12	38.63	38.43	39.17	41.06	40.29	2.05	-4.13	-4.62	-2.78	1.91
6	B	90	48.59	46.88	49.22	48.64	46.11	47.31	2.70	-0.90	4.03	2.81	-2.54
6	C	90	50.35	49.91	49.80	50.75	49.07	50.34	0.02	-0.86	-1.07	0.82	-2.52
6	A	85	40.29	37.76	38.19	38.59	39.76	39.58	1.79	-4.62	-3.52	-2.51	0.44
6	B	85	46.86	45.24	47.54	46.96	44.55	45.68	2.60	-0.95	4.08	2.85	-2.47
6	C	85	48.68	48.65	48.20	49.24	47.32	48.65	0.06	0.01	-0.92	1.22	-2.72
6	A	80	38.26	36.12	35.94	36.63	38.02	37.49	2.04	-3.65	-4.14	-2.30	1.41
6	B	80	45.00	43.48	45.38	44.9	42.84	43.79	2.76	-0.69	3.63	2.54	-2.17
6	C	80	46.92	46.62	46.62	47.37	45.7	46.69	0.07	-0.58	-0.57	1.03	-2.53
6	A	70	34.40	32.86	32.07	32.78	34.22	33.71	2.05	-2.53	-4.88	-2.77	1.50
6	B	70	40.92	39.79	41.06	40.8	38.88	39.90	2.56	-0.26	2.91	2.26	-2.55
6	C	70	42.45	41.67	42.18	42.79	41.43	42.63	-0.42	-2.24	-1.05	0.38	-2.81
6	A	60	30.24	28.79	28.15	28.78	30.11	29.61	2.15	-2.76	-4.92	-2.79	1.70
6	B	60	35.82	34.82	35.93	35.73	33.98	34.90	2.65	-0.21	2.97	2.39	-2.62
6	C	60	37.35	36.79	36.87	37.5	36.56	37.39	-0.11	-1.60	-1.40	0.29	-2.23
6	A	40	20.44	19.55	18.93	19.35	20.41	19.97	2.36	-2.14	-5.22	-3.12	2.18
6	B	40	23.90	23.09	23.78	23.64	22.81	23.26	2.74	-0.74	2.23	1.63	-1.94
6	C	40	24.61	23.99	24.46	24.76	24.04	24.60	0.02	-2.51	-0.58	0.64	-2.29
								avg	1.86	-1.84	-0.89	0.17	-1.13
								std	1.23	1.43	3.32	2.17	1.86

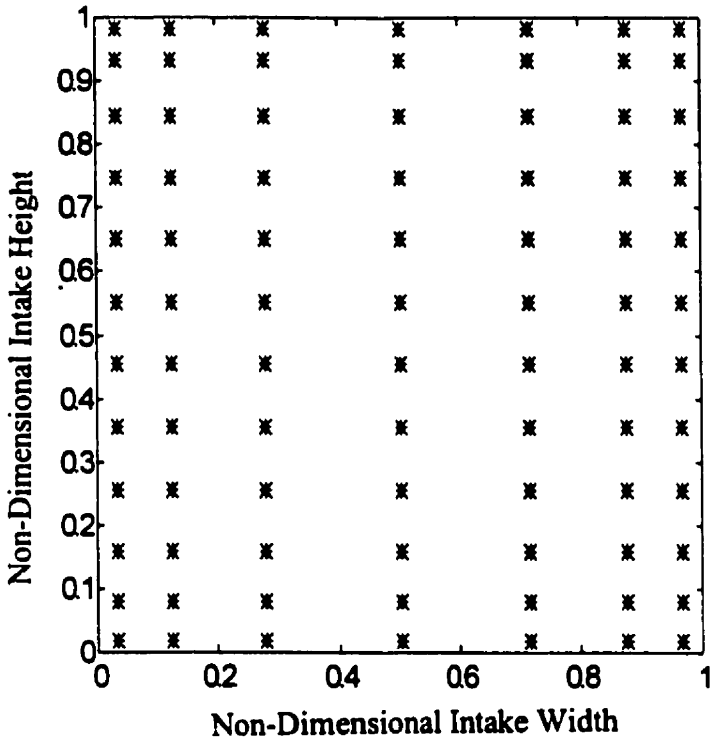

Figure 3.1. Distribution of metering points used to sample the intake velocity profile at Pine Falls Generating Station. The velocity measurements are arranged according to the German code-based distribution of velocity measurements.

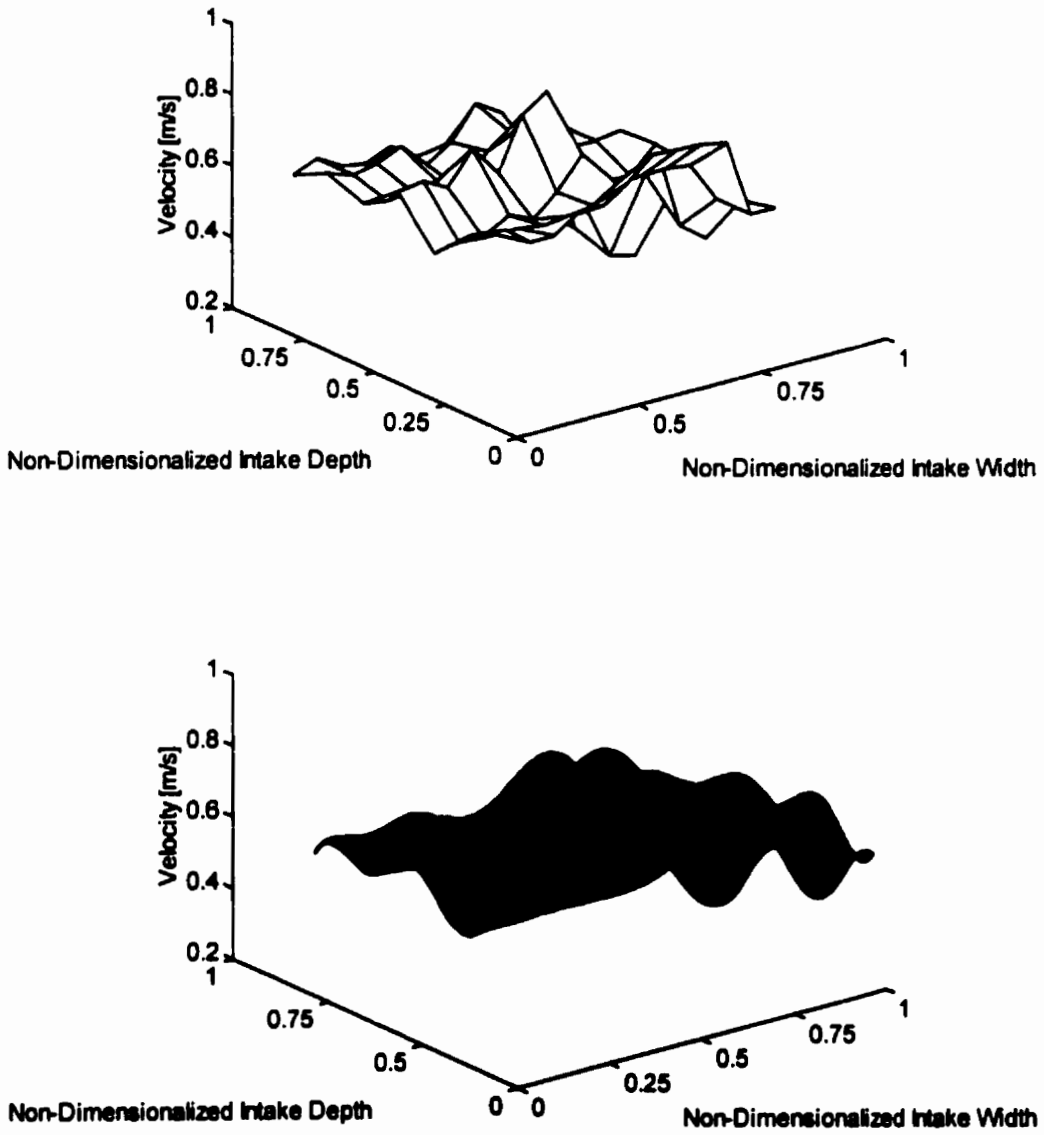

Figure 3.2 (a). Velocity profile obtained form 84 metering points. The measured points are connected by straight lines.Figure 3.2 (b). Interpolated splined surface shown in (a). The measured profile is from Pine Falls, Unit 5, intake A, 40% gate. The data was collected during October 1989 performance tests.

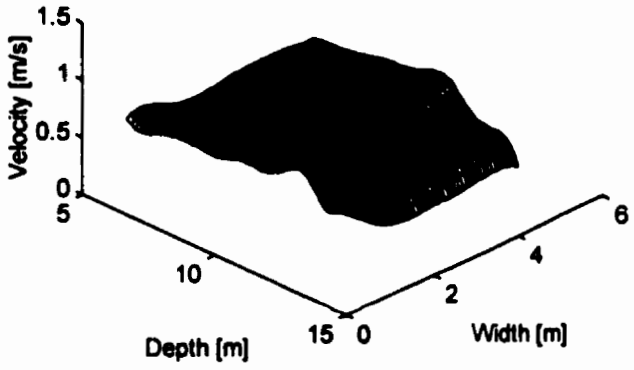

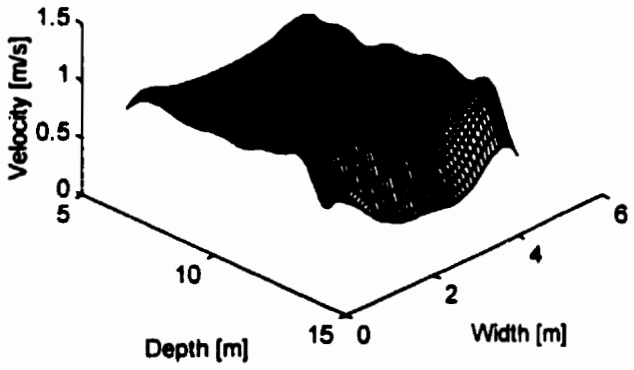

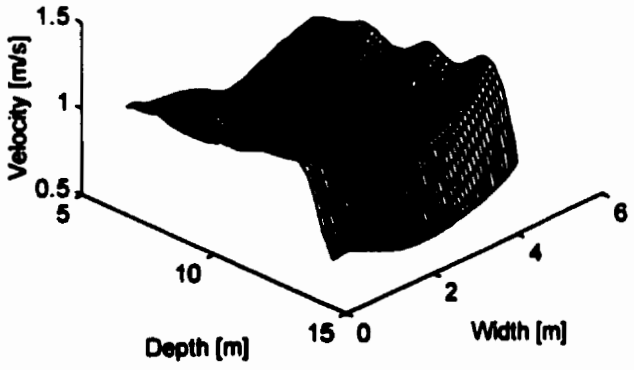

Figure 3.3 (a-c). Interpolated velocity profile for unit 3, intakes A, B, and C respectively, at 60% gate. Unit 3 is a center unit and exhibits a relatively uniform velocity profile.

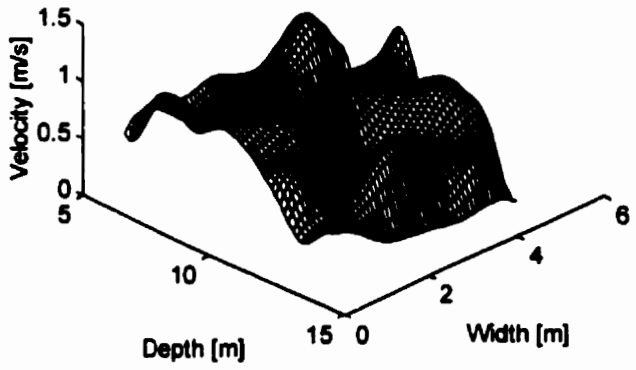

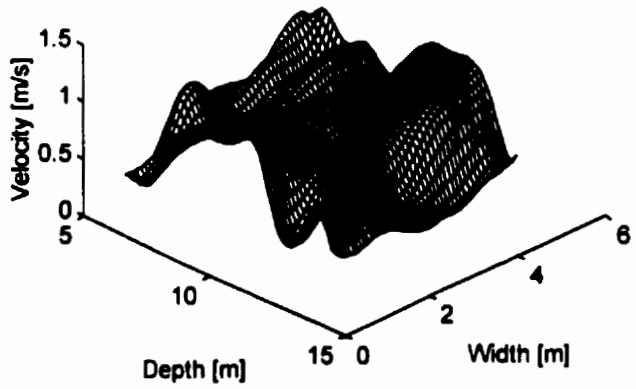

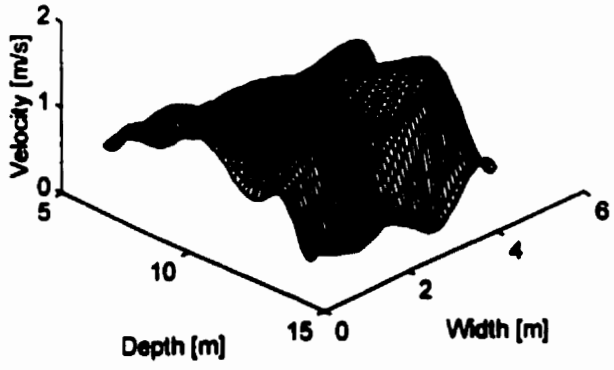

Figure 3.4 (a-c). Interpolated velocity profile for unit 6, intakes A, B, and C respectively. Unit 6 is an end unit that shows considerable velocity structure

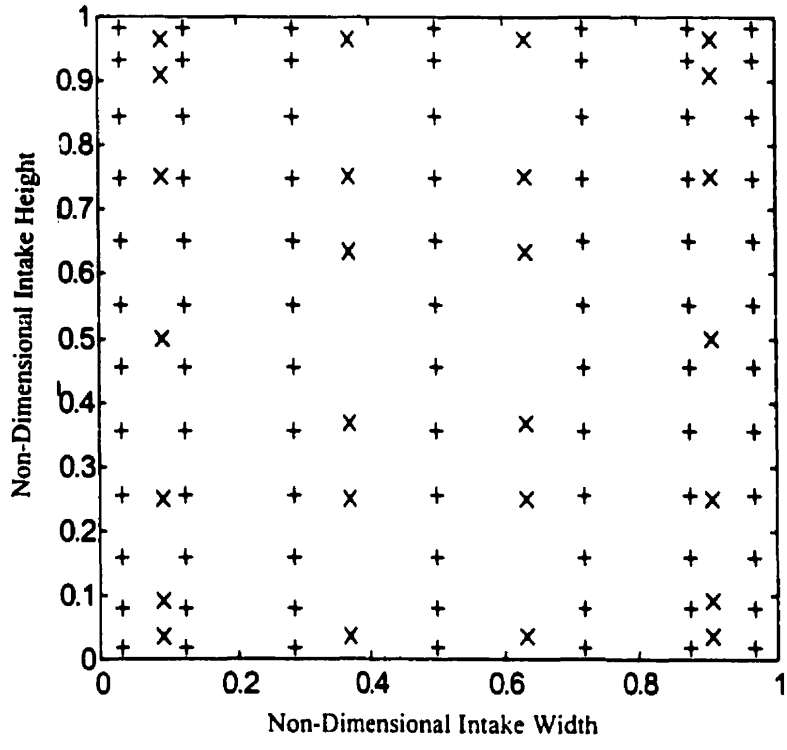

Figure 3.5. The location of the metering points required by ASME code relative to the 7x12 grid of metering (points based on German code) used for performance testing at Pine Falls Generating Station.

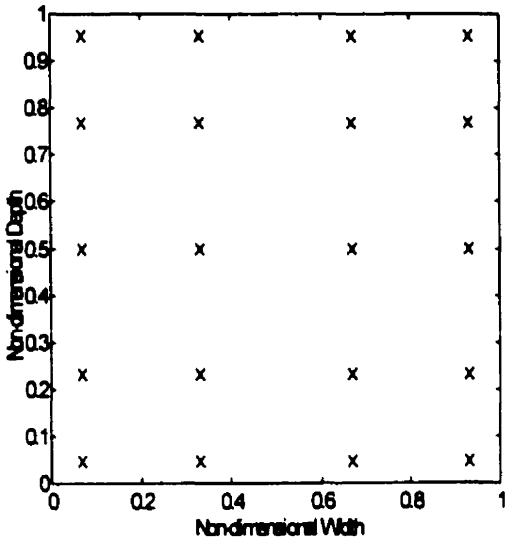

(a)

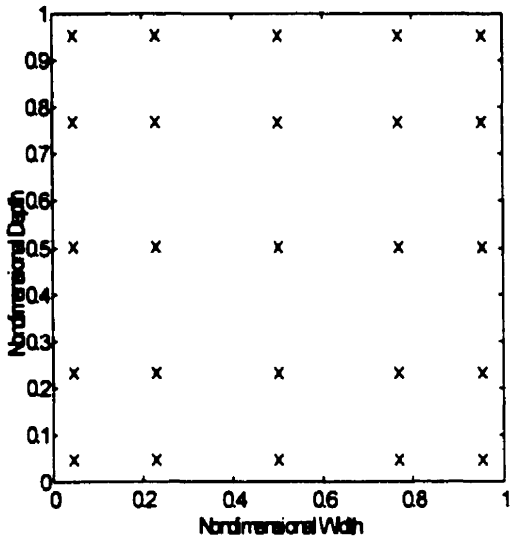

(b)

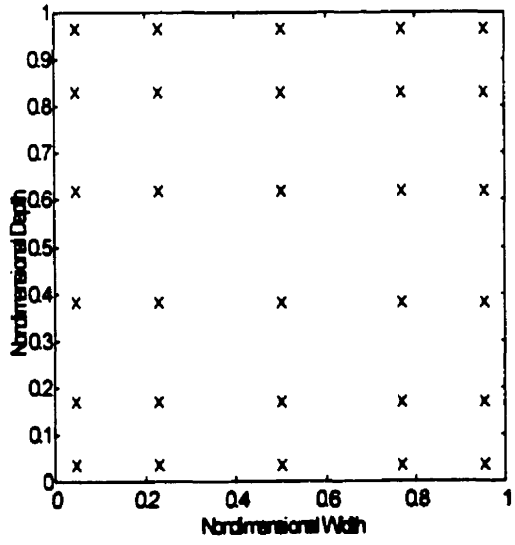

(c)

Figure 3.6 (a-c). Locations of metering points required for a 4x5, 5x5, and 5x6 GLQ respectively.

CHAPTER 4

LABORATORY TESTING

4.1 Introduction

The numerical analysis of the field data in chapter 3 suggests that Gauss-Legendre quadrature can provide more accurate estimates of discharge than either the German or ASME methods. This observation prompted a laboratory study to further investigate the findings of the analysis of the Pine Falls field data.

Testing in a laboratory environment offers a number of advantages; they are:

1. the ability to accurately measure the rate of flow volumetrically,
2. repeatability,
3. controlled conditions, and
4. range of testing conditions.

The discharge calculation methods will be tested under favorable and disturbed flow conditions over a range of discharges. By determining the accuracy of discharge estimates under a variety of flow conditions, it will be possible to evaluate the degree to which an unfavorable velocity profile influences the accuracy of a discharge estimate. Evaluation of the various sampling strategies will be based on a comparison of the discharge estimate to a reference discharge.

By "validating" a non-code based distribution of measurement points, it may be possible to obtain an accurate estimate of discharge while utilizing fewer velocity measurements. This would reduce the time required to complete a discharge measurement using the velocity-area method. Reducing the time to conduct tests would enable turbine units to return to normal operation more quickly, resulting in economic benefits.

4.2 Hydraulic Models

To undertake a laboratory investigation of the various method s of computing discharge at low-head plants, a 1/5 scale hydraulic model was used. Hydraulic models are based on a set of relationships which describe the similarities between a model and the prototype. Typically two forces predominate in a hydraulic system. When gravity and viscosity dominate, a Reynolds model is used. Reynolds models are used to model flows without a free surface. When gravity and inertia predominate a Froude model is used.

There are three types of model/prototype similarity: geometric, kinematic, and dynamic. Two objects are geometrically similar if the ratios of all corresponding length scales are equal. Geometric similitude can be expressed as

$$L_r = \frac{l_m}{l_p} \tag{4.1}$$

where l_m and l_p are the length dimensions of the model and prototype respectively, and L_r is the model scale factor. For a Froude model, the Froude number at any point in the flow is the same in the model and prototype (Sharp, 1984). The Froude number is given as

$$Fr = \frac{V}{\sqrt{gL}} \tag{4.2}$$

where V is velocity, g is acceleration due to gravity, and L is length. Therefore, it follows that

$$V_r = L_r^{1/2}. \tag{4.3}$$

where V_r is the model velocity scale. The time scale (T_r) follows from velocity which is length, divided by time,

$$T_r = L_r^{1/2}. \tag{4.4}$$

Discharge is given by

$$Q_r = L_r^{5/2}. \tag{4.5}$$

Geometric similarity is necessary to preserve the integrity of the velocity distribution. It is not, however, sufficient to guarantee full similarity between model and prototype.

From geometric and dynamic similarity follows kinematic similitude. Kinematic similitude ensures that the velocity, acceleration, and discharge are commensurate between model and prototype. It can be maintained if and only if the corresponding force ratios between the and prototype remain constant (Henderson, 1966).

In the case of a natural system such as a river, gravity is the predominant force. In this case a Froude model is used. Other forces may also exert influence over flow behavior *i.e.*, capillary, compression, and viscosity, represented by Weber, Cauchy, and Reynolds numbers respectively. Capillary effects require no consideration provided that model water depths are in excess of 25 mm. Compressibility effects are never significant in open channel flow models. Viscous effects are the most significant as these effects are exerted in a variety of situations. The only way to ensure that viscous effects can be neglected is to ensure that the Froude and Reynolds numbers are the same in the model and prototype. Alternatively, by maintaining sufficiently high Reynolds numbers, it is possible to neglect the effect of viscosity on the drag coefficient. As illustrated in figure 4.1, the relationship between drag coefficient (C_D) and R_e remains constant or independent of Reynolds number for turbulent flow.

4.3 Physical Model

The model used for this research is a 1:5 scale of an intake to a generating station. A schematic of the laboratory model is shown in figure 4.2. The area under investigation is at the intake stoplog guides (figure 4.2). This location is significant as it is the location of the metering plane used in the velocity-area method of discharge measurement.

The model scale factors for this model, derived according to equations (4.1) through (4.4) are given in Table 4.1.

Table 4.1. Model scale factors

Scale	Ratio (Model:Prototype)
Length (L_r)	0.200
Velocity ($L_r^{1/2}$)	0.447
Discharge ($L_r^{5/2}$)	0.018
Time ($L_r^{1/2}$)	0.447

4.4 Physical Characteristics

The water supply system in the HRTF consists of two low-head, high discharge pumps that pump water through a re-circulating system. Water is stored in a sump pit, from which it was pumped into a constant head tank. Flow was conveyed to the model through a 350 mm PVC pipe. The 60 and 75 hp pumps yield a total system capacity of approximately 500 l/s.

A timber flume and intake structure (figure 4.3) was used for the purposes of laboratory testing. The dimensions of the flume were 10.6 m long by 2.48 m wide by 1.60 m deep. The timber structure was made water-tight using a roller applied rubber lining (Vulkem 350).

The water supply entered the model through a supply pipe from the constant head tank. At the entrance to the flume the water supply passes through a 90° vertical elbow. Due to the vertical drop, the flow supply entering the model was highly turbulent. In order to mitigate the large scale turbulence present in the flow at the entrance, a flow straightener was fabricated. The straightener consisted of horizontally stacked 290 mm long by 76 mm diameter PVC pipes that were contained by 25 mm flattened expanded metal sheeting on both the upstream and downstream sides. Two layers of filter media were

attached to the upstream side of the straightener to further reduce large scale turbulence in the flow.

The intake area was located a distance of 3.32 m downstream of the flow straightener. Over this distance the flow was made to converge laterally from 1.60 m to 1.0 m. A trash rack was installed at the most upstream face of the intake structure, as shown in figure 4.4. The dimensions of the trash rack were 1.63 m (high) by 1.3 m (wide) by 50 mm (deep). Horizontal timbers 50 mm (high) by 1.3 m (wide) by 50 mm (deep) were cut to simulate the I-beams typical of trash rack design. Additional flow obstructions were attached to the trash racks to simulate the buildup of debris on the racks which would obstruct flow. These flow obstructions, the racks as well as the debris, were present only for a portion of the testing program. The metering plane was located 0.81 m downstream of the trash racks. The dimensions of the metering plane were 1.0 m by 1.0 m. The intake conduit extended 2.75 m downstream of the metering plane. Over this distance the conduit converged vertically to a height of 0.25 m. Downstream control of the flume was achieved by a motor driven sluice gate located a distance of 3.0 m downstream of the intake structure. From the sluice gate the flow was released to an exit chute and returned to the sump pit.

4.4.1 Velocity Measurement

Velocity measurements were made using an acoustic Doppler velocimeter (ADV). This device measures velocity using the back-scattering of an acoustic pulse in a control volume 6 mm in height and 5 mm in diameter, the center-line of which is 50 mm below the ADV transducer. The departure from the expected time of return is a function of water velocity, temperature and salinity. For the purpose of this study, water salinity was assumed to be negligible; temperature was recorded on an hourly basis, and at the beginning of each test. Due to the work done by the pumps on the water the temperature increased at a rate of approximately 1°C / hr, leveling off as the temperature approached 30°C; the rate of heat generated by pumping presumably balanced that lost to the surrounding environment.

4.4.2 Positioning System

A two-axis positioning system comprised of an aluminum frame, two lead-screws, two servo motors, an amplifier, and a motion controller was used to traverse the intake. The apparatus is shown in figure 4.5. The dimensions of the aluminum frame are 2.0 m by 0.076 m by 0.622 m; the inner portion of the frame is able to move horizontally while the entire apparatus moves vertically. Horizontal and vertical movement is on two lead screws with a pitch of 4 threads per 25 mm. A GALIL™ DMC-1020 two axis motion controller was used to control the servo motors. The DMC-1020 is a motion control card that uses a 32-bit microprocessor and has a 14-bit motor command output. Motion commands are specified using a DMC-specific programming language. Among the commands available to the DMC control card are relative and absolute positioning, speed and acceleration specifications, as well as error handling. Using the DMC motion commands it was possible to define absolute positions, program pauses to record velocity data, and control the speed of traverse.

To eliminate positioning errors, the x and y axes were manually returned to their zero (*i.e*, the most right-hand position for the x axis and the lowest position for the vertical axis) positions prior to starting each sampling strategy. The origin used for the intake was located at the bottom right-hand corner of the intake. All subsequent motions were relative to this position. The routines used for controlling the motion of the positioning system are included in Appendix B.

An ELECTRO-CRAFT BDC-25 mini-series amplifier was used to drive each servo motor. The amplifiers operate in current (torque) mode which produces a torque output from the motor proportional to the motor current. Two E-3626 brushless servo motors were used to move the lead screws.

4.4.3 Flow Measurement

The water supply to the model was measured by a MSR in-line MAGMETER (MAG) measuring device installed in the 350 mm water supply pipe. The MAG measures

discharge using the velocity reading at a single location within the pipe. Velocity is recorded using electromagnetic principles. For fully-developed, turbulent pipe flow the average velocity occurs at a distance of 11% of the pipe diameter from the pipe wall. Manufacturer recommendations specify that the MAG be installed at a distance both upstream and downstream from any flow disturbances, such as a bend. The MAG was installed 2.10 m upstream of the butterfly control valve, and 3.3 m (10 diameters) downstream of a 90° elbow. These distances exceed the manufacturer's recommendations to guarantee a uniform flow profile.

Discharge was recorded for the duration of each traverse. A time averaged value of the MAG record was used as the raw discharge value. The raw discharge was converted to a reference discharge using the calibration equation given in Appendix B.

4.5 Testing Schedule

The laboratory testing was undertaken at the Hydraulics Research and Testing Facility (HRTF) at the University of Manitoba. Since turbines are operated over a range of gate settings, it was necessary to evaluate the various discharge calculation techniques over a range of flow rates. Three discharges were selected, 175, 350, and 485 l/s. HRTF system capacity precluded testing at higher discharges. Both the 60 and 75 hp pumps were used for each of the three discharges although the capacity of the 60 hp pump would have been sufficient for the lowest discharge, both pumps were used for all tests.

In order to evaluate the effect of a less than ideal velocity profile on the accuracy of the various integration methods, flow disturbances were introduced to modify the velocity profile at the intake. A trash rack was fabricated, as shown in figure 4.4, and installed upstream of the metering plane. The velocity profile was measured following installation of the trash rack to evaluate the affect of a "clean" trash rack on the structure of the velocity profile. To simulate the existence of trash collection on the trash racks, additional flow obstructions were introduced as shown in figure 4.4. More "trash" was attached at the bottom of the racks as typically trash collects at the bottom of the intake.

The arrangements of metering points used to tests the integration techniques are given in figures 4.6a to 4.6g. Each sampling strategy was tested at three discharges, and at a favorable and disturbed flow condition. The testing schedule is given in table 4.2. A complete list of all runs is included in Appendix B as well as the exact locations of metering points. A total of 21 runs were made under favorable flow conditions. To test the repeatability of the testing approach, three realizations were made for each sampling strategy at 485 *l/s*. This resulted in a total of 35 runs conducted at the unfavorable flow conditon.

Table 4.2. Testing Schedule

Condition	*Flow*	*Integration Method*
Favorable	175 [l/s]	GLQ 2X2
Unfavorable	350 [l/s]	GLQ 3X3
	485 [l/s]	GLQ 4X4
		GLQ 5X5
		GLQ 6X6
		ASME
		German

A systematic approach was used when sampling the velocity profile to mitigate possible error that may be introduced through variable headwater or tailwater conditions and to ensure repeatability of test conditions. A constant headwater level was selected for all discharges. This level was controlled at the downstream end of the model using a vertical gate. The upstream water level was measured in relation to a benchmark set on the model. Once the discharge and corresponding tailgate settings were established the system was allowed to stabilize for 30 minutes. To further reduce sources of error and improve discharge comparisons, a single testing period was used for each discharge, *i.e.* all sampling strategies were tested consecutively, and in the same sequence for each discharge.

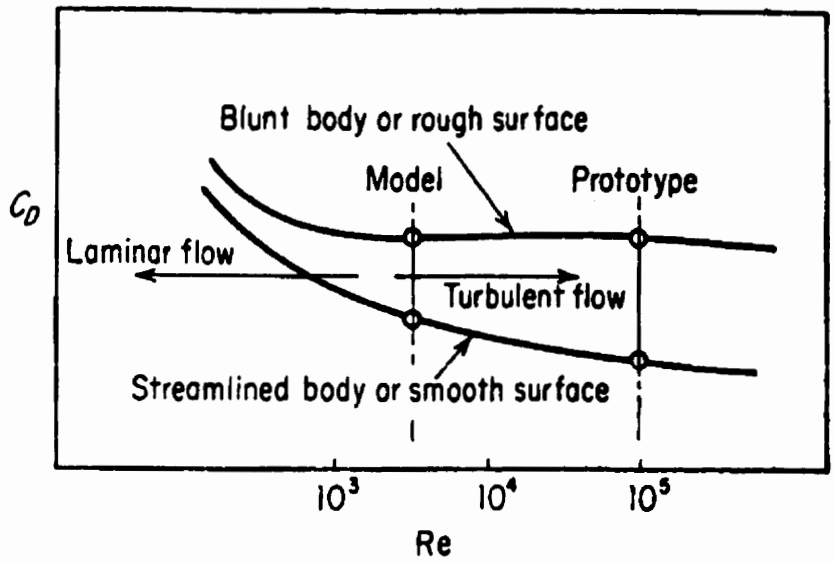

Figure 4.1. The relationship between drag coefficient (C_d) and Reynolds number (R_e). By maintaining sufficiently high R_e it is possible to neglect of viscosity on the drag coefficient (Henderson, 1966).

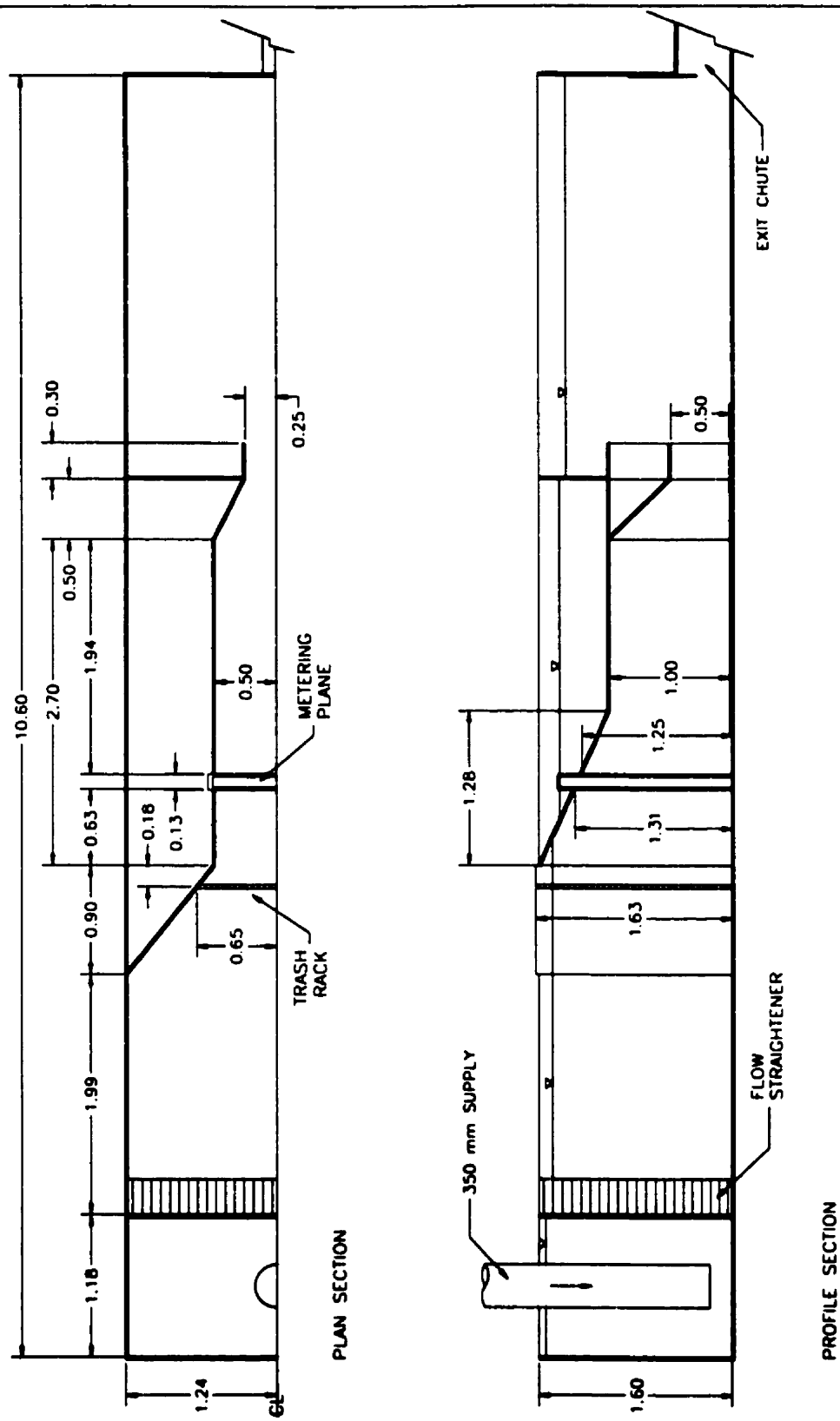

Figure 4.2. Schematic of the laboratory model. The specific area under investigation is at the metering plane.

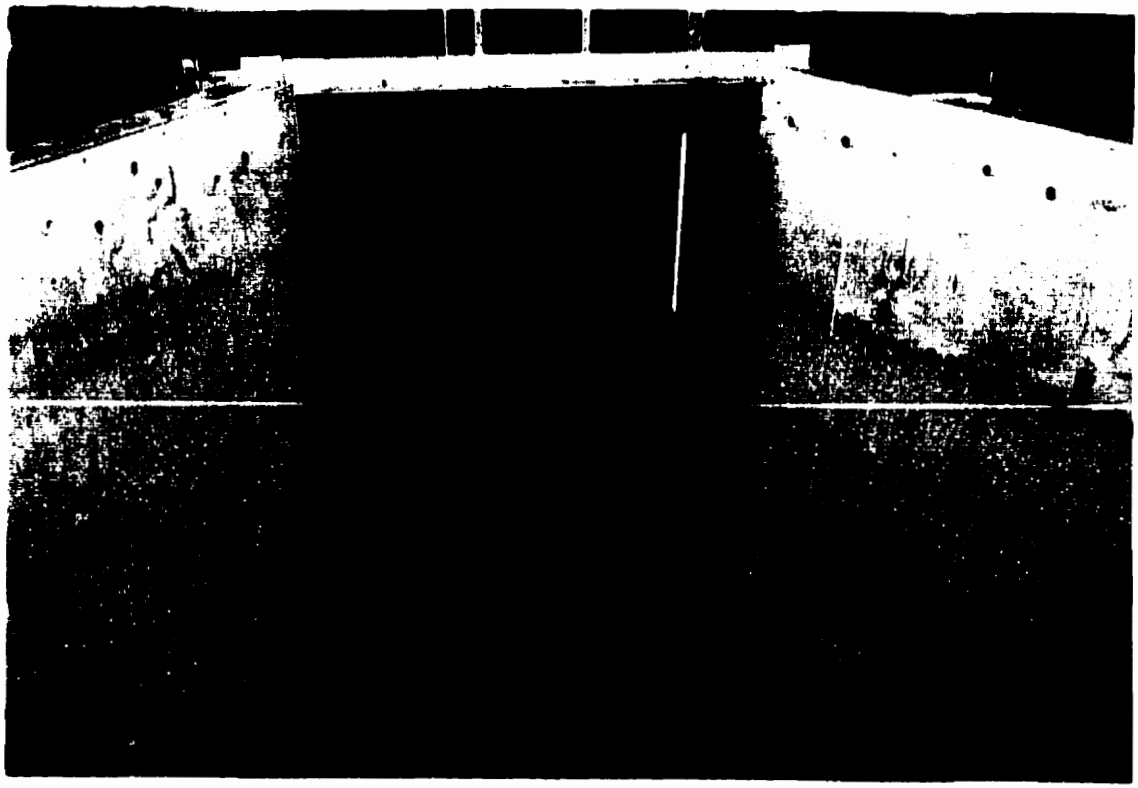

Figure 4.3. The timber flume and intake structure used for laboratory testing.

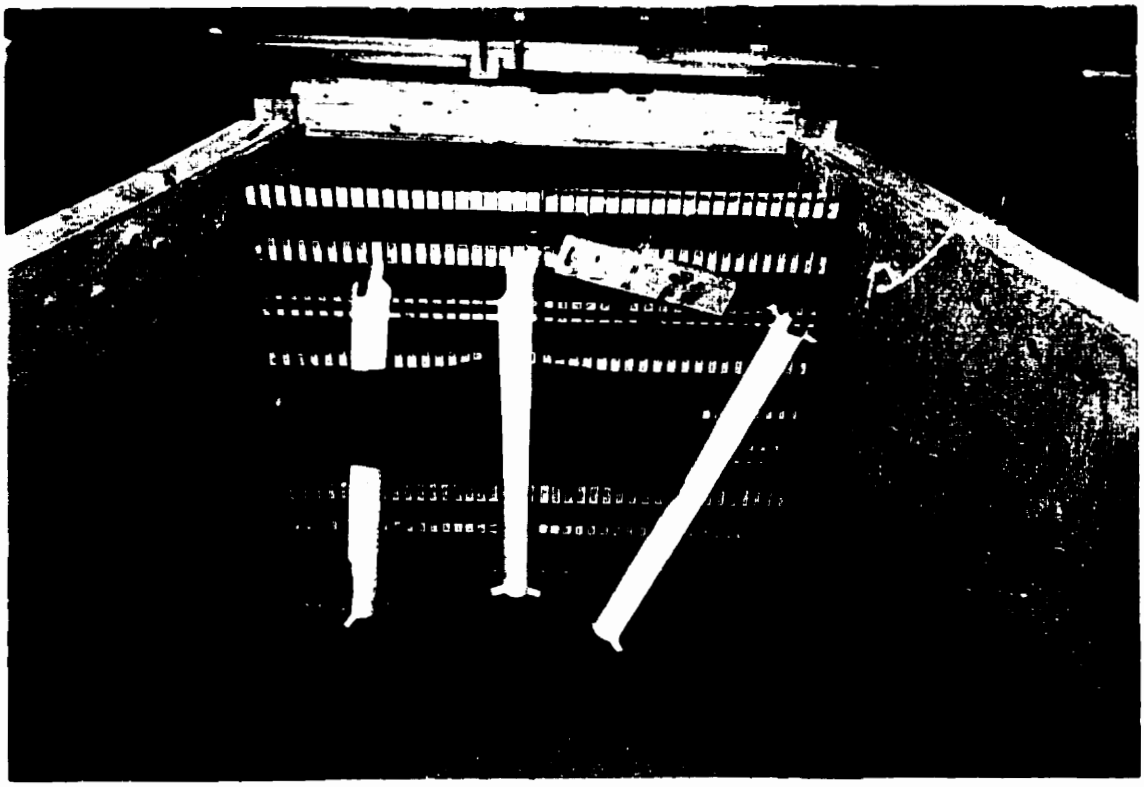

Figure 4.4. Trash rack (including debris) installed at the upstream face of the trash rack.

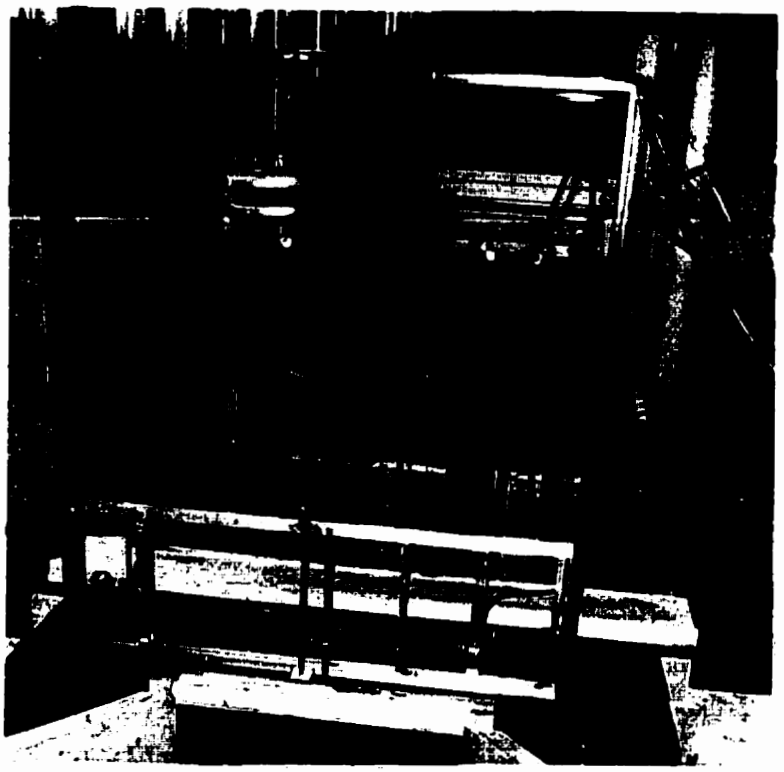

Figure 4.5. Aluminum apparatus and lead screws used to traverse the intake.

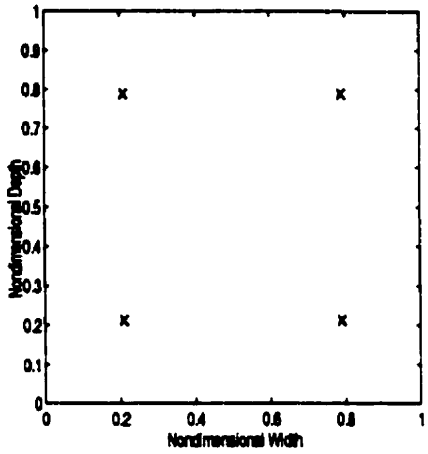
Nondimensional Depth
Nondimensional Width

(a)

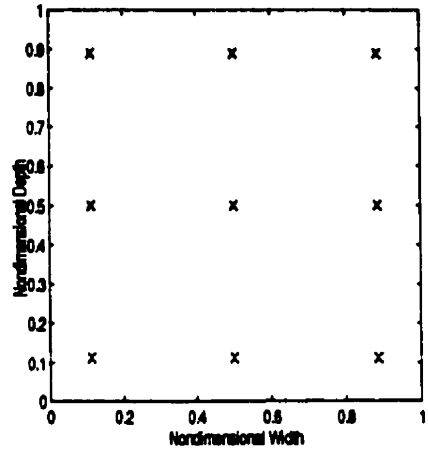
Nondimensional Depth
Nondimensional Width

(b)

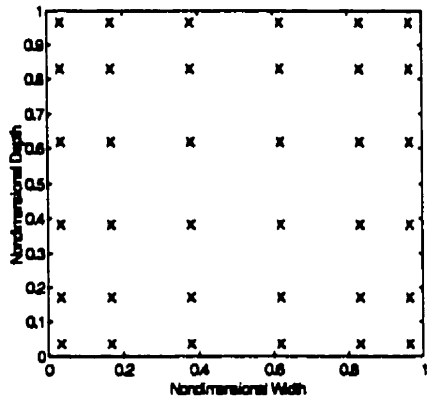
Nondimensional Depth
Nondimensional Width

(c)

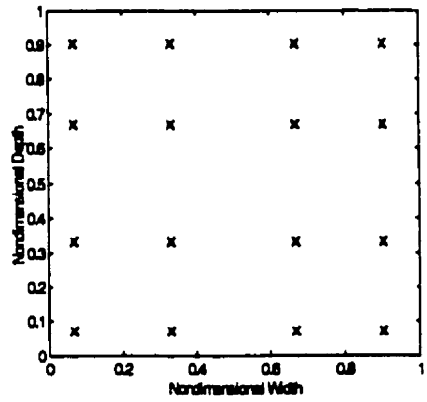
Nondimensional Depth
Nondimensional Width

(d)

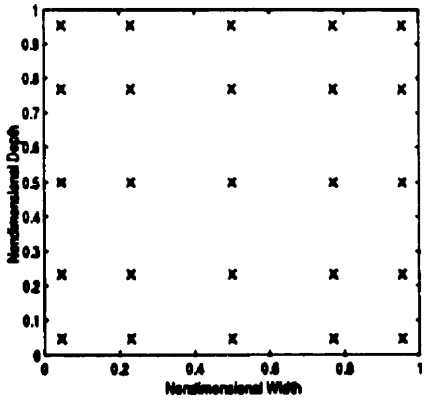
Nondimensional Depth
Nondimensional Width

(e)

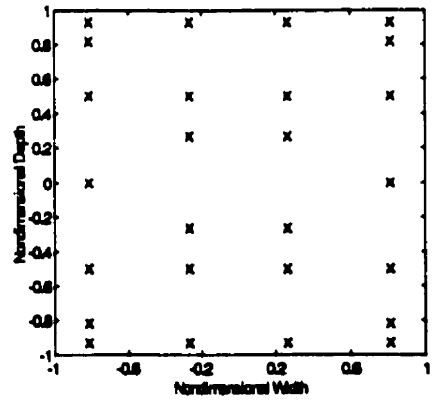
Nondimensional Depth
Nondimensional Width

(f)

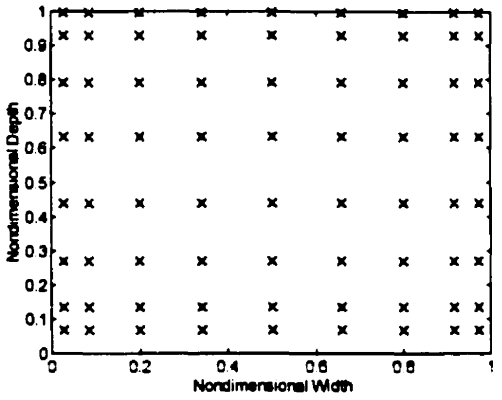

(g)

Figure 4.6. Distributions of metering points used to traverse the model intake stop-log guides. (a) GLQ 2x2; (b) GLQ 3x3 (c) GLQ 4x4 (d) GLQ 5x5 (e) GLQ 6x6 (f) ASME and (g) German.

CHAPTER 5

DATA POST-PROCESSING

It was necessary to process the raw data collected in the laboratory, prior to use in discharge calculations, and analysis. The following is an explanation of the data-post processing required for the velocity and discharge data.

5.1 Velocity Data

The method of collecting point estimates of velocity was to sample continuously at a position for two minutes, then traverse to the next position, and repeat. Velocity data was continuously collected, both while the ADV was in motion and stationary. It was therefore necessary to separate the traverse data from the stationary data set. A typical unfiltered velocity record is shown in figure 5.1. The data collected while the ADV was in motion is shown by o; velocity measurements recorded during the two minute sampling period are shown by +.

Two minutes of velocity data were collected at each position within the traverse. This sample length was chosen based on the hydraulic testing code recommendation of a two minute velocity sample at each position within the traverse. However, the model ratio is 1:5, therefore the ratio of the time scale is given by

$$T_r = L_r^{1/2} = \frac{t_m}{t_p} \qquad (5.1),$$

where T_r is the time scale and L_r is the length scale; t_m and t_p are the time intervals in the model and prototype, respectively. Then according to Froude scaling, the corresponding time period for collecting velocity data would be 54 seconds. Therefore, a 54 second window of velocity data was extracted from the 2 minute window. The average over the

54 second length was taken as the point velocity measurement. Once the grid of velocity estimates was obtained, the appropriate integration routines were applied and the calculated discharge was compared to the MAG reference discharge. The velocity records were processed using MATLAB script files (Appendix B).

5.2 Discharge Data

The MAGMETER was calibrated volumetrically to ensure the accuracy of the reference discharge used to evaluate the various integration schemes. The method of calibration, as well as the results, are included in Gawne (1997). Based on the results of the calibration the following equation was derived

$$Q_{ref} = 8.694 + 1.106 Q_{mraw} \tag{5.2}$$

where Q_{ref} is the MAG reference discharge and Q_{mraw} is the raw MAG data [l/s] (Gawne, 1997). Figure 5.2 shows a typical plot of MAG data. The variability in discharge value can be attributed to the turbulence in the pipe. A time averaged value of the MAG data was used as the reference discharge. A separate MAG file was collected for each sampling strategy to increase the accuracy of the reference discharge.

5.2.1 MAG Reference Discharge Error

The sources of error in discharge measurement are a combination of calibration error and instrument error. In the case of calibration, the sources of error are:

Volumetric tank volume calculation and calibration error of water level gauge (± 0.14%)

Leakage due to switch plate (± 0.66%) for 300 l/s

Stopwatch timing with 0.1 second scale (± 0.07%) contributes to error in discharge measurement

Random timing error combined with float gauge reading error (± 0.09%)

Water level error (± 0.53%) yields a total random error of ± 0.66%

The instrument error consists of calibration error (systematic) and the random instrumentation error. The systematic error in the MAG reading was estimated to be ± 1.0% by the manufacturer. For the purposes of calculation, this error was subdivided into ± 0.5% random and ± 0.5% systematic.

5.2.2 *Velocity Measurement Error*

Acoustic Doppler velocimetry uses the travel-time of an acoustic pulse to measure water velocity along an acoustic path. The propogation time of an acoustic pulse is a function of temperature, salinity, and pressure. Clay and Medwin (1977) provide an empirical relationship for the speed of sound in water given by

$$\begin{aligned} c_{emp} &= 1449.2 + 4.6T - 0.055T^2 + 0.00029T^3 \\ &\quad +(1.34 - 0.010T)(S-35) + 0.016z \end{aligned} \tag{5.3}$$

where c_{emp} is the empirical estimate of the speed of sound in water [m/s]; T is temperature [°C], S is salinity [ppt] and z is depth [m]. Based on this empirical relationship, a 0.05 °C error in temperature measurement would result in a 0.009 % in the (empirical) value of c. This error in sound speed results in a velocity measurement error of 0.02 %.

5.2.3 *Positioning Error*

The maximum allowable positioning error for the DMC motion controller was set to 1000 quadrature counts, or 1.3 mm in both the vertical and horizontal directions. As the dimensions of the intake are 1.0 m by 1.3 m, a positioning error of 1000 quadrature counts translates into 0.0012 % in the horizontal and 0.001 % in the vertical. Two types of motion are possible with the DMC programming, relative and absolute positioning. In the case of relative position movements, each position is relative to the previous, consequently positioning errors are accumulated. Absolute positions are relative to the defined origin. Absolute positioning was favored because it eliminated cumulative errors in position.

In the case of a significant positioning error, the weights applied in the Gauss-Legendre quadrature and the ASME integration schemes would not be accurate. Similarly the dimensions of the flow elements used in the German integration method would require modification. The positioning system was periodically interrogated using the TP (tell position) command to determine the typical positioning error. It was found that during the course of a traverse, the error was on the order of 100 quadrature counts (0.13 mm) As this positioning error is negligible, it was assumed to have no effect on the integration methods used to calculate discharge.

5.2.4 *Geometric Error*

Any error in intake measurement contributes directly to a discharge calculation error, therefore, four measurements were made of the intake height at equally spaced intervals across the intake width. Similarly, four measurements were made of the intake width at equally spaced intervals over the intake height. The estimated measurement error was 0.5 cm , or 0.5 %.

5.3 Error Calculations

Combining the errors introduced by the MAG discharge measurement, the velocity measurement error contributed by the ADV, as well as positioning errors introduced by the positioning system. The total error is calculated by

$$MSE = \frac{\sum_{i=1}^{n} e_i^2}{n} \tag{5.4}$$

where MSE is the mean squared error, e_i is the % error, n is the number of error sources; the outcome is ± 0.155 %.

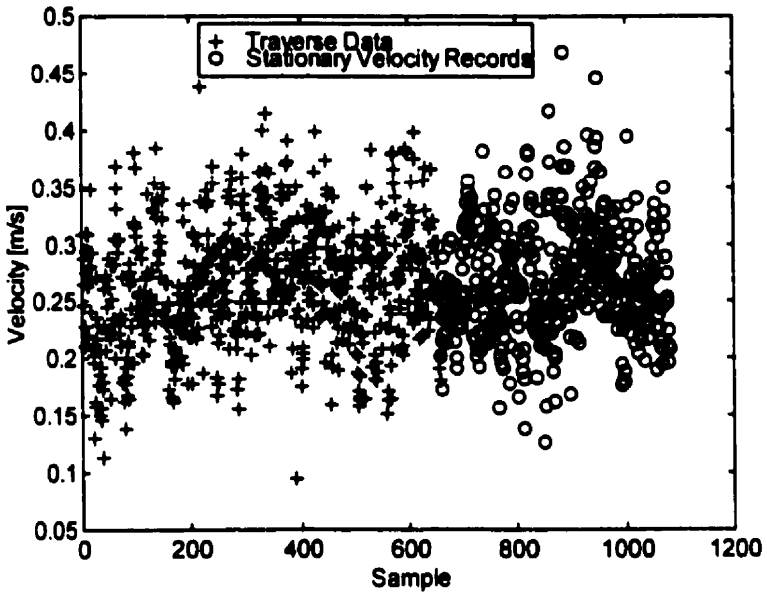

Figure 5.1: Unfiltered ADV record.

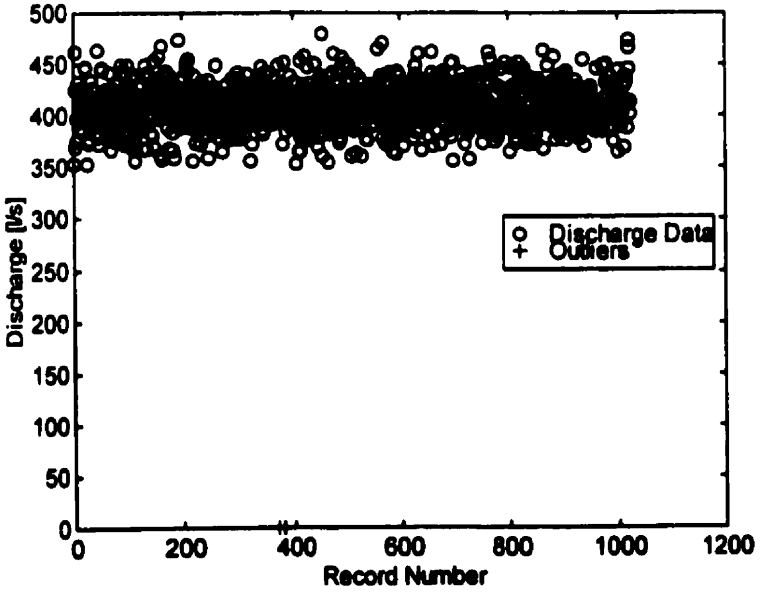

Figure 5.2 Typical plot of magmeter discharge data.

CHAPTER 6

LABORATORY RESULTS

Seven sampling strategies were tested under both favorable and disturbed flow conditions. Three discharges, 175, 350, and 485 l/s, were used to simulate the variation in turbine operating levels, *i.e.*, gate settings. The sampling strategies were evaluated based on the accuracy of the respective discharge measurement relative to the MAG reference discharge. To establish repeatability, three independent tests were conducted at a discharge of 485 *l/s* under unfavorable flow conditions. This discharge was chosen as the influence of the flow obstructions would be most pronounced at the highest discharge.

6.1 Favorable Flow Conditions

The objective of evaluating the favorable flow condition was to observe the relative change in accuracy of discharge estimate following the introduction of flow disturbance. Figure 6.1 shows the intake velocity profile for the favorable flow condition at 485 l/s. This velocity profile is based on the German sampling strategy (72 velocity measurements). This intake velocity profile is generally representative of a smoothly varying velocity profile with uniformity through the center and more variability in proximity to the boundaries. The unusually low velocities in the lower left hand corner of the intake (figure 6.1) it may be due to the intake geometry.

Investigation of the centerline velocity profile (figure 6.2) reveals the existence of variability that is not representative of fully-developed, turbulent flow. It is, however, similar in shape to the centerline velocity profile observed at low-head plants (refer to Chapter 3). Lower velocities are observed at the top of the intake and increases with depth. The observed high velocities in proximity to the bottom flow boundary may be due, in part, to the geometry of the flume at the flow entrance. The velocity profile in proximity to the top flow boundary is more representative of fully-developed flow. In this region the velocity increases with distance from the top flow boundary.

Discharge was calculated using the German, ASME, and Gauss-Legendre quadrature methods. The resulting discharge estimates are shown in table 6.1. The error associated with each estimate was calculated by

$$Error = \frac{Q_{calc} - Q_{ref}}{Q_{ref}} \times 100 \qquad (6.1)$$

where Q_{calc} is the calculated discharge based on an intake traverse, Q_{ref} is the MAG reference discharge [l/s].

Table 6.1: Summary of discharge estimates for undisturbed flow condition. The error of each discharge estimate from the reference discharge is given in ( ).

Sampling Distribution	Nominal Reference Discharge [*l/s*]		
	165 [l/s] (E %)	385 [l/s] (E %)	485 [l/s] (E %)
GLQ 2x2	176.4 (7.23)	371 (8.51)	491 (7.96)
GLQ 3x3	170.4 (2.95)	354 (3.29)	469.3 (3.21)
GLQ 4x4	168.3 (1.96)	349.9 (1.30)	469.5 (3.07)
GLQ 5x5	163 (-1.13)	343.6 (-0.57)	460.8 (1.12)
ASME	151.97 (-8.43)	321.62 (-6.44)	425.36 (-7.39)
GLQ 6x6	152.5 (-7.97)	326.2 (-4.95)	433.5 (-5.51)
German	171.6 (3.11)	360.4 (-0.03)	478.9 (4.64)

6.1.1 Gauss Legendre Quadrature

The relative accuracy of the Gauss-Legendre discharge estimate increased with the number of points used to sample the velocity profile. The 2x2 point Gauss-Legendre (GLQ 2x2) over-estimated the reference discharge on average by 7.7% and was the least accurate, while the 5x5 point yielded an estimate with an accuracy of approximately 0.04%. Contrary to the trend, however, was the estimate made by the 6x6 point Gauss-Legendre integration that underestimated Q_{ref} by approximately 5%. The accuracy of

this estimate was unexpectedly low given the number of velocity measurements. As well, the GLQ 6x6 consistently under-estimates discharge. These observations suggest that some of the GLQ 6x6 points were in areas of uncharacteristically low velocity. An explanation for the decrease in the accuracy of discharge estimate could be the proximity of the 6x6 point measurement to the flow boundaries, which are regions of high shear. In the prototype conditions the problem of edge effects may not subsist as the outermost measurement points for a GLQ 6x6 would not be in such close proximity to the boundaries.

Comparison of the velocity profiles obtained by the GLQ 5x5 and GLQ 6x6 as shown in figures 6.3 a and b, respectively, suggests that the 6x6 point GLQ strategy, while using more velocity measurements to estimate discharge, is subject to higher shear zones due to proximity to the flow boundaries; this may influence the accuracy of discharge estimation. This may have been due to an over-fitting of the velocity profile by a high order GLQ.

6.1.2 German

The discharge estimate obtained using the German code-based distribution of 72 velocity measurements is approximately 4 % greater than Q_{ref}, and is comparable to the accuracy of the GLQ 3x3 estimate which uses 9 points. Given the density of metering points used for the German discharge estimate, the accuracy is lower than anticipated. As in the case of the GLQ 6x6, the proximity of the outermost metering points to the flow boundaries may have influenced the discharge estimate at these locations.

6.1.3 ASME

The 26 point log-linear method of discharge estimation yields the least accurate estimate of discharge, underestimating Q_{REF} (on average) by 7.42 %. This result suggests that the log-linear arrangement of metering points does not adequately sample a complex, non developed velocity profile. Although the proximity of the outermost velocity measurements is higher than in prototype conditions, these results suggest that the

Although the GLQ 5x5 uses one less metering point than the ASME, the relative accuracy of discharge estimate is higher. Figure 6.4 shows the position of the 26 ASME points relative to the GLQ 5x5 sampling strategy. Although the vertical positions are similar throughout the traverse, the horizontal positions are consistently different. Through the center (horizontal) of the intake, the GLQ points lie between the ASME; the outermost GLQ points are in closer proximity to the flow boundaries in the vertical direction.

6.2 Disturbed Flow Condition

The intake velocity profile that resulted from introducing the trash-rack disturbance (figure 4.4) is shown in figure 6.5. This profile is based on the German distribution of velocity measurements. Clearly this profile cannot be well represented by a $1/n$-power law. It is however, representative of the variability present at the intake of many low-head turbine units (refer to Chapter 3). The results of the velocity-area discharge calculations are given in Table 6.2.

Table 6.2. Summary of discharge estimates for disturbed flow condition.

Sampling Distribution	Nominal Reference Discharge [*l/s*]				
	165 [l/s]	350 [l/s]	485 [l/s]		
GLQ 2x2	183.1(4.79)	361.1 (6.71)	461.1 (1.74)	470.8 (4.46)	485.3 (4.63)
GLQ 3x3	165.4 (-4.85)	344.2 (1.98)	462.2 (1.77)	459.3 (-0.37)	456.4 (1.12)
GLQ 4x4	180.4 (3.51)	348 (3.09)	462 (1.65)	464.5 (2.75)	471.2 (2.49)
GLQ 5x5	172.4 (-1.08)	344.7 (1.82)	461.9 (1.49)	450.1 (0.74)	451.2 (1.35)
ASME	169.91 (-2.73)	339.82 (0.84)	459.42 (0.76)	475.2 (-0.38)	469.8 (0.41)
GLQ 6x6	160.2 (-8.05)	325.1 (-3.29)	436.4 (-4.28)	432.7 (-5.21)	428.1 (-4.26)
German	180.5 (3.24)	356 (4.93)	474.3 (3.54)	479.7 (3.91)	477.6 (4.13)

6.2.1 Gauss-Legendre Quadrature

As was the case in the favorable flow conditions, the GLQ 5x5 integration yielded accurate results, on average 1% higher than the reference discharge. The trend observed for the GLQ distributions in the ideal flow case held for the disturbed flow condition with the accuracy of discharge estimate increasing with the higher order approximations. These results suggest that the GLQ integration schemes can provide an accurate and efficient means of estimating discharge.

6.2.2 German

The German code-based discharge estimate yields a discharge that over-estimates Q_{REF} by approximately 4.3%. The error in discharge estimate may be attributed, in part, to the proximity of the outermost velocity estimates to the flow boundaries where large shear occur. In field conditions the outermost velocity measurements are taken at a distance of at least one propeller diameter from the boundary; this distance is meant to ensure that the propeller is capable of recording accurate velocities.

In prototype conditions the proximity of velocity measurement to the flow boundary was not limited by instrument accuracy as the ADV uses a 6 mm by 5 mm control volume for velocity measurement. However, the converging intake geometry, combined with the effect of the flow obstruction resulted in a highly variable velocity profile, particularly in the vicinity of the flow boundaries. This variability was most pronounced at the bottom flow boundary, specifically at the corner where position 72 of the German distribution was located. Analysis of the velocity profile obtained by the German distribution of metering points (figure 6.5) shows a region of high shear in this corner of the intake.

The discharge estimates obtained by the German method obtained in the disturbed-flow condition are comparable to the results of the favorable flow condition. Of note is the accuracy of the lower order GLQ discharge estimates which are of greater or at least comparable accuracy to the German code-based estimate. Once again, the results suggest that the distribution of metering points is more important than the number of velocity measurements used to sample the velocity profile.

6.2.3 ASME

Although the ASME log-linear integration method uses one more velocity sample than GLQ 5x5, the accuracy of the discharge estimates are not comparable. These results suggest that the log-linear distribution of velocity estimates does not sufficiently sample the flow profile when the flow conditions are less than ideal. The measurements in proximity to the flow boundaries are made in areas of high shear, and particularly low velocity, more weight may be given to velocity measurements which are not representative of the flow profile, thereby resulting in an underestimated discharge. Although the ASME does not advocate application of the log-linear method where non-ideal flow conditions exist, the results of this analysis demonstrate the sensitivity of the log-linear integration method to a flow profile different from that, which is idealized.

The errors associated with the various sampling strategies are shown in figure 6.6. The sampling strategies are plotted in increasing number of velocity samples. From this graph it is possible to observe the trend of increasing estimate accuracy with increasing density of velocity estimates, although this trend does not persist beyond the GLQ 5x5 strategy. Based on the results of the favorable flow condition, the GLQ 5x5 provides the most accurate estimate of discharge. The observed trend suggests that the accuracy of discharge estimate does not necessarily increase with increasing density of velocity measurements. The results of this analysis are congruous with the findings of numerical Chapter 3, and suggest that it is the distribution, rather than the number of metering points which is central to accurate discharge estimation.

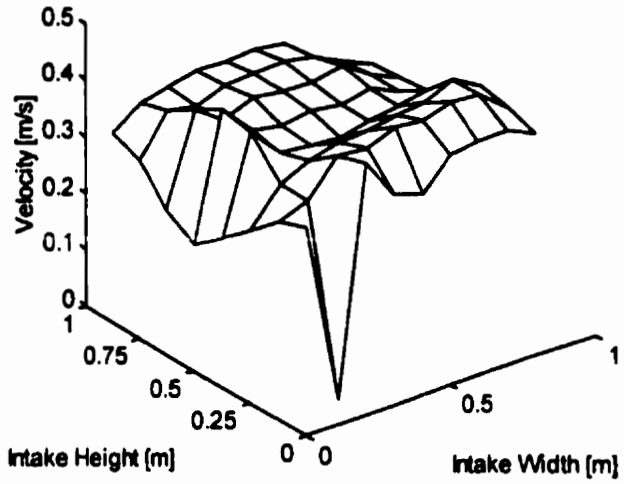

Figure 6.1. Intake velocity profile for favorable flow profile using the German distribution of velocity measurements (Q=485 l/s).

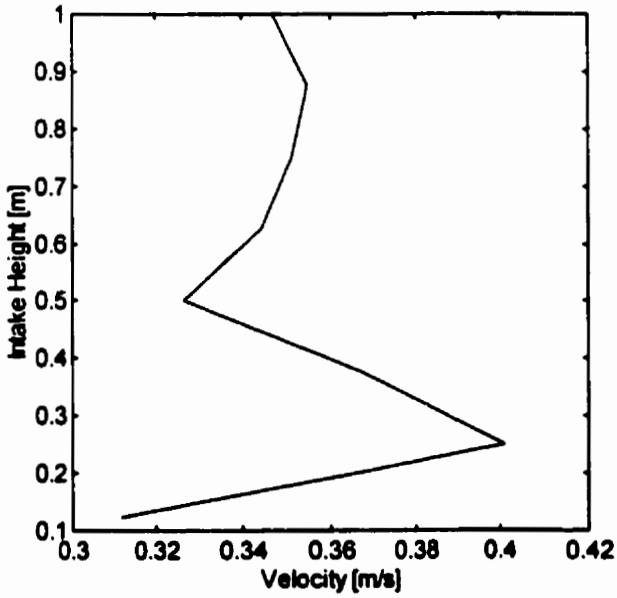

Figure 6.2. Centerline velocity profile obtained from German distribution of measurements shown in 6.1. (Q=485 l/s).

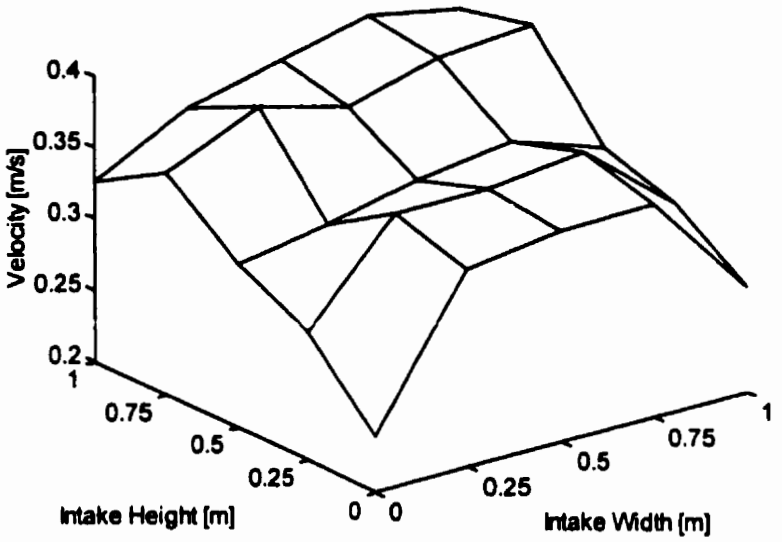

Figure 6.3 (a). Intake velocity profile for Q=485 [l/s]. The velocity measurements were obtained from a 5x5 Gauss-Legendre quadrature sampling strategy. The origin is at the bottom left corner of the intake.

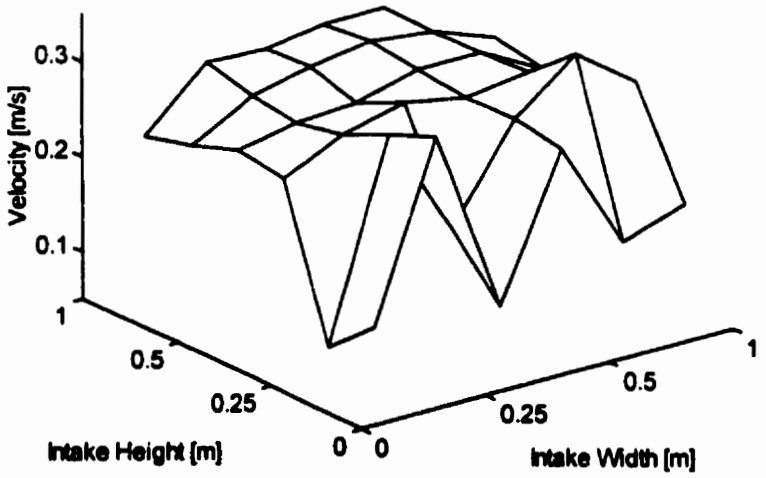

Figure 6.3 (b). Intake velocity profile for Q=485 [l/s]. The velocity measurements are obtained from a 6x6 Gauss-Legendre quadrature sampling strategy. The origin is at the bottom left corner of the intake. Comparison with the profile in (a) shows a greater number of low velocity estimates in proximity to the flow boundaries.

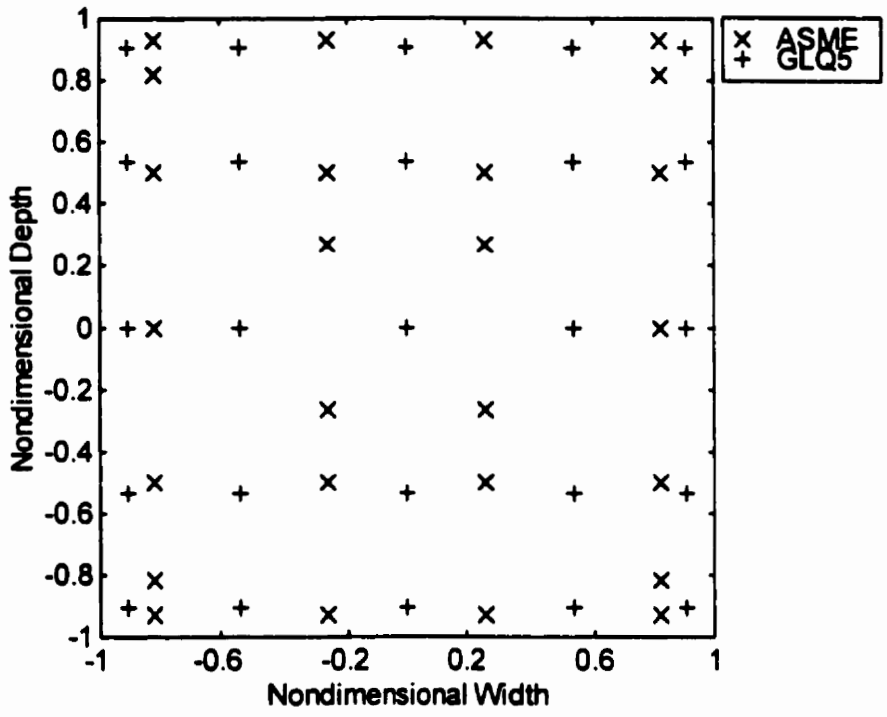

Figure 6.4. Position of metering points used for ASME (x) relative to those of GLQ 5x5 (+).

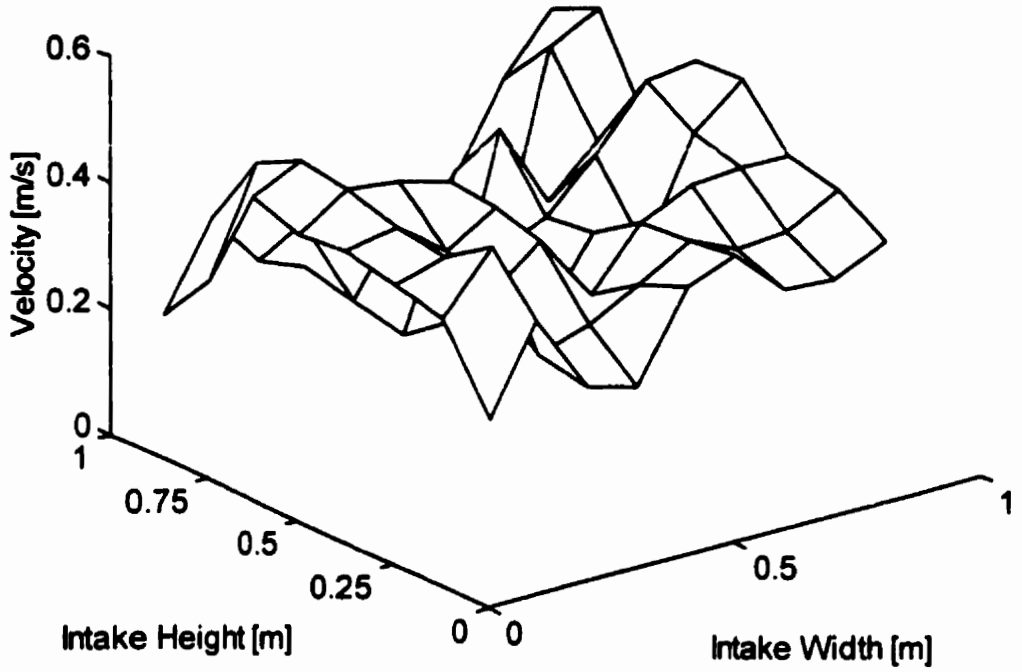

Figure 6.5. Intake velocity profile for the disturbed flow condition using the German distribution of velocity measurements (485 l/s).

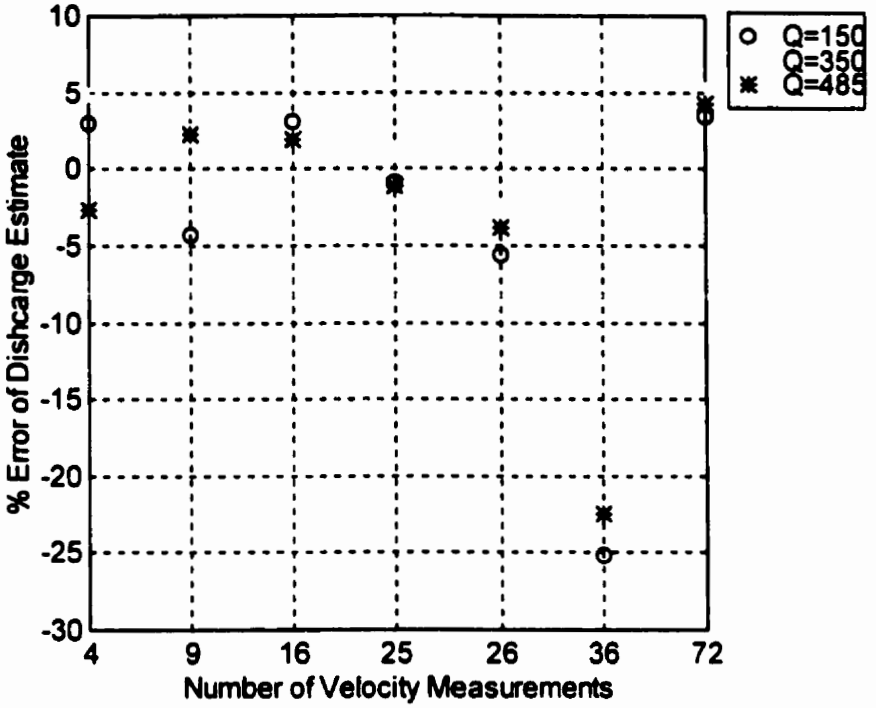

Figure 6.6. Error of discharge estimates for discharges of 165 (o), 350 (+), and 485 (*) l/s using GL 2x2, 3x3, 4x4, 5x5, ASME, GLQ 6x6 and German distributions of velocity measurements.

CHAPTER 7

REDUCED DATA SET TESTING

Although it is essential for hydroelectric utilities to determine the operating curve for turbine/generator units, measuring discharge can prove to be time consuming, labor-intensive, and costly. It is therefore advantageous to develop a testing methodology that reduces the time required to conduct discharge measurements, but does not compromise the accuracy of discharge measurement. One possible method of accomplishing this is through the application of Reduced Data Set (RDS) testing.

The Reduced Data Set (RDS) testing technique was developed based on the results of 86 velocity-area tests conducted at Manitoba Hydro's Kettle Generating Station. An observed self-similarity of the intake velocity profile for a given unit, over numerous gate settings, suggested the existence of a relationship between discharge and the horizontal velocity profile at a given position within the vertical traverse. Figure 7.1 shows the horizontal velocity profile, at a single location within the vertical traverse, for a typical unit. Successive curves show the trend in velocity profile over numerous wicket gate settings. The self-similarity of these velocity profiles over all vertical locations suggests the existence of a relationship between velocity at a single vertical position and discharge through the unit. It is this observed relationship which prompts this research. The objective of this analysis is to investigate the robustness of the RDS approach and establish the reliability of its discharge estimate. The usefulness of RDS will be examined based on a statistical analysis.

7.1 Data

The data used in this analysis were collected as part of field performance testing conducted at Kettle Generating station. Kettle is part of the Manitoba Hydro system and is located on the Nelson River. It is a low-head plant (30 m) with 12 turbine units. Each

unit has a capacity of 106 MW, yielding total plant capacity of 1272 MW. All turbine units have 3 intake openings measuring 6 m (wide) by 14 m (high).

Performance tests were conducted in accordance with the German code for hydraulic efficiency testing. Propeller-type flow meters (Ott type A) were mounted on a rigid support frame and traversed across the intake at the emergency stop-log guides for various gates. Frames were traversed simultaneously across all three intakes when testing a given unit. The distribution of metering points is shown in figure 7.2. A 9 (horizontal) by 14 (vertical) grid of metering points was obtained for each intake with close spacing in proximity to the flow boundaries, and fewer points through the center of the intake. Estimates of velocity were made based on a two-minute, time-averaged velocity. Performance tests were conducted on all 12 units at Kettle Generating station. Testing was undertaken for wicket gate settings of 25, 40, 50, 60, 65, 70, 80, 90, and 100 %.

7.2 Data Interpolation and Integration

Discharge calculations made in accordance with the German code for hydraulic efficiency are based on three representative flow elements, *viz.*, center, edge, and corner. Although the distribution of measured velocities is according to German code, to eliminate the error associated with this integration method, a numerical integration technique will be used to calculate discharge. The same numerical integration method will be used to calculate the area under the velocity-horizontal position curve (RDS index number). To facilitate integration, cubic splines were used to interpolate the measured velocity data. Cubic splines were fit to each of the horizontal and vertical arrays of measured velocities. The resulting (unique) splined surface provided a parametric description of the velocity profile. Cubic splines were fit to the arrays of measured velocities as well as to the horizontal transects at the RDS testing level.

Since the splined surface provides a detailed description of the velocity profile, the resulting velocity surface, and profile were easily integrated using trapezoidal integration. The trapezoid rule is the first of Newton-Cotes closed integration formulae. It is based on

a straight line approximation of the function, in this case velocity profile, between two points. The area under the straight line segment is an estimate of the integral of *f(x)*, between the limits *a* and *b*. The trapezoid rule is given by

$$I = (b-a)\frac{f(a)+f(b)}{2} \tag{7.1}$$

where *a* and *b* are the limits of the integral. *f(a)* and *f(b)* are the functional evaluations (velocity) at limits *a* and *b* respectively.

The error of the trapezoid integration is a function of the distance between *a* and *b*, and is given by

$$E = -\frac{1}{12}f''(\xi)(b-a)^3 \tag{7.2}$$

where ξ lies in the interval between *a* and *b*. Given the close spacing of velocity measurements on the interpolated surface (0.001) this error is negligible.

The discharge calculated by trapezoid integration of the intake velocity profile was used as the reference discharge in the RDS analysis. For the purpose of this analysis this number was calculated by trapezoidal integration of the velocity-horizontal position splined profile.

Figure 7.3 shows the measured (a) and splined (b) intake velocity profile. Similarly, figure 7.4 shows the measured velocities and splined velocity profiles for level 0.91H. The interpolation of the measured data as well as the integration were performed using MATLAB™ algorithms (Appendix C).

7.3 Evaluation of the RDS Methodology

The principle of RDS relies in the existence of a relationship between the area under the velocity-horizontal position curve at a single position within the vertical traverse (RDS index number), and the area under the complete intake velocity profile (discharge). The area under the horizontal velocity profile at a given vertical location is referred to as the RDS index number and is determined by integration of the velocity-horizontal position

curve. This relationship is determined by relating discharge to the corresponding RDS index number for a range of gate settings. Discharge was calculated for each unit and all wicket gate settings using trapezoidal integration of the splined velocity profiles. Although a single RDS testing level is typically selected when conducting field performance tests, three levels within the vertical traverse were chosen to evaluate the sensitivity of the RDS approach to vertical position within the traverse. The RDS levels were 2.1 m, 9.2 m, and 12.5 m from the top of the intake. These positions correspond to 0.15, 0.67, and 0.91 of the intake depth (H), respectively. The top ($0.15H$) and bottom ($0.91H$) were selected as they are in the vicinity of $0.11D$, which for fully developed, turbulent pipe flow is the location of the average velocity. The RDS index number was calculated for each unit, all gate settings, and the three RDS levels.

7.3.1 Statistical Analysis

The relationship between RDS index number and discharge was determined using statistical analysis. The discharge was calculated for each wicket gate setting using trapezoidal integration on the interpolated velocity profile. This was used as the reference discharge. Subsequently, the RDS index numbers were calculated, one for each of $0.15H$, $0.67H$, and $0.91H$ within the vertical traverse. The statistical relationship was investigated by graphing RDS index number and the corresponding reference discharge (figure 7.5) and determining the regression line through the data points. A separate regression analysis was performed for each turbine intake as the relationship between RDS index number and discharge may be specific to the location within the plant as well as turbine unit. The results of the statistical analysis are included in Table 7.1. All calculated discharges as well as RDS index numbers are included in Appendix D.

A least squares linear regression was fit to the data set as it is the most elementary means of investigating the relationship between a set of paired observations (in this case discharge and RDS index number). The expression for the regression line is given by

$$y = a_0 + a_1 x + e \tag{7.3}$$

where a_o and a_1 represent the intercept and slope, respectively. e is the error, or residual, between the model and observations. The overall fit of the model to the data set can be measured by the sum of the squared errors.

Two components of uncertainty exist in a linear regression: the uncertainty in the independent variable which is present prior to regression (S_t), and the uncertainty that persists after the regression fit (S_r). The relative improvement in estimate is given by $S_t - S_r$. This value can be normalized by

$$r^2 = \frac{S_t - S_r}{S_t} \tag{7.4}$$

where r^2 is the coefficient of determination and r is the correlation coefficient. In the case of a perfect fit of the regression line to the data set, $S_r = 0$ and $r^2=1$. An $r^2=1$ implies that the regression line is a perfect fit to the data set and that all error is accounted for by S_r; r^2 indicates the % of original uncertainty that can be accounted for by the model (Chapra & Canale, 1988)

As the slope of the regression line is used to predict discharge based on an RDS index factor, it is important to determine the standard error of a new prediction. The "standard deviation" for the regression line can be determined by

$$S_{y/x} = \sqrt{\frac{S_r}{n-2}} \tag{7.5}$$

where $S_{y/x}$ is the standard error of an estimate. The subscript y/x denotes the error in a predicted y based on a known x. The standard error of the estimate quantifies the spread of data points about the regression line. The uncertainty in the independent variable which present prior to regression is given by the sum of squares about the mean, denoted by S_t.

Table 7.1. Summary of statistical analysis.

		RDS @ 0.15*H*		RDS @ 0.67*H*		RDS @ 0.91H	
Unit	Intake	r^2	Std. Error	r^2	Std. Error	r^2	Std. Error
1	A	0.968	0.336	0.045	22.296	0.991	2.149
	B	1.000	0.572	0.029	26.311	0.996	1.639
	C	0.999	0.794	0.010	28.405	1.000	0.476
2	A	1.000	0.322	0.066	20.900	0.999	0.603
	B	0.999	0.578	0.049	20.846	0.999	0.494
	C	1.000	0.469	0.029	28.117	0.999	0.742
3	A	0.996	1.441	0.027	23.281	1.000	0.377
	B	1.000	0.376	0.006	26.488	1.000	0.565
	C	1.000	2.026	0.000	28.892	0.999	3.536
4	A	1.000	0.281	0.088	19.360	0.998	0.984
	B	1.000	0.419	0.074	24.427	0.997	1.332
	C	0.997	1.368	0.073	24.364	0.998	0.987
5	A	0.999	0.584	0.195	19.280	0.976	3.349
	B	1.000	0.386	0.125	25.382	0.987	3.038
	C	1.000	0.424	0.198	22.861	0.994	2.018
6	A	1.000	0.281	0.039	21.613	0.995	1.565
	B	0.999	0.623	0.283	21.924	0.999	0.724
	C	1.000	0.506	0.271	21.153	0.999	0.733
7	A	1.000	0.368	0.061	21.744	0.999	0.549
	B	1.000	0.365	0.053	22.945	0.996	1.469
	C	0.997	1.557	0.055	26.789	0.990	2.743
8	A	0.995	1.762	0.033	23.611	0.867	8.748
	B	0.997	1.518	0.010	27.073	0.988	3.035
	C	0.999	1.019	0.014	28.808	0.998	1.161
9	A	1.000	15.742	0.052	20.997	0.976	15.552
	B	0.937	6.504	0.007	25.010	0.488	16.896
	C	0.966	20.655	0.937	27.698	0.969	19.833

10	A	0.971	18.276	0.950	24.642	0.974	17.624
	B	0.992	1.969	0.208	16.596	0.986	2.262
	C	0.999	0.694	0.296	17.872	0.923	6.765
11	A	0.998	1.243	0.073	25.261	0.971	5.748
	B	0.962	3.115	0.249	13.839	0.895	5.169
	C	1.000	0.371	0.253	16.853	0.882	6.703
12	A	0.948	5.068	0.003	22.109	0.876	7.791
	B	0.975	3.061	0.088	18.576	0.281	16.492
	C	0.996	1.206	0.058	19.331	0.762	9.720
Average		***0.991***	***2.674***	***0.139***	***22.935***	***0.937***	***4.821***

7.3.1.1 RDS at 0.15H

Comparison of the statistical indicators for the three RDS index levels suggest that the strength of the relationship between the velocity-horizontal position curve and discharge is sensitive to the location selected as the RDS level. The results of this analysis suggest that the relationship between discharge and RDS index number is greatest at 0.15 *H*. An r^2 (on average) of 0.991 across all units indicates that the regression line fits the data with 99.1 % accuracy. As indicated by the standard error of estimate, it is possible to estimate discharge (on average) to within (approximately) 2.7 cms.

Figure 7.6a shows the velocity-horizontal position curve for Unit 1, intake A, for all gate settings. From these curves it is possible to infer that the self-similarity of the velocity profiles across a range of discharges is reflected in the statistical relationship between RDS index number and discharge.

7.3.1.2 RDS at 0.67H

The statistical data for an RDS level of 0.67*H* do not suggest to the existence of a strong statistical relationship between RDS index number and discharge. The r^2 coefficient is

extremely low (0.139), with the standard error in prediction of 22.9 cms. These results imply that no significant statistical relationship exists between the variables.

Analysis of the velocity-horizontal position curve at 0.67*H* in the vertical traverse confirms the findings of the statistical analysis. The velocity data from Unit 1, intake A, is shown in figure 7.6b and there is no apparent trend in the velocity profile through the range of gate settings. These results suggest that RDS at 0.67*H* cannot be used to satisfactorily estimate discharge.

7.3.1.3 RDS at 0.91H

The statistical indicators for RDS at 0.91*H* suggest a strong correlation between discharge and RDS index number. The strength of the statistical relationship is indicated by an (average) r^2 of 0.937 across all units. Further investigation of the statistical relationship and standard error of estimate indicates that RDS index number can predict discharge with an (average) expected error of 4.81 cms. Given the strong statistical relationship, and the confidence of a new prediction, RDS at 0.91*D* appears to be a reliable method of estimating discharge for Kettle Generating Station.

Figure 7.6c shows the velocity-horizontal position curves for Unit 1, intake A at RDS level 0.91*H*. The r^2 for this intake is 0.991. From these curves, it is possible to infer that a trend exists between the horizontal velocity profile and discharge at this location.

7.4 Summary

Figures 7.7 (a-c) show the standard error of discharge estimate based on RDS at 0.15*H*, 0.67*H* and 0.91*H*, respectively. Investigation of the trend in standard error of estimate for RDS at 0.15*H* suggests that the reliability of the discharge estimate is highest for units 2, 5, and 6 as they have the lowest standard error of estimate; units 8 through 12 show the highest standard error of discharge estimate. A similar trend is observed for RDS at 0.91*H* (figure 7.7 (c)). There is no clear pattern in standard error of estimate over all units for RDS at 0.67*H*. Figure 7.8 shows the r^2 for all units and all RDS levels. The

relationship between RDS level, unit number, and r^2 shows that the strongest statistical relationship exists for RDS at $0.15H$ and $0.91H$. RDS at $0.67H$ is consistently lower, over all units.

For fully-developed, turbulent pipe flow given by Von Karman's power law, velocity increases with distance from the flow boundaries. Maximum velocity (freestream) occurs at the centerline of the pipe where boundary effects are minimal; average pipe velocity occurs at $0.11D$, where D is pipe diameter. Although the intake velocity profile has more structure than the idealized profile, the development of the velocity profile in the vicinity of the boundaries is more representative of the idealized condition, in this case, than the profile through the center of the intake. Analysis of the intake velocity profile shows significant velocity structure in the vicinity of the centerline, close to $0.67H$. This variability may account for the apparent lack of statistical relationship between discharge and horizontal velocity profile at this position within the vertical traverse. Conversely, the proximity of the upper and lower RDS levels to $0.11H$ from either the top and bottom flow profiles even in the absence of full-developed turbulent flow may contribute to the apparent strength of the statistical relationship at these positions.

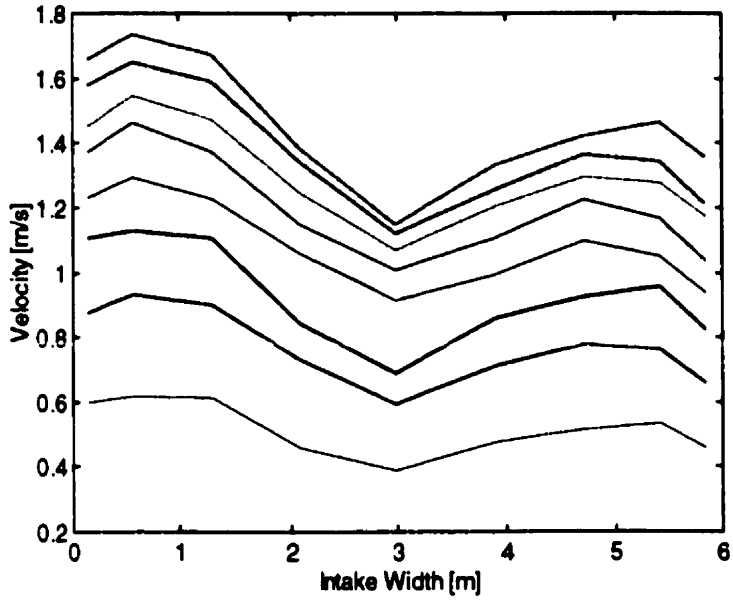

Figure 7.1. Velocity-horizontal position curves for Unit 1, intake A, at 25, 40, 50, 60, 65, 70, 80, 90, and 100 % gates at 0.91 *H*. The self-simillarity of these profiles over all vertical locations suggests the existence of a relationship between velocity profile at a single location and discharge. The velocity profiles are in order of increasing gate.

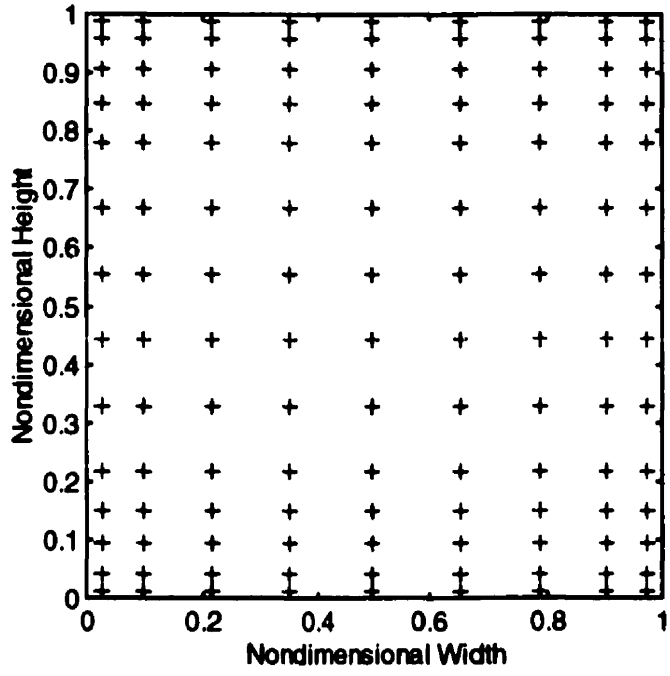

Figure 7.2. Distribution of metering points used at Kettle Generating Station. The 144 points are arranged according to German performance testing code specifications.

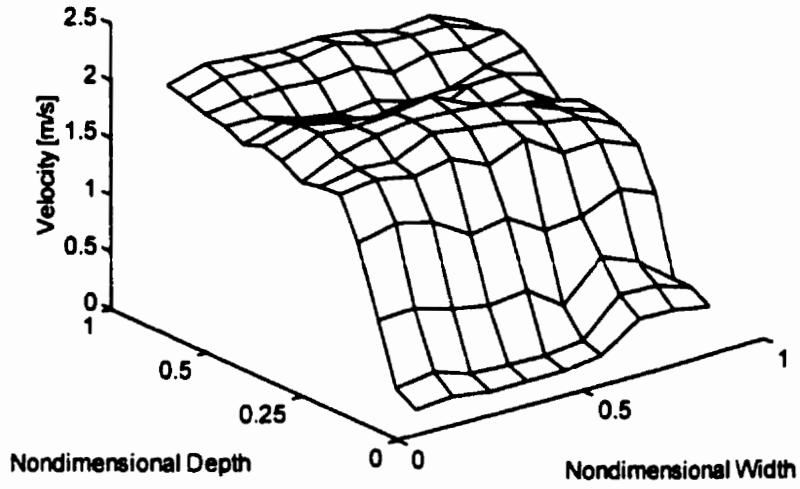

(a)

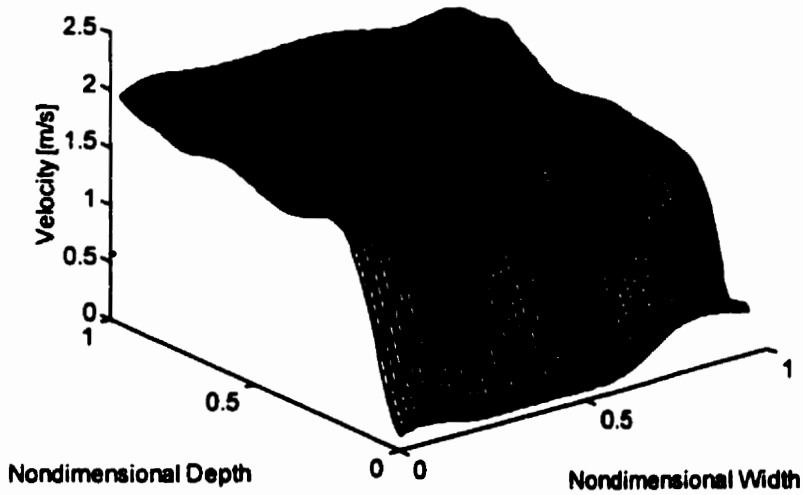

(b)

Figure 7.3 (a). Measured intake velocity profile (Unit 12, intake A, 100%). The velocity measurement are connected by straight lines. (b) Interpolated velocity profile (Unit 12, Intake A, 100%). The velocity measurements are connected by cubic splines.

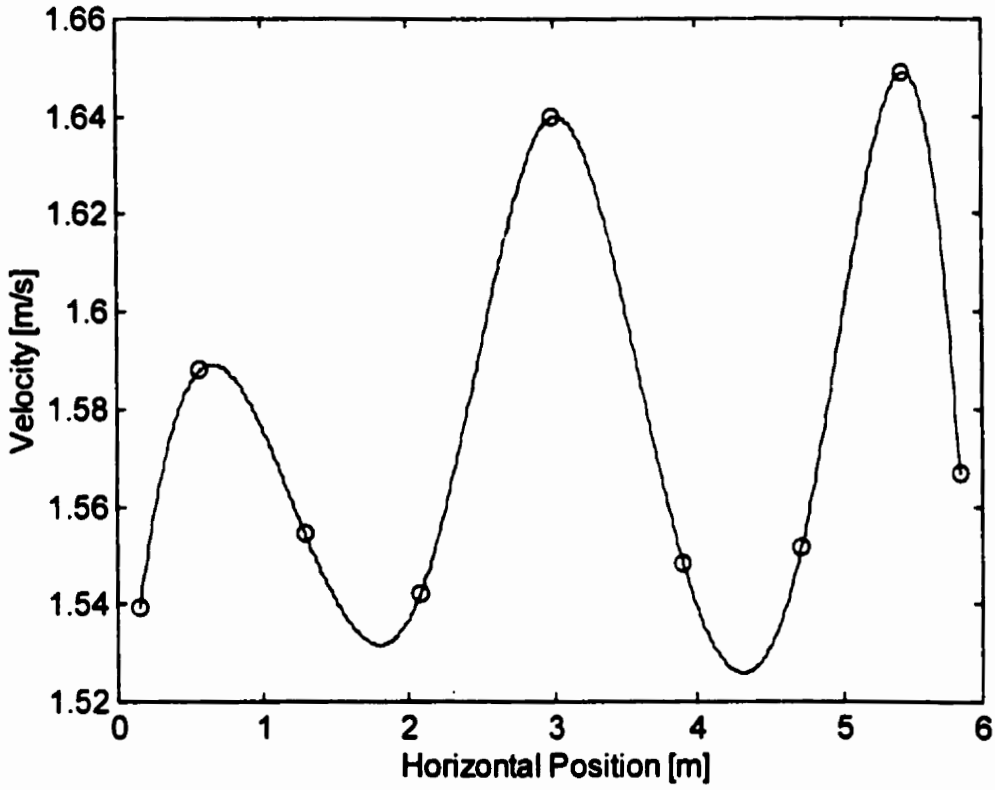

Figure 7.4. Measured velocities at 0.91 *H* (o). The splined profile (-) passes through all measured velocities (Unit 10, intake A, 100%).

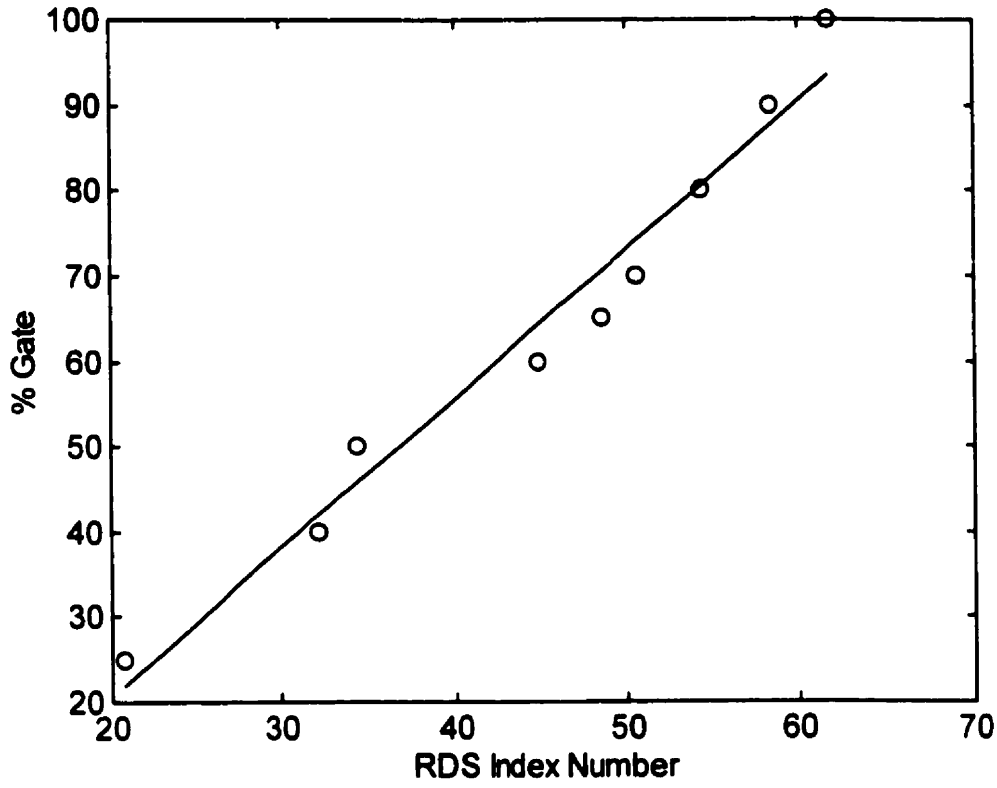

Figure 7.5. A regression line through the data points is one measure of the statistical relationship between the two variables (Unit 1, intake A at 0.91 H).

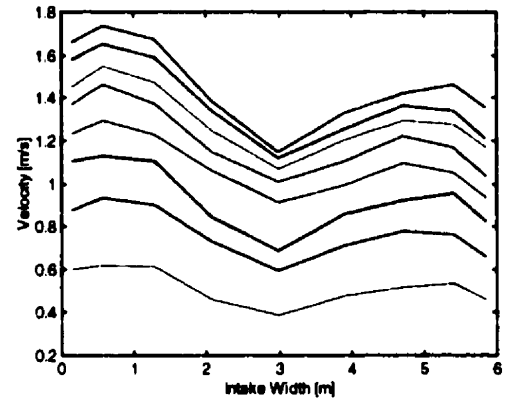

(a)

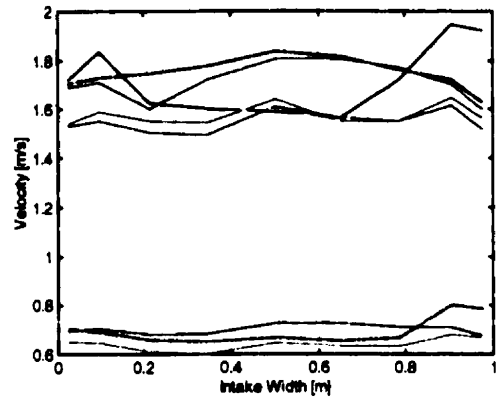

(b)

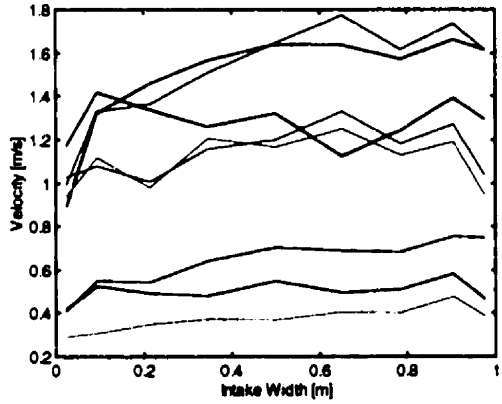

(c)

Figure 7.6(a) Velocity-horizontal position curve for Unit 1, intake A for all gate settings at RDS of 0.15 *H*. (b) Velocity horizontal position curve for Unit 1, intake A for all gate settings, at RDS of 0.67 *H*. (c) Velocity horizontal position curve for Unit 1, intake A, for all gate settings at RDS of 0.91 *H*.

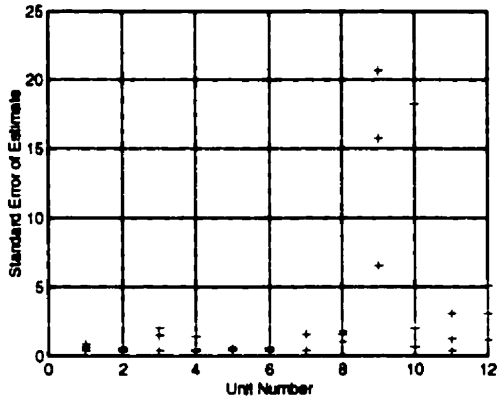

(a)

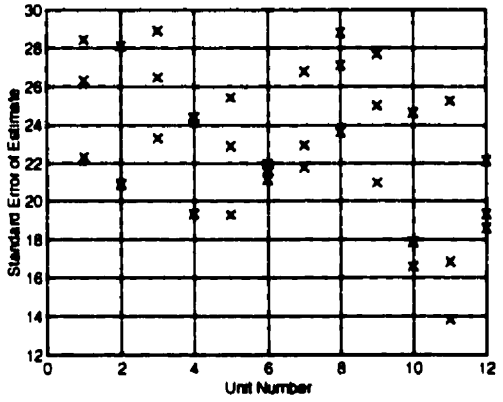

(b)

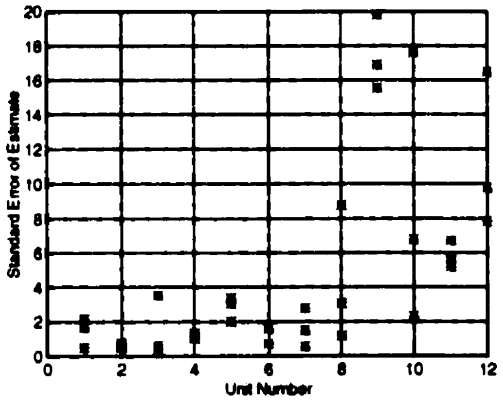

(c)

Figure 7.7 (a) Standard error of discharge estimate based on RDS at 0.15 *H (from top)* (b) Standard error of discharge estimate based on RDS at 0.67*H (from top).* (c) Standard error of discharge estimate based on RDS at 0.91 *H (from bottom).*

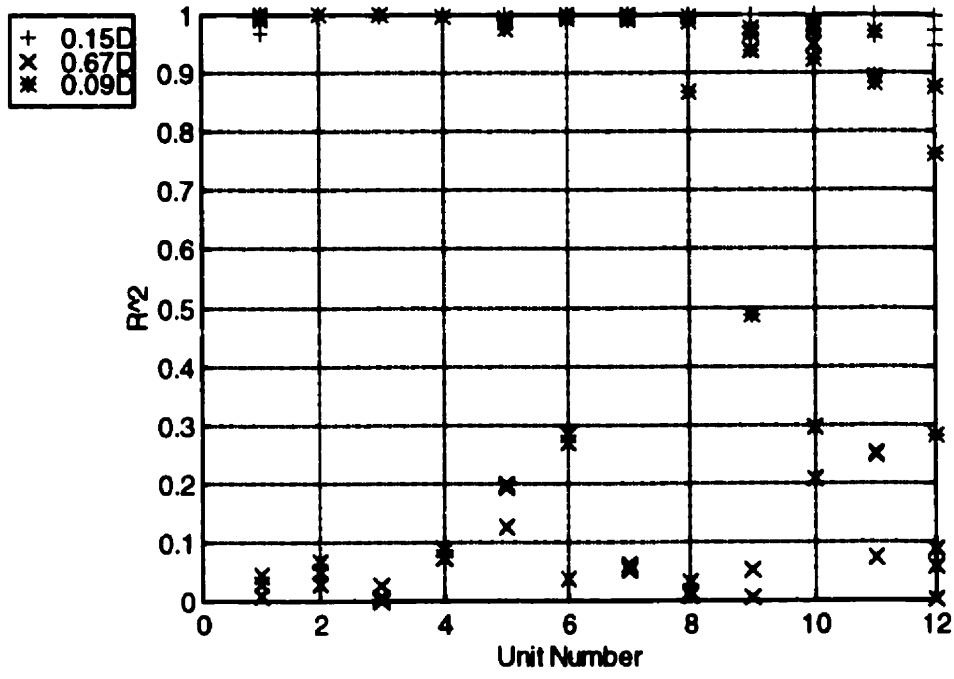

Figure 7.8. Summary of statistical analysis for three RDS levels (+) 0.15*D*, (x) 0.67*D*, (*) 0.91*D*.

CHAPTER 8

CONCLUSIONS AND RECOMMENDATIONS

8.1 Summary

Field performance tests of turbine/generator units are necessary for the efficient operation of a hydroelectric generating station. Performance tests data are used to determine the head-power-discharge relationship for a turbine/generator; this relationship is used to identify the peak operating point for a turbine. Of the variables used to determine this relationship, discharge is most difficult to measure accurately in real time and is most susceptible to measurement error. Accurate measurement of discharge, however, is critical to the accurate identification of a turbine operating curve.

Of the methods available for discharge measurement, the velocity-area method is favored by many hydroelectric utilities because it is well-suited to low-head plants with short converging intakes. Calculation of discharge by the velocity-area method involves traversing the velocity profile to obtain a grid of point estimates of velocity. The appropriate summation of these velocity measurements, times the corresponding area within the metering plane, yields an estimate of discharge.

Four codes govern the field performance testing of hydraulic turbines. These codes specify the number and distribution of velocity measurements required to estimate discharge. In general, the number and distribution is specified to adequately sample the velocity profile and are based on the assumption of fully-developed turbulent flow at the metering plane.

Investigation of the velocity at the intake of a typical low-head plant suggests that the assumed velocity profile is typically not realized. Consequently, the distributions of

metering points may not be optimal to sample the actual velocity profile, which has considerably more structure through the center, and less variability in the vicinity of the flow boundaries. This observation lead to a comparison of the techniques used to estimate discharge based on an array of velocity measurements (Chapter 3). The results of this analysis suggest that is may be possible to improve the efficacy of calculating discharge. Contrasting the results gathered using code, and non-code based integration techniques suggests that the application of a noncode-based method of computing discharge (Gauss-Legendre quadrature), provides estimates which more closely approximate discharge than either the ASME or German code-based methods. These results prompted further investigation using a laboratory model.

The results of the numerical analysis (Chapter 3) were applied to discharge estimation in a laboratory model. The intake of a low-head turbine unit was constructed for this purpose. The velocity profile was sampled according to code and noncode-based distributions of velocity measurements. Accuracy of discharge estimate, relative to a reference discharge, was the primary criteria for evaluation. The laboratory results confirmed the numerical analysis, *i.e.* basing the distribution of velocity measurements on an unrealized theoretical flow profile does not result in the most accurate estimate of discharge. Rather, an accurate estimate of discharge may be obtained using fewer velocity measurements, which, arranged to resolve the velocity profile, as in the Gauss-Legendre quadrature integration method. The implication of these findings is it is the distribution of velocity measurements, rather than the number, which is central to accurate discharge measurement. Therefore, rather than establishing the distribution of measurement points according to an unsatisfied idealized profile, more accurate results could likely be obtained by attempting to resolve the true velocity profile.

An observed relationship between the horizontal velocity profile and unit discharge at Kettle Generating station prompted analysis of a Reduced Data Set (RDS) method of estimating discharge (Chapter 7). The RDS methodology is based on a statistical

relationship between the area under the velocity-horizontal position curve (RDS index number) and discharge. The goal of the RDS method is to provide an accurate estimate of discharge using a single horizontal transect of the velocity profle. The results of this analysis suggest that given the (apparent) sensitivity of the RDS method to position within the vertical traverse, it may be concluded that is not advisable to apply the RDS method without first performing a statistical analysis on the relationship between RDS index number and discharge for all positions within the vertical traverse. Based on the results of this analysis, the optimum location for RDS data collection could be selected based on the statistical indicators of r^2 and standard error of estimate. The RDS analysis (Chapter 7) suggests that selecting an RDS level in proximity to $0.11D$ from either the top or bottom flow boundary may yield more reliable results than an RDS level in proximity to the centerline of the intake.

8.2 Conclusions

The results of this research lead to the following conclusions:

1. The distribution of measurement points based on the assumption of a velocity profile which is given by a $1/n$ power law does not result in the most accurate discharge estimate. This suggests that this distribution does not adequately sample the velocity profile.
2. An accurate estimate of discharge can be obtained using significantly fewer points than recommended by German code.
3. Using Gauss-Legendre quadrature numerical integration to sample the intake velocity profile yields accurate estimates of discharge.
4. A statistical relationship exists between the horizontal velocity profile and discharge. The strength of the relationship is dependent on position within the vertical traverse.

8.3 Recommendations

Recommendations for future research include field testing of the Gauss-Legendre quadrature integration method to investigate the most reliable GLQ distribution to be used for discharge calculation. The results of the laboratory analysis suggest that a 5x5 GLQ yields an accurate estimate of discharge, however, in field conditions, perhaps a higher order GLQ might better estimate discharge. The results of the GLQ could be compared to the discharge estimate obtained using the German code-based distribution of metering points as well as the ASME log-linear method.

The Reduced Data Set testing methodology could be further investigated using both field as well as laboratory data. Data from another generating station in addition to laboratory data could be used for verification of the Kettle results. One advantage of the laboratory setting would be to test the RDS method under a variety of conditions by varying discharge and introducing flow obstructions.

Recommendations for future laboratory research include comparing the velocity-area and acoustic methods of discharge measurement, as they are both suited to low-head plants.

REFERENCES

Abnahmeversuche an Wasserturinen, DIN 1948. (Translated)

Almquist, C., P.March, H. Pearson, H. Franseen, & B. Whitehead (1995). The Sliding Gate Method for Hydroturbine Efficiency Testing. *Waterpower* '95. pp. 793-801.

American Society of Mechanical Engineers (1985). Performance Test Codes, Hydraulic Turbines and Turbine Mode of Pump Turbines, PTC 18. The American Society of Mechanical Engineers, New York, New York.

Birch, R. & D. Lemon (1995). Non-Intrusive Flow Measurement Techniques for Hydroelectric Applications. *Waterpower* '95. pp. 2049-2058.

Chapra, S.C. & P.P. Canale (1988). Numerical Methods for Engineers. McGraw-Hill, Inc. USA.

Craeger, W.P. & J.D. Justin., (1927). Hydro-Electric Handbook. John Wiley & Sons, Inc. New York. pp.78-80.

Gawne, K.D. (1997). Developing an Acoustic Discharge Measurement Technique for Hydroelectric Performance Testing. Master of Science Thesis. Department of Civil Engineering, University of Manitoba.

Grego, G. (1996). Comparative Flowrate Measurements at the Caneva Generating Plant Unit 2, *Proceeding IGHEM Seminar – Montreal '96,* Paper n. 14.

Halas, R.N., J.C. Howe, R.J. Knowlton, P.W Ludewig, & J.B. Nystrom (1991). Field Tests of a Lewiston Pump-Generating Unit. *Waterpower '91.* Pp.1686-1695.

Hans, P.D., & H. Louka (1996). Hydraulic Performance Testing Manual. Hydraulic Engineering and Operations Department, Manitoba Hydro. Winnipeg, Canada.

Hecker, G.E. & J.B. Nystrom (1987). Which Flow Measurement Technique is Best? *Hydro Review*, June 1987. Pp. 42-48.

Henderson, F.M. (1966). Open Channel Flow. MacMillan, NY, NY.

International Electrotechnical Commission, 1991. Standard IEC-41-1991, "Field acceptance tests to determine the hydraulic performance of hydraulic turbines, storage pumps and pump-turbines."

International Standard (ISO) 3354 (1975). Measurement of clean water flow in closed conduits--Velocity-area method using current-meters. ISO 3354-1975 (E)

Lemon, D.D. (1995). Measuring Intake Flows in Hydroelectric Plants with an Acoustic Scintillation Flowmeter. *Waterpower '95*. Pp. 2039-2048.

Levesque, J.M. (1994). Measuring Flow with Pressure-Time, Current Meter Methods. *Hydro Review*, August 1994. pp. 102-109.

Mikhail, A.F., 1994. Turbine Performance Testing Using the Intake Current-Meter System (ICMS), Canadian Electrical Association, Engineering and Operating Division.

Nguyen, T.D., J.B. Nystrom, & L. Larsen (1991). Evaluation of Turbine Intake Velocity Criteria. *Waterpower '91*. Pp. 1706-1715.

Nystrom, J.B. (1991). Application of Personal Computers to Field Flow Measurement. *Waterpower '91*. Proceedings of the International Conference on Hydropower. Pp. 2254-2263.

Sharp, J.J. (1981). Hydraulic Modeling. Butterworths, Toronto.

Spencer, D. (1986). Capacity Planning with Phased-GCC Addition. *EPRI Journal*, December 1986. Pp. 40-43.

Sugishita, K., Sakurai, A., Tankaka, H. and Suzuki, T., (1996). Evaluation of Error of Acoustic Method and its Verification by Comparitive Field Tests, *Proceedings IGHEM Seminar – Montreal '96*, Paper n. 31.

Voaden, G.H. (1951). Index Testing of Hydraulic Turbines. Presented by the Hydraulic Division and presented at the Annual Meeting, New York, N.Y. November 26-December 1, 1950, of The American Society of Mechanical Engineers. Paper No. 50-A-52.

Voigt, R.L., J.S. Gulliever, & J. Woods. (1989). Field Efficiency Testing of Hydroelectric Turbines. *Waterpower* 1989. Pp. 1515-1524.

Voser, A., Bruttin, C., Prenat, J., and Staubli, T., 1996. "Improving Acoustic Flow Measurement", *International Water Power & Dam Construction*, April 1996.

Winstone, C.R., 1989. Ott meter program: Long Spruce generating station. Manitoba Hydro technical report, 89-04, 244 pp.

Yalin, M.S. (1971). Theory of Hydraulic Models. The MacMillan Press Ltd. Toronto, Canada.

APPENDIX A

Positions of Velocity Measurements Motion Control Programs

Matrices of Absolute Positions Measured in Counts

ASME

X	75628	302101	519943	746416	
Y	66299	66299	66299	66299	Bottom of Intake
	124407			124407	
	282623	282623	282623	282623	
		400282	400283		
	532961			532961	
		665641	665641		
	783301	783301	783301	783301	
	941515			941515	
	999594	999594	999594	999594	Top of Intake

Gauss Quadrature

2x2

X	173718	640105	
Y	243897	243897	
	822030	822030	

3x3

X	92646	411022	729398
Y	145142	145142	145142
	532966	532966	532966
	920789	920789	920789

4x4

X	57076	271282	550762	764968	
Y	101811	101811	101811	101811	
	362742	362742	362742	362742	
	703185	703185	703185	703185	
	964116	964116	964116	964116	

5x5

X	38562	189699	411022	632345	783482	
Y	79260	79260	79260	79260	79260	
	263365	263365	263365	263365	263365	
	532965	532965	532965	532965	532965	
	802565	802565	802565	802565	802565	
	986976	986976	986976	986976	986976	

6x6

X	27757	139250	312944	509100	682794	794287	
Y	66095	66095	66095	66095	66095	66095	
	201909	201909	201909	201909	201909	201909	
	413491	413491	413491	413491	413491	413491	
	652434	652434	652434	652434	652434	652434	
	864016	864016	864016	864016	864016	864016	
	999830	999830	999830	999830	999830	999830	

German

X	23486	70449	164401	281838	411022	540165	657635	751587	798534
Y	66329	66329	66329	66329	66329	66329	66329	66329	66329
	135423	135423	135423	135423	135423	135423	135423	135423	135423
	271607	271607	271607	271607	271607	271607	271607	271607	271607
	441838	441838	441838	441838	441838	441838	441838	441838	441838
	635100	635100	635100	635100	635100	635100	635100	635100	635100
	794316	794316	794316	794316	794316	794316	794316	794316	794316
	930500	930500	930500	930500	930500	930500	930500	930500	930500
	999594	999594	999594	999594	999594	999594	999594	999594	999594

```
#GQ2
KI 1,1
TL 9.5,9.5
ER 1000, 1000
OE 1,1
SP 16000, 16000
AC 4000, 4000
DC 4000, 4000
MG " "
MG "GQ2 -4 PT GAUSS-Q"
MG "2 MIN/STA"
MG " "
MG "CHECK ADV"
MG "VERIFY AT STATION 00000"
MG " "
MG "IF NOT, RESET DMC NOW!"
WT 4000
DP 0,0
MG "POSITION SET TO 0,0"
MG "TRAVERSING"
PA 173718,243897
BG
AM
WT 24000
MG "AT STATION 1"
MG "START ADV"
WT 120000
MG "TRAVERSING"
PA 173718,822030
BG
AM
WT 360
MG " "
MG "AT STATION 2"
WT 120000
MG "TRAVERSING"
PA 640105,822030
BG
AM
WT 6830
MG " "
MG "AT STATION 3"
WT 120000
MG "TRAVERSING"
PA 640105,243897
BG
AM
WT 500
MG " "
MG "AT STATION 4 (LAST STATION)"
WT 120000
MG "STOP LOGGING DATA NOW"
PA 0,0
BG
AM
MG "END OF PROGRAM"
EN
```

```
#GQ3
KI 1,1
TL 9.5,9.5
ER 1000, 1000
OE 1,1
SP 16000, 16000
AC 4000, 4000
DC 4000, 4000
MG " "
MG "GQ3 -9 PT GAUSS-Q"
MG "2 MIN/STA"
MG " "
MG "CHECK ADV"
MG "VERIFY AT STATION 00000"
MG " "
MG "IF NOT, RESET DMC NOW!"
WT 4000
DP 0,0
MG "POSITION SET TO 0,0"
MG "TRAVERSING"
PA 92646,145142
BG
AM
WT 18090
MG "AT STATION 1"
MG "START ADV"
WT 120000
MG "TRAVERSING"
PA 92646,532966
BG
AM
WT 3500
MG " "
MG "AT STATION 2"
WT 120000
MG "TRAVERSING"
PA 92646,920789
BG
AM
WT 2150
MG " "
MG "AT STATION 3"
WT 120000
MG "TRAVERSING"
PA 411022,920789
BG
AM
WT 6030
MG " "
MG "AT STATION 4"
WT 120000
MG "TRAVERSING"
PA 411022,532966
BG
AM
WT 2850
MG " "
MG "AT STATION 5"
WT 120000
MG "TRAVERSING"
PA 411022,145142
BG
AM
WT 2120
MG " "
MG "AT STATION 6"
WT 120000
```

```
MG "TRAVERSING"
PA 729398,145142
BG
AM
WT 6930
MG " "
MG "AT STATION 7"
WT 120000
MG "TRAVERSING"
PA 729398,532966
BG
AM
WT 2020
MG " "
MG "AT STATION 8"
WT 120000
MG "TRAVERSING"
PA 729398,920789
BG
AM
WT 2790
MG " "
MG "AT STATION 9 (LAST STATION)"
WT 120000
MG "STOP LOGGING ADV DATA"
MG "RETURNING TO STATION 0,0"
PA 0,0
BG
AM
MG "AT STATION 0, PROGRAM COMPLETE"
EN
```

```
#GQ4
KI 1,1
TL 9.5,9.5
ER 1000, 1000
OE 1,1
SP 16000, 16000
AC 4000, 4000
DC 4000, 4000
MG " "
MG "GQ4 -16 PT GAUSS-Q"
MG "2 MIN/STA"
MG " "
MG "CHECK ADV"
MG "VERIFY AT STATION 00000"
MG " "
MG "IF NOT, RESET DMC NOW!"
WT 4000
DP 0,0
MG "POSITION SET TO 0,0"
MG "TRAVERSING"
PA 57076,101811
BG
AM
WT 21300
MG "AT STATION 1"
MG "START ADV"
WT 120000
MG "TRAVERSING"
PA 57076,362742
BG
AM
WT 10070
MG " "
MG "AT STATION 2"
WT 120000
MG "TRAVERSING"
PA 57076,703185
BG
AM
WT 5500
MG " "
MG "AT STATION 3"
WT 120000
MG "TRAVERSING"
PA 57076,964116
BG
AM
WT 10500
MG " "
MG "AT STATION 4"
WT 120000
MG "TRAVERSING"
PA 271282,964116
BG
AM
WT 12940
MG " "
MG "AT STATION 5"
WT 120000
MG "TRAVERSING"
PA 271282,703185
BG
AM
WT 9400
MG " "
MG "AT STATION 6"
WT 120000
```

```
MG "TRAVERSING"
PA 271282,362742
BG
AM
WT 4480
MG " "
MG "AT STATION 7"
WT 120000
MG "TRAVERSING"
PA 271282,101811
BG
AM
WT 9930
MG " "
MG "AT STATION 8"
WT 120000
MG "TRAVERSING"
PA 550762,101811
BG
AM
WT 8730
MG " "
MG "AT STATION 9"
WT 120000
MG "TRAVERSING"
PA 550762,362742
BG
AM
WT 9930
MG " "
MG "AT STATION 10"
WT 120000
MG "TRAVERSING"
PA 550762,703185
BG
AM
WT 4500
MG " "
MG "AT STATION 11"
WT 120000
MG "TRAVERSING"
PA 550762,964116
BG
AM
WT 9400
MG " "
MG "AT STATION 12"
WT 120000
MG "TRAVERSING"
PA 764968,964116
BG
AM
WT 12400
MG " "
MG "AT STATION 13"
WT 120000
MG "TRAVERSING"
PA 764968,703185
BG
AM
WT 9400
MG " "
MG "AT STATION 14"
WT 120000
MG "TRAVERSING"
PA 764968,362742
BG
```

```
AM
WT 4480
MG " "
MG "AT STATION 15"
WT 120000
MG "TRAVERSING"
PA 764968,101811
BG
AM
WT 9930
MG " "
MG "AT STATION 16 (LAST STATION)"
WT 120000
MG "STOP LOGGING ADV DATA"
MG "RETURNING TO STATION 0,0"
PA 0,0
BG
AM
MG "AT STATION 0, PROGRAM COMPLETE"
EN
```

```
#GQ5
KI 1,1
TL 9.5,9.5
ER 1000, 1000
OE 1,1
SP 16000, 16000
AC 4000, 4000
DC 4000, 4000
MG " "
MG "GQ5 -25 PT GAUSS-Q"
MG "2 MIN/STA"
MG " "
MG "CHECK ADV"
MG "VERIFY AT STATION 00000"
MG " "
MG "IF NOT, RESET DMC NOW!"
WT 4000
DP 0,0
MG "POSITION SET TO 0,0"
MG "TRAVERSING"
PA 38562,79260
BG
AM
WT 22500
MG "AT STATION 1"
MG "START ADV"
WT 120000
MG "TRAVERSING"
PA 38562,263365
BG
AM
WT 14200
MG " "
MG "AT STATION 2"
WT 120000
MG "TRAVERSING"
PA 38562,532965
BG
AM
WT 9000
MG " "
MG "AT STATION 3"
WT 120000
MG "TRAVERSING"
PA 38562,802565
BG
AM
WT 11100
MG " "
MG "AT STATION 4"
WT 120000
MG "TRAVERSING"
PA 38562,986976
BG
AM
WT 15200
MG " "
MG "AT STATION 5"
WT 120000
MG "TRAVERSING"
PA 189699,986976
BG
AM
WT 16000
MG " "
MG "AT STATION 6"
WT 120000
```

```
MG "TRAVERSING"
PA 189699,802565
BG
AM
WT 14000
MG " "
MG "AT STATION 7"
WT 120000
MG "TRAVERSING"
PA 189699,532965
BG
AM
WT 9000
MG " "
MG "AT STATION 8"
WT 120000
MG "TRAVERSING"
PA 189699,263365
BG
AM
WT 10000
MG " "
MG "AT STATION 9"
WT 120000
MG "TRAVERSING"
PA 189699,79260
BG
AM
WT 14600
MG " "
MG "AT STATION 10"
WT 120000
MG "TRAVERSING"
PA 411022,79260
BG
AM
WT 11600
MG " "
MG "AT STATION 11"
WT 120000
MG "TRAVERSING"
PA 411022,263365
BG
AM
WT 14200
MG " "
MG "AT STATION 12"
WT 120000
MG "TRAVERSING"
PA 411022,532965
BG
AM
WT 9000
MG " "
MG "AT STATION 13"
WT 120000
MG "TRAVERSING"
PA 411022,802565
BG
AM
WT 11100
MG " "
MG "AT STATION 14"
WT 120000
MG "TRAVERSING"
PA 411022,986976
BG
```

```
AM
WT 15200
MG " "
MG "AT STATION 15"
WT 120000
MG "TRAVERSING"
PA 632345,986976
BG
AM
WT 11500
MG " "
MG "AT STATION 16"
WT 120000
MG "TRAVERSING"
PA 632345,802565
BG
AM
WT 14000
MG " "
MG "AT STATION 17"
WT 120000
MG "TRAVERSING"
PA 607675,532965
BG
AM
WT 9000
MG " "
MG "AT STATION 18"
WT 120000
MG "TRAVERSING"
PA 632345,263365
BG
AM
WT 10000
MG " "
MG "AT STATION 19"
WT 120000
MG "TRAVERSING"
PA 632345,79260
BG
AM
WT 14600
MG " "
MG "AT STATION 20"
WT 120000
MG "TRAVERSING"
PA 783482,79260
BG
AM
WT 17490
MG " "
MG "AT STATION 21"
WT 120000
MG "TRAVERSING"
PA 783482,263365
BG
AM
WT 14200
MG " "
MG "AT STATION 22"
WT 120000
MG "TRAVERSING"
PA 783482,532965
BG
AM
WT 9000
MG " "
```

```
MG "AT STATION 23"
WT 120000
MG "TRAVERSING"
PA 783482,802565
BG
AM
WT 11100
MG " "
MG "AT STATION 24"
WT 120000
MG "TRAVERSING"
PA 783482,986976
BG
AM
WT 15200
MG " "
MG "AT STATION 25 (LAST ONE)"
WT 120000
MG "STOP LOGGING ADV DATA"
MG "RETURNING TO STATION 0000"
PA 0,0
BG
AM
MG "AT STATION 0, PROGRAM COMPLETE"
MG " "
EN
```

```
#GQ6
KI 1,1
TL 9.5,9.5
ER 1000, 1000
OE 1,1
SP 16000, 16000
AC 4000, 4000
DC 4000, 4000
MG " "
MG "GQ6 -36 PT GAUSS-Q"
MG "2 MIN/STA"
MG " "
MG "CHECK ADV"
MG "VERIFY AT STATION 00000"
MG " "
MG "IF NOT, RESET DMC NOW!"
WT 4000
DP 0,0
MG "POSITION SET TO 0,0"
MG "TRAVERSING"
PA 27757,66095
BG
AM
WT 22500
MG "AT STATION 1"
MG "START ADV"
WT 120000
MG "TRAVERSING"
PA 27757,201909
BG
AM
WT 22000
MG " "
MG "AT STATION 2"
WT 120000
MG "TRAVERSING"
PA 27757,413491
BG
AM
WT 13000
MG " "
MG "AT STATION 3"
WT 120000
MG "TRAVERSING"
PA 27757,652434
BG
AM
WT 11100
MG " "
MG "AT STATION 4"
WT 120000
MG "TRAVERSING"
PA 27757,864016
BG
AM
WT 12400
MG " "
MG "AT STATION 5"
WT 120000
MG "TRAVERSING"
PA 27757,999830
BG
AM
WT 18500
MG " "
MG "AT STATION 6"
WT 120000
```

```
MG "TRAVERSING"
PA 139250,999830
BG
AM
WT 24000
MG " "
MG "AT STATION 7"
WT 120000
MG "TRAVERSING"
PA 139250,864016
BG
AM
WT 17400
MG " "
MG "AT STATION 8"
WT 120000
MG "TRAVERSING"
PA 139250,652434
BG
AM
WT 13400
MG " "
MG "AT STATION 9"
WT 120000
MG "TRAVERSING"
PA 139250,413491
BG
AM
WT 11300
MG " "
MG "AT STATION 10"
WT 120000
MG "TRAVERSING"
PA 139250,201909
BG
AM
WT 14700
MG " "
MG "AT STATION 11"
WT 120000
MG "TRAVERSING"
PA 139250,66095
BG
AM
WT 25000
MG " "
MG "AT STATION 12"
WT 120000
MG "TRAVERSING"
PA 312944,66095
BG
AM
WT 15500
MG " "
MG "AT STATION 13"
WT 120000
MG "TRAVERSING"
PA 312944,201909
BG
AM
WT 24200
MG " "
MG "AT STATION 14"
WT 120000
MG "TRAVERSING"
PA 312944,413491
BG
```

```
AM
WT 13000
MG " "
MG "AT STATION 15"
WT 120000
MG "TRAVERSING"
PA 312944,652434
BG
AM
WT 11100
MG " "
MG "AT STATION 16"
WT 120000
MG "TRAVERSING"
PA 312944,864016
BG
AM
WT 12400
MG " "
MG "AT STATION 17"
WT 120000
MG "TRAVERSING"
PA 312944,999830
BG
AM
WT 18500
MG " "
MG "AT STATION 18"
WT 120000
MG "TRAVERSING"
PA 509100,999830
BG
AM
WT 13300
MG " "
MG "AT STATION 19"
WT 120000
MG "TRAVERSING"
PA 509100,864016
BG
AM
WT 17400
MG " "
MG "AT STATION 20"
WT 120000
MG "TRAVERSING"
PA 509100,652434
BG
AM
WT 13400
MG " "
MG "AT STATION 21"
WT 120000
MG "TRAVERSING"
PA 509100,413491
BG
AM
WT 11300
MG " "
MG "AT STATION 22"
WT 120000
MG "TRAVERSING"
PA 509100,201909
BG
AM
WT 14700
MG " "
```

```
MG "AT STATION 23"
WT 120000
MG "TRAVERSING"
PA 509100,66095
BG
AM
WT 25000
MG " "
MG "AT STATION 24"
WT 120000
MG "TRAVERSING"
PA 682794,66095
BG
AM
WT 15100
MG " "
MG "AT STATION 25"
WT 120000
MG "TRAVERSING"
PA 682794,201909
BG
AM
WT 22000
MG " "
MG "AT STATION 26"
WT 120000
MG "TRAVERSING"
PA 682794,413491
BG
AM
WT 13000
MG " "
MG "AT STATION 27"
WT 120000
MG "TRAVERSING"
PA 682794,652434
BG
AM
WT 11100
MG " "
MG "AT STATION 28"
WT 120000
MG "TRAVERSING"
PA 682794,864016
BG
AM
WT 12400
MG " "
MG "AT STATION 29"
WT 120000
MG "TRAVERSING"
PA 682794,999830
BG
AM
WT 18500
MG " "
MG "AT STATION 30"
WT 120000
MG "TRAVERSING"
PA 794287,999830
BG
AM
WT 18100
MG " "
MG "AT STATION 31"
WT 120000
MG "TRAVERSING"
```

```
PA 794287,864016
BG
AM
WT 17400
MG " "
MG "AT STATION 32"
WT 120000
MG "TRAVERSING"
PA 794287,652434
BG
AM
WT 13400
MG " "
MG "AT STATION 33"
WT 120000
MG "TRAVERSING"
PA 794287,413491
BG
AM
WT 11300
MG " "
MG "AT STATION 34"
WT 120000
MG "TRAVERSING"
PA 794287,201909
BG
AM
WT 14700
MG " "
MG "AT STATION 35"
WT 120000
MG "TRAVERSING TO LAST STAION"
PA 794287,66095
BG
AM
WT 25000
MG " "
MG "AT STATION 36 (LAST ONE)"
WT 120000
MG "STOP LOGGING ADV DATA"
MG "RETURNING TO STATION 0000"
PA 0,0
BG
AM
MG " "
MG "AT STATION 0, PROGRAM COMPLETE"
MG " "
EN
```

```
#ASME
KI 1,1
TL 9.5,9.5
ER 1000, 1000
OE 1,1
SP 16000, 16000
AC 4000, 4000
DC 4000, 4000
MG " "
MG "ASME -26 PT GAUSS-Q"
MG "2 MIN/STA"
MG " "
MG "CHECK ADV"
MG "VERIFY AT STATION 00000"
MG " "
MG "IF NOT, RESET DMC NOW!"
WT 4000
MG "POSITION SET TO 0,0"
MG "TRAVERSING"
PA 75628,66299
BG
AM
WT 21000
MG "AT STATION 1"
MG "START ADV"
WT 120000
MG "TRAVERSING"
PA 75628,124407
BG
AM
WT 23000
MG " "
MG "AT STATION 2"
WT 120000
MG "TRAVERSING"
PA 75628,282623
BG
AM
WT 16200
MG " "
MG "AT STATION 3"
WT 120000
MG "TRAVERSING"
PA 75628,532961
BG
AM
WT 10800
MG " "
MG "AT STATION 4"
WT 120000
MG "TRAVERSING"
PA 75628,783301
BG
AM
WT 10100
MG " "
MG "AT STATION 5"
WT 120000
MG "TRAVERSING"
PA 75628,941515
BG
AM
WT 16400
MG " "
MG "AT STATION 6"
WT 120000
MG "TRAVERSING"
```

```
PA 75628,999594
BG
AM
WT 23000
MG " "
MG "AT STATION 7"
WT 120000
MG "TRAVERSING"
PA 302101,999594
BG
AM
WT 11400
MG " "
MG "AT STATION 8"
WT 120000
MG "TRAVERSING"
PA 302101,783301
BG
AM
WT 12590
MG " "
MG "AT STATION 9"
WT 120000
MG "TRAVERSING"
PA 302101,665641
BG
AM
WT 18780
MG " "
MG "AT STATION 10"
WT 120000
MG "TRAVERSING"
PA 302101,400282
BG
AM
WT 10490
MG " "
MG "AT STATION 11"
WT 120000
MG "TRAVERSING"
PA 302101,282623
BG
AM
WT 18580
MG " "
MG "AT STATION 12"
WT 120000
MG "TRAVERSING"
PA 302101,66299
BG
AM
WT 12530
MG " "
MG "AT STATION 13"
WT 120000
MG "TRAVERSING"
PA 519943,66299
BG
AM
WT 13000
MG " "
MG "AT STATION 14"
WT 120000
MG "TRAVERSING"
PA 519943,282623
BG
AM
```

```
WT 12530
MG " "
MG "AT STATION 15"
WT 120000
MG "TRAVERSING"
PA 519943,400282
BG
AM
WT 18580
MG " "
MG "AT STATION 16"
WT 120000
MG "TRAVERSING"
PA 519943,665641
BG
AM
WT 10490
MG " "
MG "AT STATION 17"
WT 120000
MG "TRAVERSING"
PA 519943,783301
BG
AM
WT 18780
MG " "
MG "AT STATION 18"
WT 120000
MG "TRAVERSING"
PA 519943,999594
BG
AM
WT 12590
MG " "
MG "AT STATION 19"
WT 120000
MG "TRAVERSING"
PA 746416,999594
BG
AM
WT 11630
MG " "
MG "AT STATION 20"
WT 120000
MG "TRAVERSING"
PA 746416,941515
BG
AM
WT 23000
MG " "
MG "AT STATION 21"
WT 120000
MG "TRAVERSING"
PA 746416,783301
BG
AM
WT 16400
MG " "
MG "AT STATION 22"
WT 120000
MG "TRAVERSING"
PA 746416,532961
BG
AM
WT 10100
MG " "
MG "AT STATION 23"
```

```
WT 120000
MG "TRAVERSING"
PA 746416,282623
BG
AM
WT 10800
MG " "
MG "AT STATION 24"
WT 120000
MG "TRAVERSING"
PA 746416,124407
BG
AM
WT 16200
MG " "
MG "AT STATION 25"
WT 120000
MG "TRAVERSING"
PA 746416,66299
BG
AM
WT 23000
MG " "
MG "AT STATION 26 (LAST ONE)"
WT 120000
MG "STOP LOGGING ADV DATA"
MG "RETURNING TO STATION 0000"
PA 0,0
BG
AM
MG " "
MG "AT STATION 0, PROGRAM COMPLETE"
MG " "
EN
```

```
#GERM1
KI 1,1
TL 9.5,9.5
ER 1000, 1000
OE 1,1
SP 16000, 16000
AC 4000, 4000
DC 4000, 4000
MG " "
MG "GERMAN METHOD (GERM1)"
MG "2 MIN/STA"
MG " "
MG "CHECK ADV"
MG "VERIFY AT STATION 0"
MG " "
MG "IF NOT,RESET DMC NOW!"
WT 4000
DP 0,0
MG "POSITION SET TO 0,0"
MG "TRAVERSING"
PA 23486,66329
BG
AM
WT 10000
MG " "
MG "AT STATION 1"
MG "START ADV"
WT 120000
MG "TRAVERSING"
PA 23486,135423
BG
AM
WT 21020
MG "AT STATION 2"
WT 120000
MG "TRAVERSING"
PA 23486,271607
BG
AM
WT 17570
MG "AT STATION 3"
WT 120000
MG "TRAVERSING"
PA 23486,441838
BG
AM
WT 14990
MG "AT STATION 4"
WT 120000
MG "TRAVERSING"
PA 23486,635100
BG
AM
WT 13950
MG "AT STATION 5"
WT 120000
MG "TRAVERSING"
PA 23486,794316
BG
AM
WT 16490
MG "AT STATION 6"
WT 120000
MG "TRAVERSING"
PA 23486, 930500
BG
AM
```

```
WT 17100
MG "AT STATION 7"
WT 120000
MG "TRAVERSING"
PA 23486,989594
BG
AM
WT 21540
MG "AT STATION 8"
WT 120000
MG "TRAVERSING"
PA 70449,989594
BG
AM
WT 22140
MG "AT STATION 9"
WT 120000
MG "TRAVERSING"
PA 70449,930500
BG
AM
WT 21540
MG "AT STATION 10"
WT 120000
MG "TRAVERSING"
PA 70449,794316
BG
AM
WT 17100
MG "AT STATION 11"
WT 120000
MG "TRAVERSING"
PA 70449,635100
BG
AM
WT 16490
MG "AT STATION 12"
WT 120000
MG "TRAVERSING"
PA 70449,441838
BG
AM
WT 13950
MG "AT STATION 13"
WT 120000
MG "TRAVERSING"
PA 70449,271607
BG
AM
WT 14990
MG "AT STATION 14"
WT 120000
MG "TRAVERSING"
PA 70449,135423
BG
AM
WT 17570
MG "AT STATION 15"
WT 120000
MG "TRAVERSING"
PA 70449,66329
BG
AM
WT 21020
MG "AT STATION 16"
WT 120000
MG "Traversing"
```

```
PA 164401,66329
BG
AM
WT 18440
MG "AT STATION 17"
WT 120000
MG "TRAVERSING"
PA 164401,135423
BG
AM
WT 21020
MG "AT STATION 18"
WT 120000
MG "TRAVERSING"
PA 164401,271607
BG
AM
WT 17570
MG "AT STATION 19"
WT 120000
MG "TRAVERSING"
PA 164401,441838
BG
AM
WT 14990
MG "AT STATION 20"
WT 120000
MG "TRAVERSING"
PA 164401,635100
BG
AM
WT 13950
MG "AT STATION 21"
WT 120000
MG "TRAVERSING"
PA 164401,794316
BG
AM
WT 16490
MG "AT STATION 22"
WT 120000
MG "TRAVERSING"
PA 164401,930500
BG
AM
WT 17100
MG "AT STATION 23"
WT 120000
MG "TRAVERSING"
PA 164401,989594
BG
AM
WT 21540
MG "AT STATION 24"
WT 120000
MG "TRAVERSING"
PA 281838,989594
BG
AM
WT 17140
MG "AT STATION 25"
WT 120000
MG "TRAVERSING"
PA 281838,930500
BG
AM
WT 21540
```

```
MG "AT STATION 26"
WT 120000
MG "TRAVERSING"
PA 281838,794316
BG
AM
WT 17100
MG "AT STATION 27"
WT 120000
MG "TRAVERSING"
PA 281838,635100
BG
AM
WT 16490
MG "AT STATION 28"
WT 120000
MG "TRAVERSING"
PA 281838,441838
BG
AM
WT 13950
MG "AT STATION 29"
WT 120000
MG "TRAVERSING"
PA 281838,271607
BG
AM
WT 14990
MG "AT STATION 30"
WT 120000
MG "TRAVERSING"
PA 281838,135423
BG
AM
WT 17570
MG "AT STATION 31"
WT 120000
MG "TRAVERSING"
PA 281838,66329
BG
AM
WT 21020
MG "AT STATION 32"
WT 120000
MG "TRAVERSING"
PA 411022,66329
BG
AM
WT 17000
MG "AT STATION 33"
WT 120000
MG "TRAVERSING"
PA 411022,135423
BG
AM
WT 21020
MG "AT STATION 34"
WT 120000
MG "TRAVERSING"
PA 411022,271607
BG
AM
WT 17570
MG "AT STATION 35"
WT 120000
MG "TRAVERSING"
PA 411022,411838
```

```
BG
AM
WT 14990
MG "AT STATION 36 (LAST GERM1)"
WT 120000
MG "STOP LOGGING ADV DATA"
MG "LOAD GERM2"
EN
```

```
#GERM2
DP 411022,411838
MG "TRAVERSING TO STATION 37"
PA 411022,635100
BG
AM
WT 4000
MG "START ADV"
MG "AT STATION 37"
WT 120000
MG "TRAVERSING"
PA 411022,794316
BG
AM
WT 16490
MG "AT STATION 38"
WT 120000
MG "TRAVERSING"
PA 411022,930500
BG
AM
WT 17100
MG "AT STATION 39"
WT 120000
MG "TRAVERSING"
PA 411022,989594
BG
AM
WT 21540
MG "AT STATION 40"
WT 120000
MG "TRAVERSING"
PA 540165,989594
BG
AM
WT 16700
MG "AT STATION 41"
WT 120000
MG "TRAVERSING"
PA 540165,930500
BG
AM
WT 21540
MG "AT STATION 42"
WT 120000
MG "TRAVERSING"
PA 540165,794316
BG
AM
WT 17100
MG "AT STATION 43"
WT 120000
MG "TRAVERSING"
PA 540165,635100
BG
AM
WT 16490
MG "AT STATION 44"
WT 120000
MG "TRAVERSING"
PA 540165,441838
BG
AM
WT 13950
MG "AT STATION 45"
WT 120000
MG "TRAVERSING"
```

```
PA 540165,271607
BG
AM
WT 14990
MG "AT STATION 46"
WT 120000
MG "TRAVERSING"
PA 540165,135423
BG
AM
WT 17570
MG "AT STATION 47"
WT 120000
MG "TRAVERSING"
PA 540165,66329
BG
AM
WT 21020
MG "AT STATION 48"
WT 120000
MG "TRAVERSING"
PA 657635,66329
BG
AM
WT 17250
MG "AT STATION 49"
WT 120000
MG "TRAVERSING"
PA 657635,135423
BG
AM
WT 21020
MG "AT STATION 50"
WT 120000
MG "TRAVERSING"
PA 657635,271607
BG
AM
WT 17570
MG "AT STATION 51"
WT 120000
MG "TRAVERSING"
PA 657635,441838
BG
AM
WT 14990
MG "AT STATION 52"
WT 120000
MG "TRAVERSING"
PA 657635,635100
BG
AM
WT 13950
MG "AT STATION 53"
WT 120000
MG "TRAVERSING"
PA 657635,794316
BG
AM
WT 16490
MG "AT STATION 54"
WT 120000
MG "TRAVERSING"
PA 657635,930500
BG
AM
WT 17100
```

```
MG "AT STATION 55"
WT 120000
MG "TRAVERSING"
PA 657635,989594
BG
AM
WT 21540
MG "AT STATION 56"
WT 120000
MG "TRAVERSING"
PA 751587,989594
BG
AM
WT 19000
MG "AT STATION 57"
WT 120000
MG "TRAVERSING"
PA 751587,930500
BG
AM
WT 21020
MG "AT STATION 58"
WT 120000
MG "TRAVERSING"
PA 751587,794316
BG
AM
WT 17570
MG "AT STATION 59"
WT 120000
MG "TRAVERSING"
PA 751587,635100
BG
AM
WT 14990
MG "AT STATION 60"
WT 120000
MG "TRAVERSING"
PA 751587,441838
BG
AM
WT 13950
MG "AT STATION 61"
WT 120000
MG "TRAVERSING"
PA 751857,271607
BG
AM
WT 16490
MG "AT STATION 62"
WT 120000
MG "TRAVERSING"
PA 751857,135423
BG
AM
WT 17100
MG "AT STATION 63"
WT 120000
MG "TRAVERSING"
PA 751857,66329
BG
AM
WT 21540
MG "AT STATION 64"
WT 120000
MG "TRAVERSING"
PA 798534,66329
```

```
BG
AM
WT 22300
MG "AT STATION 65"
WT 120000
MG "TRAVERSING"
PA 798534,135423
BG
AM
WT 21020
MG "AT STATION 66"
WT 120000
MG "TRAVERSING"
PA 798534,271607
BG
AM
WT 17570
MG "AT STATION 67"
WT 120000
MG "TRAVERSING TO 68"
PA 798534,441838
BG
AM
WT 14990
MG "AT STATION 68"
WT 120000
MG "TRAVERSING"
PA 798534,635100
BG
AM
WT 13950
MG "AT STATION 69"
WT 120000
MG "TRAVERSING"
PA 798534,794316
BG
AM
WT 16490
MG "AT STATION 70"
WT 120000
MG "TRAVERSING"
PA 798534,930500
BG
AM
WT 17100
MG "AT STATION 71"
WT 120000
MG "TRAVERSING"
PA 798534,999594
BG
AM
WT 21540
MG "AT STATION 72(LAST)"
WT 120000
MG "STOP LOGGING DATA"
MG "RETURN TO 0,0"
PA 0,0
BG
AM
MG "END OF PROGRAM, AT 0,0"
EN
```

APPENDIX B

Laboratory Testing Results
Matlab™ Script Files for Data-Post Processing

Integration Method	File	Q calc	Q ref	
2x2	0605c	176.4	164.5	Favorable Flow
3x3	0605d	170.4	165.38	
4x4	0605e	168.3	165.08	
5x5	0605f	163	164.87	
6x6	0605g	152.5	165.71	
asme	0605h	118.2	165.96	
germ	0605i & j	171.6	166.43	
2x2	0606a	491	454.78	
3x3	0606b	469.3	454.2	
4x4	0606d	469.5	455.53	
5x5	0609a	460.8	455.68	
asme	0609b	329.4	459.28	
germ	0609c & d	478.4	457.18	
2x2	0610a	371	341.89	
3x3	0610b	354	342.34	
6x6	0610c	326.2	343.19	
asme	0610d	250.9	343.75	
germ	0610e & f	360.5	345.17	
5x5	0610g	343.6	345.58	
4x4	0610h	351.5	345.4	
germ	0613a & b	466.5	458.48	
germ	0614a & b	472.3	457.92	
2x2	0615a	462.9	456.46	
3x3	0615b	477.1	455.87	
4x4	0615c	461.1	456.87	
5x5	0615d	456.7	457.23	
6x6	0615e	443.5	458.31	
asme	0615f	353.9	458.98	
2x2	0616a	461.1	453.23	Disturbed Flow
3x3	0616b	462.2	454.01	
4x4	0616c	462	454.52	
5x5	0616d	451.9	455.13	
6x6	0616e	436.4	455.91	
asme	0616f	356.9	455.91	
germ	0616g & h	474.3	458.08	
2x2	0617a	361.1	338.39	
3x3	0617b	344.2	336.57	
3x3	0617c	348.3	337.4	
4x4	0617d	348	337.58	
5x5	0617e	344.7	338.53	
6x6	0618a	325.1	336.16	
asme	0618b	266.5	336.99	
germ	0618c & d	356	339.26	
2x2	0618e	183.1	174.73	
3x3	0618f	165.4	173.42	
4x4	0618g	180.4	174.28	
5x5	0618h	172.4	174.29	
6x6	0618i	160.2	174.23	
asme	0618j	132.1	174.68	
germ	0618k & l	180.5	174.83	
6x6	0611a	435.4	458.8	
2x2	0704a	470.8	460.68	
3x3	0704b	459.3	460.16	
4x4	0704c	464.5	462.29	
5x5	0704d	450.1	463.4	
6x6	0704e	432.7	464.87	
asme	0704f	475.2	466.06	
germ	0704g &h	481.9	464.94	
2x2	0707a	485.3	463.82	
3x3	0707b	456.4	461.77	
4x4	0707c	471.2	462.65	
5x5	0707d	451.2	464.22	
6x6	0707e	428.1	465.47	
asme	0707f	469.8	466.1	
germ	0707g &h	479.7	468.44	
germ	0708a & b	477.6	465.12	

```
%***********************************************
%This function calculates the discharge
%for gauss 2x2 distribution.
%It is called by the matlab script file adv.m
%***********************************************
%Load data files

load sontek\adv0707a.vel;
veldat=adv0707a(:,4)/100; %convert from cm/s to m/s

startline=660
endline=1080

for position=1:4;
                        vel(position)=mean(veldat(startline:endline));
                                    startline=endline+1920;
                                    endline=startline+1080;
end


vel=vel';

vel2=vel;
%%*****************************************************************************************
%
%
%The following portion of the script file is used to re-arrange the
%velocity measurements into the correct order to be used in the
%integration of the velocity profile.
%
%for 2x2 the measured points are ordered as follows:
%                                          1,2,4,3

%define 2 vectors for each set of positions
%vel##a is the original data file, without re-arrangement of velocities
%vel##m is the manipulated data file.
%Vel####m is a nxm array of velocity measurements.

vel2a=vel2;
vel2m(1,2)=vel2a(3);
vel2m(2,2)=vel2a(4);
vel2m(1,1)=vel2a(1);
vel2m(2,1)=vel2a(2);

%The following is the code for GQ integration:
%
%gx=vel2m*wx;
%gy=gx.*wy;
%qgl2=sum(gy)*(0.5*(bx-ax)*0.5*(by-ay));

%Transforming the positions to -1 to +1 requires the following equation
%xd=2x-(b+a)/(b-a)
%where x is the measured position,
%a and b are the limits of the integral
%xd is the required position between -1 and +1
%The velocity measurements were made at the specified GQ locations.
%So no transforms are needed in post processing.
%
%The dimensions of the intake are:
%

                                          ax=0
                                          ay=0
                                         bx=1.04
                                         by=1.27

                                  [bf2,wf2]=gaussint(-1,+1,2);
```

```
                                        gx=vel2m*wf2;
    gy=gx.*wf2;
    qgl2=sum(gy)*(0.5*(bx-ax)*0.5*(by-ay))
                              save qgl2 qgl2 -ascii -double -tabs
end
```

```
%function Gauss3(n)

%*********************************************
%This function calculates the discharge
%for gauss 3x3 distribution.
%It is called by the matlab script file adv.m
%*********************************************
 %*************************************************************************************
%Load data files
load sontek\adv0707b.vel;
veldat=adv0707b(:,4)/100;

startline=660
endline=1080

for position=1:9;
                      vel(position)=mean(veldat(startline:endline));
                                  startline=endline+1920;
                                  endline=startline+1080;
end

vel=vel';
vel3=vel;

%*************************************************************************************
%
%
%The following portion of the script file is used to re-arrange the
%velocity measurements into the correct order to be used in the
%integration of the velocity profile.
%for 3x3 the measured points are ordered as follows:
%                                    1,2,3,6,5,4,7,8,9
%define 2 vectors for each set of positions
%vel##a is the original data file, without re-arrangement of velocities
%vel##m is the manipulated data file.
%Vel####m is a nxm array of velocity measurements.

vel3a=vel3;
vel3m(1,2)=vel3a(6);
vel3m(2,2)=vel3a(5);
vel3m(3,2)=vel3a(4);
vel3m(1,1)=vel3a(1);
vel3m(2,1)=vel3a(2);
vel3m(3,1)=vel3a(3);
vel3m(1,3)=vel3a(7);
vel3m(2,3)=vel3a(8);
vel3m(3,3)=vel3a(9);

%The following is the code for GQ integration:
%
[bp3,wf3]=gaussint(-1,+1,3);
%gx=vel3m*wx;
%gy=gx.*wy;
%qql3=sum(gy)*(0.5*(bx-ax)*0.5*(by-ay));

%Transforming the positions to -1 to +1 requries the following equation
%xd=2x-(b+a)/(b-a)
%where x is the measured position,
%a and b are the limits of the integral
%xd is the required position between -1 and +1
%The velocity measurements were made at the specified GQ locations.
%So no transforms are needed in post processing.
%
%The dimensions of the intake are:
%
                                        ax=0
```

```
                                        ay=0
                                       bx=1.04
                                       by=1.27

                                    gx=vel3m*wf3;
    gy=gx.*wf3;
    qgl3=sum(gy)*(0.5*(bx-ax)*0.5*(by-ay))
                            save qgl3 qgl3 -ascii -double -tabs
end
```

```
%*********************************************
%This function calculates the discharge
%for gauss 4x4 distribution.
%It is called by the matlab script file adv.m
%*********************************************

%Load data files
load sontek\adv0704c.vel;
veldat=adv0704c(:,4)/100;

startline=660;
endline=1080;

for position=1:16;
                    vel(position)=mean(veldat(startline:endline));
                              startline=endline+1920;
                              endline=startline+1080;
end


vel=vel';
vel4=vel;

%*************************************************************************************
%
%
%The following portion of the script file is used to re-arrange the
%velocity measurements into the correct order to be used in the
%integration of the velocity profile.
%for 4x4 the measured points are ordered as follows:
%                         1,2,3,4,8,7,6,5,9,10,11,12,16,15,14,13
%define 2 vectors for each set of positions
%vel##a is the original data file, without re-arrangement of velocities
%vel##m is the manipulated data file.
%Vel####m is a nxm array of velocity measurements.

vel4a=vel4;
vel4m(1,2)=vel4a(8);
vel4m(2,2)=vel4a(7);
vel4m(3,2)=vel4a(6);
vel4m(4,2)=vel4a(5);
vel4m(1,4)=vel4a(16);
vel4m(2,4)=vel4a(15);
vel4m(3,4)=vel4a(14);
vel4m(4,4)=vel4a(13);
vel4m(1,1)=vel4a(1);
vel4m(2,1)=vel4a(2);
vel4m(3,1)=vel4a(3);
vel4m(4,1)=vel4a(4);
vel4m(1,3)=vel4a(9);
vel4m(2,3)=vel4a(10);
vel4m(3,3)=vel4a(11);
vel4m(4,3)=vel4a(12);

%The following is the code for GQ integration:
%

%gx=vel4m*wx;
%gy=gx.*wy;
%qgl4=sum(gy)*(0.5*(bx-ax)*0.5*(by-ay));

%Transforming the positions to -1 to +1 requries the following equation
%xd=2x-(b+a)/(b-a)
%where x is the measured position,
%a and b are the limits of the integral
%xd is the required position between -1 and +1
%The velocity measurements were made at the specified GQ locations.
```

```
%So no transforms are needed in post processing.
%
%The dimensions of the intake are:
%
                                        ax=0    ;
                                         ay=0   ;
                                        bx=1.04;
                                        by=1.27;

                                    [bf,wf]=gaussint(-1,+1,4);

                                          gx=vel4m*wf;
    gy=gx.*wf;
    qgl4=sum(gy)*(0.5*(bx-ax)*0.5*(by-ay))
                                save qgl4 qgl4 -ascii -double -tabs
end
```

```
%*********************************************

%This function calculates the discharge

%for gauss 5x5 distribution.

%It is called by the matlab script file adv.m
%*********************************************
%*****************************************************************************************
%Load data files
load sontek\adv0707d.vel;
veldat=adv0707d(:,4)/100;

startline=660
endline=1080

for position=1:25;
                        vel(position)=mean(veldat(startline:endline))
                                    startline=endline+1920
                                    endline=startline+1080
end

vel=vel';
vel5=vel;

%*****************************************************************************************
%
%
%The following portion of the script file is used to re-arrange the
%velocity measurements into the correct order to be used in the
%integration of the velocity profile.
%for 5x5 the measured points are ordered as follows:
%           1,2,3,4,10,9,8,7,6,11,12,13,14,15,20,19,18,17,16,21,22,23,24,25
%define 2 vectors for each set of positions
%vel##a is the original data file, without re-arrangement of velocities
%vel##m is the manipulated data file.
%Vel####m is a nxm array of velocity measurements.

vel5a=vel5;
vel5m(1,2)=vel5a(10);
vel5m(2,2)=vel5a(9);
vel5m(3,2)=vel5a(8);
vel5m(4,2)=vel5a(7);
vel5m(5,2)=vel5a(6);
vel5m(1,4)=vel5a(20);
vel5m(2,4)=vel5a(19);
vel5m(3,4)=vel5a(18);
vel5m(4,4)=vel5a(17);
vel5m(5,4)=vel5a(16);
vel5m(1,1)=vel5a(1);
vel5m(2,1)=vel5a(2);
vel5m(3,1)=vel5a(3);
vel5m(4,1)=vel5a(4);
vel5m(5,1)=vel5a(5);
vel5m(1,3)=vel5a(11);
vel5m(2,3)=vel5a(12);
vel5m(3,3)=vel5a(13);
vel5m(4,3)=vel5a(14);
vel5m(5,3)=vel5a(15);
vel5m(1,5)=vel5a(21);
vel5m(2,5)=vel5a(22);
vel5m(3,5)=vel5a(23);
vel5m(4,5)=vel5a(24);
vel5m(5,5)=vel5a(25);

%The following is the code for GQ integration:
%
```

```
[bp5,wf5]=gaussint(-1,+1,5);

%gx=vel5m*wx;
%gy=gx.*wy;
%qgl5=sum(gy)*(0.5*(bx-ax)*0.5*(by-ay));

%Transforming the positions to -1 to +1 requries the following equation
%xd=2x-(b+a)/(b-a)
%where x is the measured position,
%a and b are the limits of the integral
%xd is the required position between -1 and +1
%The velocity measurements were made at the specified GQ locations.
%So no transforms are needed in post processing.
%
%The dimensions of the intake are:
%

                                          ax=0
                                          ay=0
                                         bx=1.04
                                         by=1.27

                                       gx=vel5m*wf5;
    gy=gx.*wf5;
    qgl5=sum(gy)*(0.5*(bx-ax)*0.5*(by-ay))
                              save qgl5 qgl5 -ascii -double -tabs
end
```

```
%*********************************************
%This function calculates the discharge
%for gauss 6x6 distribution.
%It is called by the matlab script file adv.m
%
%*****************************************************************************
%Load data files
load sontek\adv0610c.vel;
veldat=adv0610c(:,4)/100;

startline=660
endline=1080

for position=1:36;
                    vel(position)=mean(veldat(startline:endline));
                              startline=endline+1920;
                              endline=startline+1080;
end



vel=vel';
vel6=vel;

%*****************************************************************************
%
%
%The following portion of the script file is used to re-arrange the
%velocity measurements into the correct order to be used in the
%integration of the velocity profile.
%for 6x6 the measured points are ordered as follows:
%              1,2,3,4,5,6,12,11,10,9,8,7,13,14,15,16,17,18,24,23,22,21,20,
%                        19,25,26,27,28,29,30,36,35,34,33,32,31
%define 2 vectors for each set of positions
%vel##a is the original data file, without re-arrangement of velocities
%vel##m is the manipulated data file.
%Vel####m is a nxm array of velocity measurements.

vel6a=vel6;
vel6m(1,2)=vel6a(12);
vel6m(2,2)=vel6a(11);
vel6m(3,2)=vel6a(10);
vel6m(4,2)=vel6a(9);
vel6m(5,2)=vel6a(8);
vel6m(6,2)=vel6a(7);
vel6m(1,4)=vel6a(24);
vel6m(2,4)=vel6a(23);
vel6m(3,4)=vel6a(22);
vel6m(4,4)=vel6a(21);
vel6m(5,4)=vel6a(20);
vel6m(6,4)=vel6a(19);
vel6m(1,6)=vel6a(36);
vel6m(2,6)=vel6a(35);
vel6m(3,6)=vel6a(34);
vel6m(4,6)=vel6a(33);
vel6m(5,6)=vel6a(32);
vel6m(6,6)=vel6a(31);
vel6m(1,1)=vel6a(1);
vel6m(2,1)=vel6a(2);
vel6m(3,1)=vel6a(3);
vel6m(4,1)=vel6a(4);
vel6m(5,1)=vel6a(5);
vel6m(6,1)=vel6a(6);
vel6m(1,3)=vel6a(13);
vel6m(2,3)=vel6a(14);
vel6m(3,3)=vel6a(15);
vel6m(4,3)=vel6a(16);
```

```
vel6m(5,3)=vel6a(17);
vel6m(6,3)=vel6a(18);
vel6m(1,5)=vel6a(25);
vel6m(2,5)=vel6a(26);
vel6m(3,5)=vel6a(27);
vel6m(4,5)=vel6a(28);
vel6m(5,5)=vel6a(29);
vel6m(6,5)=vel6a(30);

%The following is the code for GQ integration:
%
[bp6,wf6]=gaussint(-1,+1,6);

%gx=vel6m*wx;
%gy=gx.*wy;
%qgl6=sum(gy)*(0.5*(bx-ax)*0.5*(by-ay));

%Transforming the positions to -1 to +1 requries the following equation
%xd=2x-(b+a)/(b-a)
%where x is the measured position,
%a and b are the limits of the integral
%xd is the required position between -1 and +1
%The velocity measurements were made at the specified GQ locations.
%So no transforms are needed in post processing.
%
%The dimensions of the intake are:
%

                                        ax=0
                                        ay=0
                                       bx=1.04
                                       by=1.27

                                    gx=vel6m*wf6;
    gy=gx.*wf6;
    qgl6=sum(gy)*(0.5*(bx-ax)*0.5*(by-ay))
                              save qgl6 qgl6 -ascii -double -tabs

end
```

```
%*********************************************
%This function calculates the discharge
%for the asme distribution.
%It is called by the matlab script file adv.m
%*****************************************************************************
%Load data files
load sontek\adv0707f.vel;
veldat=adv0707f(:,4)/100;

startline=660
endline=1080

for position=1:26;
                    vel(position)=mean(veldat(startline:endline));
                              startline=endline+1920;
                              endline=startline+1080;
end

vel=vel';
vel=vel';
velasa=vel;

%*****************************************************************************
%
%
%The following portion of the script file is used to re-arrange the
%velocity measurements into the correct order to be used in the
%integration of the velocity profile.
%for ASME the measured points are ordered as follows:
%for ASME the measured points are ordered as follows:
%          1,2,3,4,5,6,7,13,12,11,10,9,8,14,15,16,17,18,19,26,25,24,23,22,21,20
%define 2 vectors for each set of positions
%vel##a is the original data file, without re-arrangement of velocities
%vel##m is the manipulated data file.
%Vel####m is a nxm array of velocity measurements.

velasm(1,1)=velasa(1);
velasm(2,1)=velasa(2);
velasm(3,1)=velasa(3);
velasm(4,1)=0;
velasm(5,1)=velasa(4);
velasm(6,1)=0;
velasm(7,1)=velasa(5);
velasm(8,1)=velasa(6);
velasm(9,1)=velasa(7);
velasm(1,2)=velasa(13);
velasm(2,2)=0;
velasm(3,2)=velasa(12);
velasm(4,2)=velasa(11);
velasm(5,2)=0;
velasm(6,2)=velasa(10);
velasm(7,2)=velasa(9);
velasm(8,2)=0;
velasm(9,2)=velasa(8);
velasm(1,3)=velasa(14);
velasm(2,3)=0;
velasm(3,3)=velasa(15);
velasm(4,3)=velasa(16);
velasm(5,3)=0;
velasm(6,3)=velasa(17);
velasm(7,3)=velasa(18);
velasm(8,3)=0;
velasm(9,3)=velasa(19);
velasm(1,4)=velasa(26);
velasm(2,4)=velasa(25);
velasm(3,4)=velasa(24);
velasm(4,4)=0;
```

```
velasm(5,4)=velasa(23);
velasm(6,4)=0;
velasm(7,4)=velasa(22);
velasm(8,4)=velasa(21);
velasm(9,4)=velasa(20);


%The dimensions of the intake are:
%
                                        ax=0
                                        ay=0
                                      bx=1.04;
                                      by=1.27;

%**********************ASME log-linear integration**********************************
%The ASME integration method is based on using a weighted average of velocity
%measurements across the intake.
%Greater emphasis is placed on the velocities measured in proximity to the boundaries.
%Less emphasis is placed on the velocities measured near the center of the intake where
%the flow is assumed to be more uniform.
%The ASME distribution of metering points is based on the assumption that the flow
%profile can be represented by a 1/7th power law.

    asmwt=[2 3 3 2;2 0 0 2;5 3 3 5;0 6 6 0;6 0 0 6; 0 6 6 0;5 3 3 5;2 0 0 2;2 3 3 2];
mult=velasm(1,1)*asmwt(1,1)+velasm(1,2)*asmwt(1,2)+velasm(1,3)*asmwt(1,3)+velasm(1,4)*asm
wt(1,4)+velasm(2,1)*asmwt(2,1)+velasm(2,2)*asmwt(2,2)+velasm(2,3)*asmwt(2,3)+velasm(2,4)*
asmwt(2,4)+velasm(3,1)*asmwt(3,1)+velasm(3,2)*asmwt(3,2)+velasm(3,3)*asmwt(3,3)+velasm(3,
4)*asmwt(3,4)+velasm(4,1)*asmwt(4,1)+velasm(4,2)*asmwt(4,2)+velasm(4,3)*asmwt(4,3)+velasm
(4,4)*asmwt(4,4)+velasm(5,1)*asmwt(5,1)+velasm(5,2)*asmwt(5,2)+velasm(5,3)*asmwt(5,3)+vel
asm(5,4)*asmwt(5,4)+velasm(6,1)*asmwt(6,1)+velasm(6,2)*asmwt(6,2)+velasm(6,3)*asmwt(6,3)+
velasm(6,4)*asmwt(6,4)+
velasm(7,1)*asmwt(7,1)+velasm(7,2)*asmwt(7,2)+velasm(7,3)*asmwt(7,3)+velasm(7,4)*asmwt(7,
4)+velasm(8,1)*asmwt(8,1)+velasm(8,2)*asmwt(8,2)+velasm(8,3)*asmwt(8,3)+velasm(8,4)*asmwt
(8,4)+velasm(9,1)*asmwt(9,1)+velasm(9,2)*asmwt(9,2)+velasm(9,3)*asmwt(9,3)+velasm(9,4)*as
mwt(9,4);
                                    qasm=(mult/96)*1.04*1.27;
                                save qasm qasm -ascii -double -tabs

end
```

```
%function qgerm=germ(n,veldat,vel);

%*********************************************

%function germ(n,veldat,vel);

%This function calculates the dishcarge

%for the asme distribution.

%It is called by the matlab script file adv.m
%*********************************************
%Load the data files:
load sontek\adv0708a.vel; %for Germ1
veldat1=adv0708a(:,4)/100;

load sontek\adv0708b.vel; %for Germ2
veldat2=adv0708b(:,4)/100;

n=36
startline=660
endline=1080

for position=1:36;
                    vel1(position)=mean(veldat1(startline:endline));
                                startline=endline+1920;
                                endline=startline+1080;
end

startline=660
endline=1080

for position=1:36;
                    vel2(position)=mean(veldat2(startline:endline));
                                startline=endline+1920;
                                endline=startline+1080;
end

vel1=vel1';
vel2=vel2';
%velgerm=vel;
vel=[vel1;vel2]; %concatenate Germ1 and Germ2

%*******************German Integration*********************************************
%The German integration method is based on calculating flow through three
%representative flow areas; edge, corner, and center.
%The shape of the elements, as well as the distribution of metering points
%is based on a flow profile which can be represented by a 1/7th power law.
%
%The formula for edge elements is given by:
%
%                                          W and H are the width and height dimensions of the eleme
%                                                                          V=(V1+V2)/2
%The formula for corner elements is given by:
%
%                                          W and H are the width and height dimensions of the eleme
%                                                    V is the velocity at the corner
%The formula for center elements is given by:
%
%                                                                      V=(V1+V2+V3+V4)/4
%                                          W and H are the width and height dimensions of the eleme

%The *0.01 at the end of each element discharge
%equation is to convert the velocity from cm/s to m/s.
%All element dimensions are in meters.
%The resulting discharge will be in cms.
%
```

```
%*************************************************************************
%                                                                    Edge
%
                velgerm(1)=((vel(1)+vel(2))/2)*29.8e-3*87.75e-3*7/8;
                velgerm(2)=(vel(3)+vel(2))/2*29.8e-3*172.95e-3*7/8;
                velgerm(3)=(vel(3)+vel(4))/2*29.8e-3*216.19e-3*7/8;
                velgerm(4)=(vel(4)+vel(5))/2*29.8e-3*245.4e-3*7/8;
                velgerm(5)=(vel(5)+vel(6))/2*29.8e-3*202.2e-3*7/8;
                velgerm(6)=(vel(7)+vel(6))/2*29.8e-3*375.16e-3*7/8;
                velgerm(7)=(vel(7)+vel(8))/2*29.8e-3*87.75e-3*7/8;
                velgerm(8)=(vel(8)+vel(9))/2*59.64e-3*52e-3*7/8;
                velgerm(9)=(vel(24)+vel(9))/2*119.32e-3*52e-3*7/8;
               velgerm(10)=(vel(24)+vel(25))/2*149.14e-3*52e-3*7/8;
                velgerm(11)=(vel(25)+vel(40))/2*164.1e-3*52e-3*7/8;
                velgerm(12)=(vel(41)+vel(40))/2*164.1e-3*52e-3*7/8;
                velgerm(13)=(vel(41)+vel(56))/2*149.2e-3*52e-3*7/8;
               velgerm(14)=(vel(56)+vel(57))/2*119.32e-3*52e-3*7/8;
                velgerm(15)=(vel(57)+vel(72))/2*59.6e-3*52e-3*7/8;
              velgerm(16)=(vel(72)+vel(71))/2*29.86e-3*87.75e-3*7/8;
             velgerm(17)=(vel(70)+vel(71))/2*172.95e-3*29.86e-3*7/8;
              velgerm(18)=(vel(70)+vel(69))/2*202.2e-3*29.86e-3*7/8;
              velgerm(19)=(vel(69)+vel(68))/2*245.4e-3*29.86e-3*7/8;
              velgerm(20)=(vel(68)+vel(67))/2*216.2e-3*29.86e-3*7/8;
             velgerm(21)=(vel(67)+vel(66))/2*172.95e-3*29.86e-3*7/8;
              velgerm(22)=(vel(66)+vel(65))/2*87.75e-3*29.86e-3*7/8;

%*************************************************************************
%                                                          Center Elements
%
%The heights and widths of the center elements are given in
%vectors germh and germw respectively.

          germw=[0.05964,0.11932,0.2685,0.1641,0.164,0.1492,0.1197,0.0596];
           germh=[0.08775,0.17295,0.21619,0.24544,0.20220,0.17295,0.08775];

           velgerm(23)=(vel(1)+vel(16)+vel(2)+vel(15))/4*germh(1)*germw(1);
           velgerm(24)=(vel(2)+vel(15)+vel(3)+vel(14))/4*germh(2)*germw(1);
           velgerm(25)=(vel(3)+vel(4)+vel(13)+vel(14))/4*germh(3)*germw(1);
           velgerm(26)=(vel(4)+vel(13)+vel(12)+vel(5))/4*germh(4)*germw(1);
           velgerm(27)=(vel(5)+vel(11)+vel(12)+vel(6))/4*germh(5)*germw(1);
           velgerm(28)=(vel(7)+vel(11)+vel(10)+vel(6))/4*germh(6)*germw(1);
            velgerm(29)=(vel(7)+vel(8)+vel(10)+vel(9))/4*germh(7)*germw(1);
          velgerm(30)=(vel(15)+vel(16)+vel(17)+vel(18))/4*germw(2)*germh(1);
          velgerm(31)=(vel(15)+vel(18)+vel(14)+vel(19))/4*germw(2)*germh(2);
          velgerm(32)=(vel(14)+vel(19)+vel(13)+vel(20))/4*germw(2)*germh(3);
          velgerm(33)=(vel(12)+vel(21)+vel(13)+vel(20))/4*germw(2)*germh(4);
          velgerm(34)=(vel(12)+vel(21)+vel(11)+vel(22))/4*germw(2)*germh(5);
          velgerm(35)=(vel(11)+vel(22)+vel(10)+vel(23))/4*germw(2)*germh(6);
           velgerm(36)=(vel(10)+vel(23)+vel(9)+vel(24))/4*germw(2)*germh(7);
          velgerm(37)=(vel(17)+vel(32)+vel(18)+vel(31))/4*germw(3)*germh(1);
          velgerm(38)=(vel(18)+vel(31)+vel(19)+vel(30))/4*germw(3)*germh(2);
          velgerm(39)=(vel(19)+vel(30)+vel(20)+vel(29))/4*germw(3)*germh(3);
          velgerm(40)=(vel(20)+vel(29)+vel(21)+vel(28))/4*germw(3)*germh(4);
          velgerm(41)=(vel(21)+vel(28)+vel(22)+vel(27))/4*germw(3)*germh(5);
          velgerm(42)=(vel(22)+vel(27)+vel(23)+vel(26))/4*germw(3)*germh(6);
          velgerm(42)=(vel(23)+vel(24)+vel(25)+vel(26))/4*germw(3)*germh(7);
          velgerm(43)=(vel(31)+vel(32)+vel(33)+vel(34))/4*germw(4)*germh(1);
          velgerm(44)=(vel(30)+vel(31)+vel(34)+vel(35))/4*germw(4)*germh(2);
          velgerm(45)=(vel(30)+vel(35)+vel(29)+vel(36))/4*germw(4)*germh(3);
          velgerm(46)=(vel(29)+vel(36)+vel(28)+vel(37))/4*germw(4)*germh(4);
          velgerm(47)=(vel(27)+vel(28)+vel(37)+vel(38))/4*germw(4)*germh(5);
          velgerm(48)=(vel(27)+vel(38)+vel(26)+vel(39))/4*germw(4)*germh(6);
          velgerm(49)=(vel(26)+vel(29)+vel(25)+vel(40))/4*germw(4)*germh(7);
          velgerm(50)=(vel(33)+vel(48)+vel(34)+vel(47))/4*germw(5)*germh(1);
          velgerm(51)=(vel(34)+vel(47)+vel(35)+vel(46))/4*germw(5)*germh(2);
          velgerm(52)=(vel(35)+vel(46)+vel(36)+vel(45))/4*germw(5)*germh(3);
          velgerm(53)=(vel(36)+vel(45)+vel(37)+vel(44))/4*germw(5)*germh(4);
```

```
velgerm(54)=(vel(37)+vel(44)+vel(38)+vel(43))/4*germw(5)*germh(5);
velgerm(55)=(vel(38)+vel(43)+vel(39)+vel(42))/4*germw(5)*germh(6);
velgerm(56)=(vel(39)+vel(42)+vel(40)+vel(41))/4*germw(5)*germh(7);
velgerm(57)=(vel(48)+vel(49)+vel(47)+vel(50))/4*germw(6)*germh(1);
velgerm(58)=(vel(47)+vel(50)+vel(46)+vel(51))/4*germw(6)*germh(2);
velgerm(59)=(vel(46)+vel(51)+vel(45)+vel(52))/4*germw(6)*germh(3);
velgerm(60)=(vel(45)+vel(52)+vel(44)+vel(53))/4*germw(6)*germh(4);
velgerm(61)=(vel(44)+vel(53)+vel(43)+vel(54))/4*germw(6)*germh(5);
velgerm(62)=(vel(43)+vel(54)+vel(42)+vel(54))/4*germw(6)*germh(6);
velgerm(63)=(vel(42)+vel(55)+vel(41)+vel(56))/4*germw(6)*germh(7);
velgerm(64)=(vel(49)+vel(64)+vel(50)+vel(63))/4*germw(7)*germh(1);
velgerm(65)=(vel(50)+vel(63)+vel(51)+vel(62))/4*germw(7)*germh(2);
velgerm(66)=(vel(51)+vel(62)+vel(52)+vel(61))/4*germw(7)*germh(3);
velgerm(67)=(vel(52)+vel(61)+vel(53)+vel(60))/4*germw(7)*germh(4);
velgerm(68)=(vel(53)+vel(60)+vel(54)+vel(59))/4*germw(7)*germh(5);
velgerm(69)=(vel(54)+vel(59)+vel(55)+vel(58))/4*germw(7)*germh(6);
velgerm(70)=(vel(55)+vel(58)+vel(56)+vel(57))/4*germw(7)*germh(7);
velgerm(71)=(vel(63)+vel(64)+vel(65)+vel(66))/4*germw(8)*germh(1);
velgerm(72)=(vel(63)+vel(62)+vel(67)+vel(66))/4*germw(8)*germh(2);
velgerm(73)=(vel(61)+vel(62)+vel(67)+vel(68))/4*germw(8)*germh(3);
velgerm(74)=(vel(60)+vel(61)+vel(68)+vel(69))/4*germw(8)*germh(4);
velgerm(75)=(vel(60)+vel(69)+vel(59)+vel(70))/4*germw(8)*germh(5);
velgerm(76)=(vel(59)+vel(70)+vel(58)+vel(71))/4*germw(8)*germh(6);
velgerm(77)=(vel(58)+vel(71)+vel(57)+vel(72))/4*germw(8)*germh(7);

%*****************************************************************************
%                                                                  Corner Elements
%
%The formula for corner elements is given by:
%                                                                      49/60*V*H*W
%
%where:                          v is the corner velocity
%                                                          H is the element height
%                                                           W is the element width

                        velgerm(78)=vel(1)*49/60*34.2e-3*29.83e-3;
                         velgerm(79)=vel(8)*49/60*52e-3*29.83e-3;
                        velgerm(80)=vel(72)*49/60*52e-3*29.86e-3;
                        velgerm(81)=vel(65)*49/60*52e-3*29.86e-3;
%*****************************************************************************
%                                                                  Total Discharge
%
%Total discharge is calculated as the summation of the individual flow elements.

                                  qgerm=sum(velgerm);
                            save qgerm qgerm -ascii -double -tabs

%*****************************************************************************
%The intake velocity profile for the intake is given by the matrix
%of velocities as measured by the German distribution of metering points.
%To plot the profile, the vector of German velocities must be rearranged
%into a matrix.
%The matrix is given by profile

%vel(25:32)=flipud(vel(25:32));
%vel(41:48)=flipud(vel(41:48));
%vel(57:64)=flipud(vel(57:64));

 profile(:,1)=flipud(vel(1:8));
 profile(:,2)=vel(9:16);
 profile(:,3)=flipud(vel(17:24));
  profile(:,4)=vel(25:32);
 profile(:,5)=flipud(vel(33:40));
 profile(:,6)=vel(41:48);
 profile(:,7)=flipud(vel(49:56));
 profile(:,8)=vel(57:64);
 profile(:,9)=flipud(vel(65:72));
```

```
 mesh(fliplr(profile))

end
```

List of all Laboratory Tests

APPENDIX C

MATLAB™ Script Files used for RDS Analysis

```
%This script file is used to calculate the RDS factor
%for each Ott meter test conducted at Kettle Generating Station.
%The RDS factor is taken as the integrated area under the velocity-
%horizontal position curve for a given elevation within the
%Ott meter traverse.

load rds1266.dat
vel3=rds1266*0.3048;
load rds924.dat;
vel1=rds924*0.3048;
load rds1158.dat;
vel2=rds1158*0.3048;

%The horizontal locations of the velocity measurements are:
xm=[0.02541942,    0.095577021,    0.21403152,    0.347229283,    0.499745806,    0.652262328,
0.78596848,0.904422979, 0.9745805];

% Define the required data points
xrqd=[0.025:0.01:0.974];

                                        for i=1:345
                                                zzj=spline(xm,vel3(i,:),xrqd);
                                                                        zzj=zzj';
                                              rdsfact(i)=trapz(xrqd,zzj)*5.69;
                                                                        clear zzj
                                            end


figure(1)
set(gca,'XTickLabels',[-1:0.5:1])
hold on
plot(zzj(1,:),'m-')
plot(zzj(4,:),'b-')
plot(zzj(7,:),'c-')
plot(zzj(9,:),'g-')
legend('m-','25% Gate', 'b-','60%','c-','80%','g-','100%')
title('Unit 1 A: Velocity Profiles @ 0.15H from Top of Intake')
hold off
print rds1  -f1 -dmeta
clear zzj

for k=1:9
zzj(k,:)=spline(x,vel2(k,:),xrqd);
end

figure(2)
set(gca,'XTickLabels',[-1:0.5:1])
hold on
plot(zzj(1,:),'m-')
plot(zzj(4,:),'b-')
plot(zzj(7,:),'c-')
plot(zzj(9,:),'g-')
legend('m-','25% Gate', 'b-','60%','c-','80%','g-','100%')
title('Unit 1 A: Velocity Profiles 0.67H from Top of Intake')
hold off

for k=1:9
zzj(k,:)=spline(x,vel3(k,:),xrqd);
end

figure(3)
set(gca,'XTickLabels',[-1:0.5:1])
hold on
plot(zzj(1,:),'m-')
plot(zzj(4,:),'b-')
plot(zzj(7,:),'c-')
```

```
plot(zzj(9,:),'g-')
legend('m-','25% Gate', 'b-','60%','c-','80%','g-','100%')
title('Unit 1 A: Velocity Profiles 0.91H from Top of Intake')
hold off


end

%Files fact1, fact2, and fact3 contain the array of velocity factors
%for RDS testing levels 92.4, 115.8, and 126.6 ft respectively.
```

```
% Script file to perform 3D cubic spline interpolation
% on a grid of Ott meter measurements.
% xm & ym are the metering point coordinates expressed
% as a proportion of the intake opening, in the horizontal and vertical directions

load c:\users\pam\matlab\ketvel.dat;
zm=ketvel;

load c:\users\pam\matlab\ket_gate.dat;
gt=ket_gate;

% The relative location of the measured velocity points are
xm=[0.02541942,   0.095577021,   0.21403152,   0.347229283,   0.499745806,   0.652262328,
0.78596848,0.904422979, 0.9745805];
ym=[0.011061947,       0.039823009,       0.092920354,       0.150442478,       0.216814159,
0.329646018,0.442477876,  0.555309735,  0.668141593,  0.78097345,  0.84734513,  0.90707964,
0.95796460, 0.988938053];

% The area of the intake in ft^2 is:
AREA=(879.249/2);

% Define the required data points
xrqd=[0.025:0.001:0.974];
yrqd=[0.011:0.001:0.988];

[xg,xgq]=gaussint(0,1,20);
[yg,ygq]=gaussint(0,1,20);

% Sub-divide the matrix of kettle velocity measurements into 9x14 matrices

q=zeros(1,1);

zj=zeros(length(ym),length(xm));
zj=zeros(length(ym),length(xrqd));
zzj=zeros(length(ym),length(xm));

for test=1
                              startline=((test-1)*14)+1;
                               endline=(startline+13);

                                                  % Perform the interpolation along rows
                              for j=(startline:endline)
                                          zj(j-startline+1,:)=spline(xm,zm(j,:),xrqd);
                                       end

                                                % Perform the interpolation along columns
                          zzj=zeros(length(yrqd),size(xrqd,2));
                                       zzj=zzj';
                                        zj=zj';

    for k=1:size(xrqd,2)
                                                          zzj(k,:)=spline(ym,zj(k,:),yrqd);
    end

                                       zzj=zzj';
                                       %clear zj

                           %zj=zeros(length(yrqd),length(xrqd))                              ;

% perform GQ integration procedure
    asum=0;
                                        tsum=0;
                                       for i=1:m
                                       for j=1:m
                                                        a1=ygq(i).*xgq(j).*zzj(i,j);
                                                                    asum=asum+a1;
                                          end
```

```
tsum=tsum+asum;
    asum=0;
      end

  q=tsum*AREA;                                    end
```

APPENDIX D

RDS Results

Table D.1. Reference Discharge and RDS Discharge Estimates

				Q Estimate (RDS)		
Unit	Intake	Gate	Q ref	0.15 *H*	0.67 *H*	0.91 *H*
1	A	25	127.27	110.00	92.51	20.69
1	A	40	190.66	65.05	107.11	32.21
1	A	50	227.02	80.50	37.92	34.43
1	A	60	269.65	62.66	75.81	44.97
1	A	65	286.15	78.13	87.36	48.59
1	A	70	299.83	86.45	46.96	50.62
1	A	80	321.54	93.16	94.44	54.25
1	A	90	340.96	97.69	105.41	58.34
1	A	100	359.47	92.55	47.18	61.74
1	B	25	150.61	65.05	97.14	26.60
1	B	40	225.06	77.17	111.90	39.72
1	B	50	271.76	85.98	54.91	49.38
1	B	60	316.47	61.71	77.52	54.48
1	B	65	338.75	73.97	91.85	60.33
1	B	70	350.57	82.10	68.03	60.76
1	B	80	375.58	90.55	95.69	65.07
1	B	90	403.08	95.18	111.91	71.37
1	B	100	424.96	97.92	67.91	75.60
1	C	25	160.51	69.66	100.24	34.37
1	C	40	242.44	83.65	113.79	51.91
1	C	50	292.51	95.39	65.79	62.84
1	C	60	342.07	69.77	81.89	72.31
1	C	65	361.42	84.06	94.41	77.19
1	C	70	377.26	91.83	80.52	80.30
1	C	80	405.13	100.89	99.99	85.86
1	C	90	430.07	108.87	116.70	91.45
1	C	100	454.23	111.54	81.06	96.08
2	A	25	151.23	116.43	96.41	30.71
2	A	40	224.77	71.69	108.85	44.83
2	A	50	267.94	86.49	41.31	54.14
2	A	60	303.66	71.22	82.16	61.22
2	A	65	315.25	87.45	93.34	63.99
2	A	70	325.53	94.74	47.22	66.32
2	A	80	346.06	100.33	94.03	69.25
2	A	90	359.98	106.52	108.57	72.75
2	A	100	373.51	103.96	48.33	75.04
2	B	25	151.95	73.42	98.71	40.19

				Q Estimate (RDS)		
Unit	Intake	Gate	Q ref	0.15 *H*	0.67 *H*	0.91 *H*
2	B	40	225.29	88.92	113.88	58.82
2	B	50	266.38	96.98	61.71	69.19
2	B	60	300.99	74.50	85.39	78.19
2	B	65	314.78	86.29	98.53	82.77
2	B	70	324.71	93.58	68.94	84.95
2	B	80	344.88	102.60	97.94	89.54
2	B	90	358.87	106.70	113.04	94.18
2	B	100	372.50	111.10	67.61	97.33
2	C	25	198.95	65.92	103.13	36.92
2	C	40	293.61	77.07	117.59	54.77
2	C	50	349.72	77.73	73.15	64.88
2	C	60	395.53	53.32	89.56	72.70
2	C	65	414.80	64.03	102.33	77.88
2	C	70	428.37	70.88	83.05	80.22
2	C	80	453.53	78.28	101.84	84.94
2	C	90	474.19	81.50	117.58	88.47
2	C	100	492.65	89.90	83.43	92.29
3	A	25	131.19	108.27	80.11	24.97
3	A	40	196.11	64.83	92.62	37.80
3	A	50	238.44	79.39	37.47	45.75
3	A	60	278.23	61.59	72.87	53.35
3	A	65	298.20	77.76	84.04	57.07
3	A	70	313.13	86.51	42.11	60.13
3	A	80	335.01	93.61	84.81	63.85
3	A	90	352.62	99.03	98.20	66.95
3	A	100	369.09	111.77	41.03	70.64
3	B	25	150.36	65.91	83.69	32.90
3	B	40	221.21	74.15	96.33	48.63
3	B	50	266.92	74.27	54.37	58.37
3	B	60	314.95	55.12	76.62	68.12
3	B	65	336.69	66.53	87.97	72.84
3	B	70	352.26	73.35	62.46	75.62
3	B	80	377.63	80.08	89.44	80.49
3	B	90	399.15	84.12	102.96	85.64
3	B	100	418.42	95.13	59.49	89.94
3	C	25	160.02	63.18	86.95	33.33
3	C	40	237.59	75.61	100.30	50.18
3	C	50	285.69	81.54	64.70	61.43

				Q Estimate (RDS)		
Unit	Intake	Gate	Q ref	0.15 *H*	0.67 *H*	0.91 *H*
3	C	60	336.30	63.17	79.17	70.61
3	C	65	359.38	74.82	91.71	75.69
3	C	70	376.07	82.08	75.72	79.25
3	C	80	401.03	89.39	93.77	83.89
3	C	90	425.50	94.24	108.82	88.10
3	C	100	446.39	99.35	71.39	93.92
4	A	25	143.87	109.36	98.38	19.86
4	A	40	208.80	69.43	113.32	28.90
4	A	50	246.48	83.50	32.90	34.45
4	A	60	280.26	64.85	75.21	37.66
4	A	65	297.81	79.46	92.61	40.26
4	A	70	304.08	82.52	38.39	41.93
4	A	80	324.54	92.25	88.07	44.54
4	A	90	340.66	97.01	101.49	46.12
4	A	100	346.38	104.04	47.54	47.42
4	B	25	179.82	64.29	101.70	30.67
4	B	40	259.73	77.48	117.72	44.44
4	B	50	309.76	88.31	53.39	53.38
4	B	60	351.24	66.65	82.13	60.68
4	B	65	373.52	77.22	98.10	62.50
4	B	70	380.16	82.50	60.81	65.87
4	B	80	406.04	91.60	90.40	68.84
4	B	90	425.36	97.37	108.31	73.19
4	B	100	434.47	99.02	71.65	73.33
4	C	25	178.97	70.18	105.78	27.03
4	C	40	259.42	85.50	126.17	39.39
4	C	50	307.86	96.64	66.96	46.59
4	C	60	350.76	74.16	86.46	53.07
4	C	65	369.20	85.77	102.26	54.84
4	C	70	380.00	91.31	73.21	58.34
4	C	80	405.16	100.49	95.27	61.67
4	C	90	424.48	107.01	113.52	64 52
4	C	100	433.11	110.28	85.39	65.54
5	A	25	139.72	103.38	97.53	15.72
5	A	40	206.62	64.70	113.55	25.20
5	A	50	248.98	78.98	39.80	30.47
5	A	60	289.30	87.99	70.16	36.91
5	A	65	296.16	69.32	85.82	34.96

				Q Estimate (RDS)		
Unit	Intake	Gate	Q ref	0.15 *H*	0.67 *H*	0.91 *H*
5	A	70	311.04	72.01	99.07	40.59
5	A	80	329.37	82.67	45.79	41.36
5	A	90	345.67	90.43	90.52	42.18
5	A	100	356.32	103.51	43.71	41.80
5	B	25	183.89	61.78	101.21	35.24
5	B	40	268.63	75.85	121.30	51.37
5	B	50	319.45	81.67	40.77	59.62
5	B	60	371.82	90.16	79.51	71.21
5	B	65	385.17	66.01	90.85	70.18
5	B	70	399.72	68.77	99.14	71.32
5	B	80	422.14	79.88	67.01	81.19
5	B	90	443.14	86.92	92.89	83.82
5	B	100	459.21	96.94	66.74	84.41
5	C	25	172.03	68.29	106.29	26.03
5	C	40	251.41	83.59	126.98	38.15
5	C	50	301.02	97.31	59.49	44.51
5	C	60	349.74	105.69	83.33	51.89
5	C	65	361.08	77.88	94.82	52.50
5	C	70	375.94	81.24	44.64	55.55
5	C	80	396.50	93.95	78.78	55.54
5	C	90	416.51	101.85	95.86	60.47
5	C	100	431.88	107.56	82.39	63.47
6	A	25	148.11	103.16	111.32	19.85
6	A	40	220.74	63.15	71.76	30.30
6	A	50	263.86	78.42	99.94	37.57
6	A	60	297.24	88.27	113.83	41.34
6	A	65	310.93	94.11	40.14	43.29
6	A	70	326.15	96.97	69.64	48.26
6	A	80	342.91	74.52	80.40	49.14
6	A	90	362.22	86.38	94.85	52.32
6	A	100	372.95	97.44	101.30	54.34
6	B	25	180.81	57.06	47.91	32.87
6	B	40	265.67	69.44	83.91	48.89
6	B	50	317.51	78.15	103.24	58.73
6	B	60	358.15	85.30	119.10	65.29
6	B	65	373.28	92.70	60.26	68.00
6	B	70	389.45	94.45	79.20	70.57
6	B	80	411.27	71.73	83.47	74.30

				Q Estimate (RDS)		
Unit	Intake	Gate	Q ref	0.15 *H*	0.67 *H*	0.91 *H*
6	B	90	430.74	84.11	98.27	77.76
6	B	100	446.33	92.39	106.43	80.89
6	C	25	171.84	66.26	48.17	32.99
6	C	40	253.06	79.32	94.81	48.04
6	C	50	301.24	88.36	109.18	56.95
6	C	60	339.46	96.57	119.68	63.83
6	C	65	355.45	96.52	69.45	66.70
6	C	70	370.76	98.35	82.74	69.46
6	C	80	391.44	75.04	89.47	72.78
6	C	90	411.96	87.49	97.09	75.93
6	C	100	426.64	102.15	109.64	78.39
7	A	25	152.25	98.79	77.28	33.62
7	A	40	225.55	61.86	90.53	49.21
7	A	50	270.20	76.91	106.43	59.01
7	A	60	306.14	84.85	46.15	66.79
7	A	65	319.80	91.09	82.36	69.76
7	A	70	331.81	96.43	96.87	71.93
7	A	80	351.34	101.77	112.72	76.23
7	A	90	368.39	107.26	55.35	80.75
7	A	100	382.63	94.87	44.64	82.40
7	B	25	160.19	51.66	88.83	36.87
7	B	40	236.87	67.09	93.21	52.91
7	B	50	283.50	74.18	110.18	62.59
7	B	60	319.21	78.78	71.62	71.59
7	B	65	334.82	81.72	94.75	75.00
7	B	70	349.65	86.48	99.91	76.88
7	B	80	368.77	91.71	116.49	81.27
7	B	90	385.44	94.74	66.35	85.52
7	B	100	405.05	86.27	67.48	86.56
7	C	25	185.79	57.02	92.74	18.09
7	C	40	273.11	73.79	99.41	28.67
7	C	50	325.46	82.94	108.32	35.04
7	C	60	372.53	88.35	84.91	40.12
7	C	65	389.85	91.14	99.44	42.76
7	C	70	402.55	96.81	106.72	45.10
7	C	80	427.88	102.47	114.15	48.76
7	C	90	448.25	104.75	73.11	49.16
7	C	100	468.92	96.98	78.22	55.76

				Q Estimate (RDS)		
Unit	Intake	Gate	Q ref	0.15 *H*	0.67 *H*	0.91 *H*
8	A	25	122.85	94.17	94.88	9.49
8	A	40	194.92	52.78	60.35	19.77
8	A	50	236.39	66.85	84.80	22.69
8	A	60	273.56	76.39	101.55	33.07
8	A	65	291.47	85.20	63.91	34.48
8	A	70	306.15	92.68	90.00	35.08
8	A	80	329.23	96.70	107.77	29.86
8	A	90	354.23	105.25	42.60	48.38
8	A	100	367.10	91.85	78.45	40.05
8	B	25	144.53	48.62	100.11	23.55
8	B	40	221.77	63.20	72.43	35.84
8	B	50	270.70	71.42	90.11	46.23
8	B	60	319.60	79.44	107.78	57.55
8	B	65	336.59	81.99	76.59	55.88
8	B	70	354.63	89.63	95.89	58.77
8	B	80	377.40	96.18	114.64	65.88
8	B	90	401.31	105.06	67.05	66.44
8	B	100	421.14	84.40	83.84	72.55
8	C	25	154.89	50.35	104.73	22.44
8	C	40	236.63	65.02	79.13	36.70
8	C	50	289.48	73.56	94.67	44.93
8	C	60	339.34	82.46	113.21	52.88
8	C	65	359.70	89.71	83.99	56.28
8	C	70	378.50	93.22	99.80	59.12
8	C	80	402.41	99.52	120.04	63.95
8	C	90	429.03	108.94	73.01	66.10
8	C	100	449.69	87.86	87.34	70.49
9	A	25	146.28	94.62	93.83	17.25
9	A	25	153.62	57.71	50.83	21.37
9	A	40	225.31	61.68	95.03	31.38
9	A	50	266.76	74.22	106.17	38.81
9	A	60	300.41	81.39	117.93	38.98
9	A	65	312.02	88.53	47.56	44.15
9	A	70	322.54	93.16	88.11	45.14
9	A	80	340.67	94.15	97.40	45.83
9	A	90	357.94	95.09	110.40	48.23
9	A	100	371.64	82.98	78.00	49.51
9	A	100	378.12	90.36	88.06	54.65

				Q Estimate (RDS)		
Unit	Intake	Gate	Q ref	0.15 *H*	0.67 *H*	0.91 *H*
9	B	25	172.38	58.62	104.83	39.62
9	B	25	176.76	62.36	71.01	38.59
9	B	40	259.95	74.53	93.77	57.32
9	B	50	305.24	83.93	112.39	66.40
9	B	60	347.53	90.86	115.53	76.60
9	B	65	361.29	94.02	66.00	81.39
9	B	70	371.50	96.64	88.80	82.78
9	B	80	392.62	100.25	103.34	88.14
9	B	90	410.72	103.23	108.62	91.47
9	B	100	426.68	79.01	87.16	98.11
9	B	100	432.25	88.74	91.54	95.31
9	C	25	181.08	57.60	108.23	37.26
9	C	25	185.36	62.09	87.58	38.64
9	C	40	271.99	73.79	105.42	56.63
9	C	50	319.46	83.74	113.17	64.53
9	C	60	360.59	89.71	116.77	70.90
9	C	65	381.44	91.35	80.86	79.99
9	C	70	393.28	95.49	99.58	83.48
9	C	80	414.89	100.37	103.59	88.08
9	C	90	434.86	102.66	107.61	90.98
9	C	100	452.15	78.83	85.03	95.48
9	C	100	454.50	86.97	93.02	96.52
10	A	25	148.37	82.18	78.78	23.38
10	A	40	227.60	50.19	39.00	40.90
10	A	50	269.04	68.32	80.24	51.39
10	A	50	263.04	76.64	96.32	48.07
10	A	60	302.62	76.29	33.94	55.48
10	A	65	316.40	85.70	70.40	58.80
10	A	65	312.54	90.72	83.07	61.23
10	A	70	317.45	94.82	29.09	58.31
10	A	80	341.13	70.96	58.51	64.88
10	A	90	364.80	82.26	65.96	71.13
10	A	100	375.67	95.92	31.01	70.02
10	A	100	371.39	77.37	66.08	71.78
10	B	25	170.42	46.62	83.57	31.44
10	B	40	257.56	63.62	57.69	47.63
10	B	50	301.08	74.92	85.60	55.32
10	B	50	296.85	76.15	101.93	54.67

				Q Estimate (RDS)		
Unit	Intake	Gate	Q ref	0.15 *H*	0.67 *H*	0.91 *H*
10	B	60	338.80	84.27	49.91	61.78
10	B	65	353.05	87.77	74.69	64.33
10	B	65	349.39	90.90	88.86	64.57
10	B	70	356.39	80.25	43.80	66.46
10	B	80	379.94	64.22	60.60	69.29
10	B	90	404.96	74.21	69.04	76.84
10	B	100	420.29	103.03	46.60	78.88
10	B	100	414.68	71.21	69.55	79.01
10	C	25	180.25	50.20	87.78	39.84
10	C	40	272.71	67.65	69.21	59.21
10	C	50	320.01	80.03	89.48	68.84
10	C	50	312.85	81.71	107.20	68.24
10	C	60	358.45	90.76	61.56	77.79
10	C	65	375.78	93.97	78.08	79.95
10	C	65	366.52	96.98	93.33	79.26
10	C	70	378.63	105.60	51.97	82.57
10	C	80	405.44	75.52	62.65	88.28
10	C	90	430.87	90.03	72.12	95.09
10	C	100	444.47	109.73	56.05	94.61
10	C	100	436.89	75.82	73.32	95.76
11	A	40	208.88	92.16	81.98	37.37
11	A	50	251.82	66.60	93.96	46.28
11	A	55	275.43	74.55	47.11	48.58
11	A	60	292.41	80.11	93.75	51.89
11	A	65	312.18	84.46	106.54	56.23
11	A	70	327.84	83.83	31.06	56.94
11	A	80	353.13	61.21	65.84	62.10
11	A	90	377.78	72.79	79.91	69.58
11	A	100	393.74	91.92	41.67	71.20
11	B	40	228.97	57.74	86.36	45.33
11	B	50	272.97	65.15	98.34	55.53
11	B	55	297.75	70.52	68.76	58.17
11	B	60	319.43	74.62	97.06	63.21
11	B	65	338.51	78.78	111.75	66.13
11	B	70	356.24	95.30	46.60	71.91
11	B	80	383.05	69.70	71.28	76.68
11	B	90	407.27	80.71	83.70	84.30
11	B	100	427.61	82.42	61.38	88.96

				Q Estimate (RDS)		
Unit	Intake	Gate	Q ref	0.15 *H*	0.67 *H*	0.91 *H*
11	C	40	228.52	74.86	89.11	33.03
11	C	50	274.16	82.62	102.21	41.45
11	C	55	298.94	87.96	82.44	45.04
11	C	60	319.56	93.21	101.61	46.57
11	C	65	340.36	98.69	114.99	50.81
11	C	70	356.67	92.19	56.88	51.60
11	C	80	384.28	65.54	74.88	57.78
11	C	90	406.39	76.76	87.01	56.31
11	C	100	426.76	95.22	72.53	60.43
12	A	25	155.77	84.80	80.85	12.56
12	A	40	241.15	54.90	95.91	23.15
12	A	50	268.87	67.16	37.63	28.70
12	A	55	287.20	75.22	78.31	29.51
12	A	60	317.77	82.86	93.56	31.23
12	A	65	322.73	86.41	35.94	33.53
12	A	70	330.24	68.10	70.87	34.26
12	A	75	336.84	74.61	82.18	36.16
12	A	80	349.51	82.74	45.87	34.55
12	A	85	352.99	86.32	89.84	35.77
12	A	90	382.33	91.43	103.63	38.42
12	A	100	394.28	79.79	38.10	38.54
12	B	25	172.64	57.11	85.39	27.44
12	B	40	242.70	72.71	101.33	39.63
12	B	50	297.32	79.89	55.11	45.32
12	B	55	318.07	85.39	83.80	51.21
12	B	60	323.24	90.66	98.00	52.11
12	B	65	353.35	97.70	53.09	58.21
12	B	70	361.38	69.26	75.12	56.49
12	B	75	373.41	78.96	85.98	61.79
12	B	80	379.99	89.84	66.71	58.23
12	B	85	391.41	93.13	95.29	64.23
12	B	90	390.26	100.87	108.94	65.85
12	B	100	398.59	88.24	56.35	65.61
12	C	25	183.70	55.35	89.56	22.54
12	C	40	256.20	66.42	106.45	32.41
12	C	50	310.10	75.74	66.06	37.48
12	C	55	339.71	81.62	85.25	51.04
12	C	60	341.95	83.51	103.18	45.00

				Q Estimate (RDS)		
Unit	Intake	Gate	Q ref	0.15 *H*	0.67 *H*	0.91 *H*
12	C	65	372.96	94.11	61.67	52.36
12	C	70	379.54	66.15	76.75	48.54
12	C	75	395.77	75.09	87.78	56.88
12	C	80	397.68	84.13	79.28	44.53
12	C	85	413.74	89.84	97.07	60.47
12	C	90	414.15	92.44	110.60	61.13
12	C	100	418.73	78.93	66.56	55.15